SOC stock assessment in drylands based on a combined ecohydrology and aerial imagery approach

a case study in the Negev Desert, Israel

Dissertation

Zur Erlangung des akademischen Grades

Inauguraldissertation
Zur Erlangung der Würde eines Doktors der Philosophie
vorgelegt der
Philosophisch-Naturwissenschaftlichen Fakultät der
Universität Basel

Harald Hikel
aus Marktbreit (Deutschland)

Basel, 2014

Genehmigt durch die Philosophisch-Naturwissenschaftliche Fakultät auf Antrag von

Prof. Dr. Nikolaus Kuhn
(Universität Basel)
Fakultätsverantwortlicher / Dissertationsleiter

Dr. Holly Croft
(University of Toronto)
Korreferent

Basel, den 23.04.2013
Prof. Dr. Jörg Schibler
Dekan

Abstract

The global soil system forms the largest pool of terrestrial organic carbon. The inventory of soil organic carbon (SOC) is required for greenhouse gas inventories and carbon mitigation projects. Especially in (semi-) arid ecosystems the size and the dynamics of the SOC pool still lack sufficient investigation. Based on the increasing interest in reliable estimates of SOC stocks in drylands, this thesis aims for the quantification of SOC stocks and patterns in the Northern Highlands of the Negev Desert (Israel) on a regional scale considering SOC spatial heterogeneity at a local scale.

The Negev Highlands were chosen as an ideal study site because they represent a characteristic arid environment and several studies regarding lithology, hydrology and vegetation have been carried out there.

Because of the high spatial heterogeneity of environmental conditions at local scale in this area, slope sections with different ecohydrologic characteristics (e.g. soil, vegetation) were sampled and SOC stocks were calculated. To identify controlling factors of SOC stocks on rocky desert slopes, soil properties, vegetation coverage, SOC concentrations and stocks were compared between distinctive ecohydrological environments (EHEs). The EHEs are characterized by similar surface conditions (such as geology, rock/soil ratio and soil distribution), water supply and vegetation density. Rock-soil interaction and the relevance of soil volume for storing plant available water and hence the water supply for vegetation coverage determining SOC concentrations and stocks were further examined. Rainfall simulation experiments were therefore conducted to determine the amount of rainfall required to fill the available soil water storage capacity. The design and the selection of the plots aimed specifically at observing infiltration into small soil patches on a micro-scale relevant for prevalent vegetation coverage. Based on this experimental procedure the relationship between environmental properties and SOC concentrations and stocks regarding the distinctive EHEs could be identified at local scale. For the determination of local scale SOC spatial heterogeneity at regional scale an approach towards automated mapping of EHEs was developed. Therefore spatial vegetation pattern indices were calculated based on the analysis of hyperspectral and orthoimage datasets. The indices were then used as variables in a decision tree model for automated mapping of EHEs. For the quantification of SOC stocks at regional scale considering local scale spatial heterogeneity of SOC concentrations and driving processes, a GIS-based image analysis approach was developed using vegetation coverage and EHEs as proxy indicators for SOC concentrations and patterns. The calculated SOC stocks indicate that rocky desert slopes contain a significant amount of SOC of soil-covered areas of 1.54 kg C m^{-2}, with an average SOC stock over the entire study site of 0.58 kg C m^{-2}. The calculated SOC-stock for the total area ($1km^2$) is 1.19t C ha^{-1}. Based on the results of this thesis, the understanding of ecohydrological conditions and processes and remote sensing techniques were combined in one methodological approach. This implemented procedure provides the precise estimation of SOC-stocks in arid environments by combining field data and digital image processing approaches.

Zusammenfassung

Böden stellen weltweit den grössten Speicher von terrestrischem organischem Kohlenstoff dar. Durch die Quantifizierung von organischem Kohlenstoff in Böden besteht die Möglichkeit, sowohl Treibhausgasinventare zu erstellen als auch Massnahmen zur Verringerung von Kohlenstoffemissionen einzuleiten. Insbesondere in (semi-)ariden Gebieten ist sowohl die Grösse als auch die Dynamik des organischen Kohlenstoffspeichers noch weitgehend eine unbekannte Grösse. Kohlenstoffinventare werden generell für unterschiedliche Skalen berechnet (lokal, regional, global). Insbesondere auf regionaler und globaler Skala ist die Quantifizierung von organischem Kohlenstoff mit grossen Ungenauigkeiten verbunden, da die räumliche Heterogenität von Kohlenstoffkonzentration und -verteilung auf lokaler Ebene aufgrund des methodischen Vorgehens nicht berücksichtigt werden kann. Ausgehend von dem steigenden internationalen wissenschaftlichen Interesse an einer zuverlässigen und präzisen Inventarisierung von Kohlenstoff in Trockengebieten ist das Ziel dieser Arbeit die Quantifizierung von Kohlenstoffvorrat und -verteilung in den Northern Highlands der Negev Wüste, Israel. Die Berechnung wurde hierbei auf regionaler Skala durchgeführt, wobei die räumliche Heterogenität der Kohlenstoffkonzentrationen auf lokaler Ebene mit einbezogen wurde. Die Negev Highlands wurden als Untersuchungsgebiet ausgewählt, da diese ein charakteristisches Trockengebiet darstellen und dort bereits zahlreiche Studien zu Lithologie, Hydrologie und Vegetation durchgeführt wurden, die als Grundlage für die vorliegende Untersuchung genutzt werden konnten.

Das Untersuchungsgebiet ist auf lokaler Skala geprägt durch eine hohe räumliche Heterogenität der ökologischen Gegebenheiten. Aufgrund dessen wurden Hangbereiche mit unterschiedlichen ökohydrologischen Eigenschaften (z.B. Boden, Vegetation) beprobt und sowohl Kohlenstoffkonzentrationen als auch -vorräte berechnet. Um die Faktoren zu identifizieren, welche die Kohlenstoffvorräte beeinflussen, wurden Bodeneigenschaften, Vegetationsbedeckung und Kohlenstoffkonzentrationen zwischen unterschiedlichen Ökohydrologischen Einheiten verglichen, wobei jede Ökohydrologische Einheit durch charakteristische Oberflächeneigenschaften (z.B. Geologie, Boden/Stein Verhältnis, Verteilung von Boden), Wasserversorgung und Vegetationsdichte charakterisiert ist. In einem nächsten Schritt wurde das Zusammenwirken von Boden- und Steinflächen und die Bedeutung von Bodenvolumen für die Speicherung von pflanzenverfügbarem Wasser untersucht. Wasserversorgung spielt in Trockengebieten eine wichtige Rolle, da diese Vegetationsdichte und -verteilung bestimmt und sich somit direkt auf Kohlenstoffkonzentrationen und -vorräte auswirkt. Mit Hilfe von Beregnungsexperimenten wurde die Niederschlagsmenge ermittelt, die notwendig ist, um die Wasserspeicherkapazität des Bodens zu füllen. Die Auswahl und Form der Versuchsflächen zielte speziell darauf ab, die Infiltrationsmenge in kleine Bodenflächen auf Mikro-Skala zu berechnen. Aufgrund dieses methodischen Vorgehens war es möglich, den Zusammenhang zwischen den ökologischen Gegebenheiten und Kohlenstoffkonzentrationen und -vorräten in den unterschiedlichen Ökohydrologischen Einheiten auf lokaler Skala zu identifizieren. Um die räumliche Heterogenität von organischem Kohlenstoff auf lokaler Ebene auch auf grösseren

Skalen quantifizieren zu können, wurde ein Ansatz zur automatischen Kartierung der Ökohydrologischen Einheiten auf regionaler Skala entwickelt. Hierzu wurden Vegetationsindizes berechnet, die aus der Analyse von Hyperspektral- und Orthobildern abgeleitet wurden. Die Indizes wurden anschliessend als Variablen in einem Entscheidungsbaummodell verwendet. Um ein Kohlenstoffinventar auf regionaler Skala für das Untersuchungsgebiet zu erstellen, wurde eine Geographisches Informationssystem (GIS) gestützte Bildanalysemethode entwickelt. Durch die Verwendung von Vegetationsbedeckung und Ökohydrologische Einheiten als Proxy-Indikatoren für Kohlenstoffkonzentrationen und -verteilung konnte die räumliche Heterogenität von Kohlenstoffkonzentrationen und -vorräten auf lokaler Ebene berücksichtigt werden. Die daraus berechneten Kohlenstoffvorräte zeigen, dass Wüstenböden eine signifikante Menge Kohlenstoff von 1.54 kg C m^{-2} enthalten, mit einem durchschnittlichen Wert von 0.58 kg C m^{-2}. Das berechnete Kohlenstoffinventar für das gesamte Untersuchungsgebiet beträgt 1.19t C ha^{-1}. Die entwickelte und angewendete Methode gewährleistet eine präzise Quantifizierung von Kohlenstoffinventaren in Trockengebieten, indem die Analyse von ökohydrologischen Gegebenheiten und Prozessen durch Feldmessungen, die Auswertung von Fernerkundungsdaten und Bildverarbeitungsverfahren in einem Ansatz kombiniert wurden.

Contents

List of Figures **10**

List of Tables **12**

1. Introduction **13**
1.1 Benefits and limitations of SOC inventories 13
1.2 SOC assessment at regional scale 14
1.3 Research questions 15
2. Carbon stocks and their assessment in drylands **17**
2.1 Soil organic carbon and the global carbon cycle 17
2.2 SOC stocks and controlling environmental properties in drylands 18
2.2.1 Soil 18
2.2.2 Climate and water redistribution 19
2.2.3 Vegetation 19
2.3 Problems with SOC inventory 20
2.4 Remote sensing 21
2.5 Study area and environmental settings 24
2.5.1 Climate 24
2.5.2 Lithology 24
2.5.3 Soil 24
2.5.4 Vegetation 25
2.5.5 Ecohydrology 25
2.6 Methods 26
3. Research Paper* **29**
Soil organic carbon in the rocky desert of northern Negev (Israel)
Hoffmann U., Yair A., Hikel H., Kuhn N.J.
In: Journal of Soils and Sediments (2012), 12: 811-825.
Abstract 30
1. Introduction 30
1.1 Soil organic carbon and the global carbon cycle 30
1.2 Carbon stocks in drylands 31
1.3 SOC-stock calculation and links to soil-forming factors 31
1.4 Estimation of dryland SOC stocks 31
2. Study site 32
3. Methods 34
3.1 Ecohydrologic units along rocky desert slopes at Sede Boqer 34
3.2 Soil sampling and data analysis 34
3.3 Laboratory and statistical SOC analysis 35
4. Results 37
4.1 Variability of SOC stocks and controlling soil properties 37
4.2 SOC stocks, soil properties and ecohydrology 37

*the numbering of headings is used as in the Research Paper

5. Discussion 38
5.1 SOC stocks, surface characteristics, and vegetation 38
5.2 Surface processes and SOC stocks 41
5.3 SOC stock comparison with other drylands 41
6. Conclusions 42
References 42
4. Research Paper* **45**
Experimental investigation of soil ecohydrology on rocky desert slopes in the Negev Highlands, Israel
Hikel H., Yair A., Schwanghart W., Hoffmann U., Straehl S., Kuhn N.J.
In: Zeitschrift für Geomorphologie (2012),57, Suppl.1: 039-058
Abstract 46
1. Introduction 46
2. Rainfall simulation as a tool for runoff measurements on rocky desert slopes 48
3. Study area 49
4. Material and Methods 53
4.1 Plot selection and description 53
4.2 Rainfall simulation and infiltration measurements 55
5. Results and Discussion 57
6. Conclusion 62
References 62
5. Research Paper* **67**
Combining remote sensing and spatial statistics for the analysis of shrub patterns in arid regions
Hikel H., Jarmer T., Kuhn N.J., Shoshany M., Schwanghart W.
Abstract 68
1. Introduction 69
2. Study area and environmental settings 70
3. Material and Methods 72
3.1 Available Data 72
3.2 Data acquisition and preparation 73
3.2.1 Mapping 73
3.2.2 Hyperspectral imaging 73
3.2.3 Laser scanning 74
3.2.4 Derivation of plant canopy from ground based imagery 74
3.3 Vegetation pattern analysis and explorative data analysis 76
3.4 Decision Tree Modelling 77
4. Results and interpretation 78
4.1 Vegetation density 78
4.2 Scale dependence of vegetation pattern indices 78
4.3 Decision tree 80
5. Discussion 85
6. Conclusion 87
Reference 87

*the numbering of headings is used as in the Research Paper

6. Research Paper* **91**
Spatial prediction of SOC-patterns in the Negev Desert (Israel) based on vegetation distribution and surface heterogeneity
Hikel H. & Kuhn N.J.
Abstract 92
1. Introduction 93
   1.1 Soil organic carbon stocks in drylands 93
   1.2 Spatial variability of carbon sequestration 93
   1.3 Remote sensing and quantification of SOC-stocks 94
2. Study site 94
3. Methods 96
   3.1 Measurement of aerial photograph 97
   3.2 Mapping EHEs 97
   3.3 Calculation of SOC-stock 97
4. Results 98
   4.1 Determination of vegetation coverage 98
   4.2 Automated mapping of EHEs 98
   4.3 SOC-stock and SOC-patterns 98
5. Discussion 101
   5.1 SOC stocks, surface properties and vegetation 101
   5.2 Estimation of SOC using remotely sensed data 103
   5.3 SOC-stock comparison with other drylands 104
6. Summary and conclusions 105
   References 106

7. Synthesis **111**
7.1 Relationship between surface characteristics, vegetation coverage and SOC 111
7.2 Relationship between environmental properties and vegetation coverage 112
7.3 Automated mapping of ecohydrological environments (EHEs) 112
7.4 Spatial prediction of SOC stock and patterns 113
7.5 Discussion of the guided research questions 114

8. Outlook **120**

Acknowledgements **122**

References **123**

*the numbering of headings is used as in the Research Paper

List of Figures

Chapter 2 - Carbon stocks and their assessment…

Fig. 1: Schematic representation of the climate-soil-vegetation system 18

Chapter 3* - Soil organic carbon in the rocky desert…

Fig. 1: Location of the study site and sampling points 33
Fig. 2: Geological cross section with lithological formations of the study site 33
Fig. 3: SOC concentration, vegetation coverage and soil depth against aspect 38
Fig. 4: SOC concentration, vegetation coverage and soil depth against ecohydrological units and aspect 39
Fig. 5: SOC concentration as a function of depth below surface, plotted for every sample 40
Fig. 6: Scatterplot of SOC concentration and $SOC_{stock, ehu}$ of sampled soils versus vegetation coverage and soil depth 40

Chapter 4* - Experimental investigation of soil ecohydrology…

Fig. 1: Map of Israel and location of the study site 49
Fig. 2: Relationship between rock-soil ratio and vegetation density 50
Fig. 3: Lithological formations within the studied catchment 50
Fig. 4: Overview of the different soil bedding types 51
Fig. 5: Portable nozzle simulator 55
Fig. 6: Frequency analysis of the magnitude of rainfall events 56
Fig. 7: Naturally crusted soil patch 56
Fig. 8: Naturally sized micro-catchment 56
Fig. 9: Infiltration observed on plots during rainfall simulation tests 59
Fig. 10: Relationship between soil volume, total infiltration and rock-soil ratio 61
Fig. 11: Relationship between soil volume, rock-soil ratio and volumetric water content 61

Chapter 5* - Combining remote sensing and spatial statistics…

Fig. 1: Map of Israel and location of study site 70
Fig. 2: Lithological formations within the studied catchment 71
Fig. 3: Map of the studied catchment 72
Fig. 4: Schematic illustration of the procedure to obtain trunk locations regarding horizontal and vertical viewing angle of individual plants 75
Fig. 5: Planform extent of high-resolution vegetation canopy data 75
Fig. 6: Boxplots, linear regression and RMSE comparing both remote sensing datasets 79
Fig. 7: Tree classification results of EHEs 82
Fig. 8: Results of the decision tree based classification model 84

Chapter 6* - Spatial prediction of SOC-patterns…

Fig. 1: Study area and experimental catchment site 95
Fig. 2: Lithological formations within the studied catchment 96
Fig. 3: Relationship between the different vegetation density analysis methods 98
Fig. 4: Binary image showing vegetation distribution within the study area 99
Fig. 5: Results of the decision tree based classification model 100

Fig. 6: Spatial distribution of SOC-patterns within the study area 101
Fig. 7: Conceptual model of the effect of surface properties, water availability and vegetation coverage on SOC concentrations 102
Chapter 7 - Synthesis
Fig. 2: Conceptual model of the effect of surface properties, water availability and vegetation coverage on SOC concentrations 114

List of Tables*

Chapter 3 - Soil organic carbon in the rocky desert…

Table 1: Observed and mapped properties of the ecohydrological units in the study area 35

Table 2: Mean soil depth, median soil and vegetation coverage and minimum, median, mean, max and standard deviation of SOC stocks with respect to aspect and ecohydrological units 36

Table 3: Minima, median, mean, maxima and standard deviation of measured soil properties relevant for the calculation of SOC stock 38

Table 4: Global comparison of SOC and SOC stock in different arid environments 41

Chapter 4 - Experimental investigation of soil ecohydrology…

Table 1: Observed and mapped properties of ecohydrological units 52

Table 2: Measured surface properties of ecohydrological units 54

Table 3: Infiltration and runoff properties of ecohydrological units 58

Chapter 5 - Combining remote sensing and spatial statistics…

Table 1: Average percentage of vegetation density for the different EHEs as calculated from the orthoimage and hyperspectral image analysis and obtained by field observation 78

Table 2: Results of the multiple mean comparison between vegetation indices 80

Table 3: Discriminatory power (%) and normalized discriminatory power (%) of the three vegetation pattern indices in the decision tree model 83

Table 4: Results of the decision tree analysis showing the observed and predicted classification of the EHEs 83

Chapter 6 - Spatial prediction of SOC-patterns…

Table 1: Average vegetation density for the different EHEs calculated from the orthoimage and obtained from field observation 98

Table 2: Area, vegetation covered area, $SOC_{stock, ehe}$ and $SOC_{stock, total}$ with respect to the different EHEs 100

Table 3: Calculated SOC-stock (t C) for an extent of $1km^2$ based on studies in several arid environments 105

1. Introduction

The global soil system is the largest terrestrial reservoir of organic carbon and therefore plays a key role in the global carbon cycle (Amundson 2001, Kirschbaum 2000, Kutsch et al. 2009). Due to the fact that atmosphere, biosphere and pedosphere are closely connected by the exchange of C, small changes in the soil organic carbon (SOC) pool can have significant implications for atmospheric CO_2-concentrations (Smith 2004). In the context of global warming there is increased international scientific interest in SOC stocks and fluxes in terrestrial ecosystems. Here the focus is to use soils as a carbon sink as demanded by the Kyoto Protocol (Houghton 2007, Mishra et al. 2009, Wigley & Schimel 2005). The size and dynamics of the global SOC pool lack sufficient investigation (Aufdenkampe et al. 2011, Doetterl et al. 2012b, Quinton et al. 2010, Seip 2001). Spatial variation of SOC is significantly influenced by environmental factors such as climate (Djukic et al. 2010, Jobbágy & Jackson 2000), topography (Egli et al. 2009, Garcia-Pausas et al. 2007), soil and bedrock materials (Doetterl et al. 2012a, Leifeld et al. 2005, Tan et al. 2004), vegetation (Luyssaert et al. 2008, Zhou et al. 2006), and disturbances due to surface processes (Berhe et al. 2008, Yoo et al. 2006) and human activity (Bell & Worral 2009, Morgan et al. 2010). Especially in dynamic geomorphic systems, which are sensitive to climate change, precise measurements and estimates of the spatial distribution of SOC stocks are necessary to quantify the SOC sink and source capacity of soils in changing environments (Aufdenkampe et al. 2011, Smith et al. 2003, Trumbore 2009).

1.1 Benefits and limitations of SOC inventories

During the last 15 years studies of SOC have contributed to carbon accounting and understanding its role and feedback in the global carbon cycle and within the climate system (Berhe et al. 2008, Kirschbaum 2000, Perruchoud et al. 2000, Post & Kwon 2000, Rosenbloom et al. 2006, Van Wesemael et al. 2010). Studies predominantly focus on (i) the relation of SOC stocks to environmental conditions (temperature, topography, soil, vegetation, human activity), (ii) the amount and residence time of SOC content under various environmental conditions, (iii) changes of SOC stocks under changing climate conditions and (iv) management and policy purposes (Bell & Worral 2009, Berhe et al. 2008, Bolstad & Vose 2001, Don et al. 2011, Egli et al. 2009, Heckmann et al. 2009, Hoffmann et al. 2009, Luyssaert et al. 2008, Spielvogel et al. 2009). Generally SOC stocks are calculated for different scales (Doetterl et al. 2012a, b). Thereby studies focus on (i) local scale homogeneous study sites where data are derived from plots or transects (up to 200m). For the calculation of SOC stocks therefore, one relevant environmental variable changes with time or space whilst the other environmental variables remain constant; (ii) regional scale which ranges up to a few km^2. The study sites are generally selected in such a way that the spatial variability of SOC is characterized by more or less homogeneous surface properties or rather climate patterns; (iii) global scale where the spatial variability of the relevant surface properties is simplified by model assumptions (Friedlingstein et al. 2006, Grüneberg et al. 2010, Hancock et al. 2010, Leifeld et al. 2005, Sheikh et al. 2009, Xu et al. 2010, Zeng et al. 2004). Simplifying assumptions are generally applied to SOC studies due to the spatial variability of control mechanisms of environmental conditions on SOC stocks. Especially at regional and global scale, studies are based on simplified relations (Cox et al. 2000, Jones et al. 2005), where uncertainty associated with small scale variability is not considered. The above-mentioned circumstances (i), (ii) and (iii) introduce large uncertainties of regional and global SOC estimates. Studies focusing on the influence of erosion processes on the carbon cycle suggest a net uptake of carbon, but the results of these studies show a high variability and range between 0.1 and 1.0 Pg C y^{-1} (Doetterl et al. 2012b). In contrast, local scale studies are conducted at plots or transects characterized by homogeneous environmental conditions. However, the interaction of the controlling variable at local scale is in general not representative of larger areas with heterogeneous environmental conditions (Doetterl et al. 2012a, b).

1.2 SOC assessment at regional scale

In the last 15 years SOC studies have largely focused on inventories at plot scale or along transects (Cerdan et al. 2010, Coleman & Jenkinson 1999, Doetterl 2012b). To inventorise at regional or global scale as required by the Kyoto Protocol, interpolation between point measurements is used to predict values for locations that lack sampled points. This technique is based on spatial autocorrelation, which measures the degree of dependence between near and distant points (Li & Heap 2011), but due to the large spatial variability of environmental factors, soil properties and limited sampling densities, SOC stocks are not well represented and require more detailed investigation (Doetterl et al. 2012a). In turn, hyperspectral remote sensing is a practical method of data collection at larger spatial scales. Different modelling techniques are used to predict SOC from continuous reflectance spectra (wavelength range 0.4-2.5µm) or derivatives (Baumgartner et al. 1985, Ben-Dor & Banin 1994, 1995, Brown et al. 2006, Hummel et al. 2001, Reeves et al. 2002, Udelhoven et al. 2003, Viscarra Rossel et al. 2006), but a major drawback of this approach is that it is restricted to soil devoid of any vegetation (Schwanghart & Jarmer 2011). Furthermore the analysis of SOC concentrations by remote sensing is limited to the topsoil (the uppermost layer of soil, ~2cm depth). The variations of SOC concentrations with depth are not discernible (Stallard 1998). Alternatively for the quantification of SOC stocks, surface cover is determined by remote sensing which in turn is linked afterwards to SOC concentrations. In general, point data of SOC concentrations reflect the interactions of environmental properties and processes at a small spatial scale but the up-scaling from point and plot data to larger areas is problematic (Hill & Schuett 2000). In contrast, remotely sensed aerial data cover a large spatial extend, but spatial resolution is a limiting factor for the quantification of surface heterogeneity (Doetterl et al. 2012b) such as topography, surface properties or vegetation patterns. Despite the fact that down-scaling methods provide ways to obtain information on subgrid-scale, parameterization schemes of small-scale heterogeneity are required (Zhang et al. 1998). High-resolution imagery (10m and higher) has recently become more freely available. This enables the detection of a variety of environmental parameters and ecologic information over small spatial extent but with higher spatial resolution (Mulder et al. 2011). But the point-to-area data problem is still a major challenge for SOC studies.

This evidence emphasizes the need to quantify spatial heterogeneity and its scale dependency at a local scale to understand, characterize and estimate size and dynamics of SOC stocks at a regional scale. Yair and colleagues (Boeken & Shachak 1994, Olsvig-Whittaker et al. 1983, Schreiber et al. 1995, Yair & Raz-Yassif 2004, Yair & Shachak 1982) studied lithology, hydrology and vegetation in a local scale experimental watershed in the Negev Desert, Israel. The results of the studies showed that particularly the distinctive ecohydrological conditions in arid environments lead to a large spatial variability of soil and surface properties and vegetation coverage. In turn, the spatial patterns of environmental factors determine SOC concentrations and stocks at local scale. Yair and colleagues (Boeken & Shachak 1994, Olsvig-Whittaker et al. 1983, Schreiber et al. 1995, Yair & Raz-Yassif 2004, Yair & Shachak 1982) therefore defined distinctive ecohydrological environments (EHEs) characterized by similar surface conditions (such as geology, rock/soil ratio, soil distribution), water supply and vegetation density. The differences of vegetation density between EHEs imply an effect of ecohydrology on SOC stocks. The interactions between ecohydrology, vegetation density and SOC within the different distinctive EHEs were not part of their studies, but offer the opportunity to assess SOC stocks using remote sensed data of vegetation. Combining the identification of distinctive EHEs using field measurements and the detection of these distinctive EHEs at unmeasured locations by characteristic environmental properties using remote sensing techniques offers a methodological procedure solving the spatial point-to-area data problem.

1.3 Research questions

Arid environments are regarded as “hotspots” of climate change with large, rapid and variable responses to even the smallest changes in conditions (Farage et al. 2003, Lal 2003, Yair 1990). Global dryland soils contain 15.5% of the world’s total SOC to 1m depth and thus represent a major C pool (Lal 2003, Lal 2001, Schimel et al. 2000). The carbon exchange between soil and atmosphere of these ecosystems may therefore have a strong impact on the global carbon cycle (Lal 2009). However, the importance of arid environments in the global carbon cycle has received limited attention (Asner et al. 2003, Schimel 2010). For the estimation of changes in SOC stocks due to climate change, further research to provide methods for the assessment of regional SOC stocks and patterns in arid environments is needed. These methods have to consider the spatial heterogeneity of ecohydrological and environmental conditions (Chapter 2, Carbon stocks and their assessment in drylands, 2.4.5; Chapter 3, Research Paper, 2; Chapter 4, Research Paper, 3; Chapter 5, Research Paper, 2) at local scale, determining SOC concentrations and patterns.

The study was conducted in the Negev Desert (Israel), which is representative of an arid ecosystem (Olsvig-Whittaker et al. 1983, Yair 1994, Yair & Danin 1980). This area was ideal because of the well-studied lithology, hydrology and vegetation by Yair and colleagues (Boeken & Shachak 1994, Olsvig-Whittaker et al. 1983, Schreiber et al. 1995, Yair & Raz-Yassif 2004, Yair & Shachak 1982). Detailed SOC inventories focusing on the influence of spatial heterogeneity of environmental factors are still missing and were therefore part of this PhD research project, preceding the GIS and remote sensing.

Thus the following research questions stimulated the present PhD-thesis:

1. How much are surface properties, water availability and vegetation coverage related to SOC concentrations and stocks?
2. At which level of detail and accuracy can SOC inventories be made using field measurements, remote sensing and digital image processing?
3. How does the image analysis approach contribute to reducing the uncertainty of SOC inventories in heterogeneous arid environments?

Guided by these questions, this thesis aims at the development of a GIS-based image analysis approach for the quantification of SOC stocks and patterns on a regional scale considering SOC spatial heterogeneity at a local scale in arid environments.

The main objectives of this thesis are (i) to determine the relationship between soil, vegetation and SOC stocks (Chapter 3, Research Paper; Chapter 4, Research Paper), (ii) to identify relevant vegetation indices for the determination of EHEs by remote sensing (Chapter 5, Research Paper) and (iii) to quantify SOC stocks based on (i) and (ii).

The outcome is a methodological procedure combining field sampling and mapping based on remote sensing relating to land cover and Geographic Information System (GIS) analysis. This approach is intended to provide reliable estimates of SOC stocks at regional scale in arid environments.

The PhD thesis is structured as follows: Chapter 2 provides an overview of the current state of knowledge regarding dynamics of dryland ecosystems, SOC variability and SOC assessment. Chapters 3-6 were written as stand-alone manuscripts for publication in peer-reviewed journals. The major aim of chapter 3 was to quantify the relationship between surface characteristics and vegetation coverage and spatial patterns of SOC concentrations and SOC stocks. To identify controlling factors of SOC stocks on rocky desert slopes, soil properties, vegetation coverage and SOC concentrations and stocks were compared between different EHEs. In chapter 4, a method is developed for examining the interactions between rainfall and surface characteristics of rocky desert slopes. Based on this experimental procedure, the relationship between soil and vegetation for the different EHEs were characterized in detail, where each EHE reflects dominant processes and surface properties and specific hydro-geomorphological responses in reaction to rainfall. The spatial heterogeneity of SOC concentrations is determined by the relationship between vegetation density and soil volume. Chapter 5 presents an approach towards automated mapping of EHEs in arid areas on the basis of vegetation patterns. The dependence of different vegetation pattern indices on the spatial resolution of high and low resolution image data was investigated and indices identified that are sensitive to the resolution difference. This approach allows the identification of EHEs at different scales and is transferable to other arid areas. The major aim of chapter 6 was the estimation of SOC stocks and patterns at regional scale considering spatial heterogeneity of environmental properties at local scale. Therefore a GIS-based image analysis approach was developed using vegetation coverage and EHEs as proxy indicators for SOC concentrations. Finally, chapter 7 synthesizes and concludes the findings of the four studies and provides a conceptual model of the effects of surface properties, water availability and vegetation coverage on SOC concentrations. The chapter concludes with an evaluation of the relevance of the implemented image analysis approach for the reliable estimation of SOC stocks and patterns in arid environments.

2. Carbon stocks and their assessment in drylands

2.1 Soil organic carbon and the global carbon cycle

The global soil system is the largest terrestrial reservoir of organic carbon which stores about 1500 GT in the top one meter of the Earth's surface (Amundson 2001, Kutsch et al. 2009). Thereof 55% is represented by soil organic carbon (SOC), which is twice as large as the atmospheric carbon pool (Schlesinger et al. 2000, Stutter et al. 2009). Soils represent one of the most dynamic components of the global carbon cycle due to the fact that SOC has a short residence time and due to its reactive, labile character (Batjes 1996, Doetterl et al. 2012a, b, Houghton 2007, Quinton et al. 2010, Wigley & Schimel 2005). This implies that SOC is sensitive to environmental changes. At the moment small changes in SOC-content could potentially significantly increase, or mitigate current atmospheric CO_2 increase. Within the UN Framework convention on climate change (IPCC 2007), nations are admonished and advised to budget and decrease CO_2 emissions. This has increased public and scientific interest regarding the impact of soils on the global carbon cycle and on carbon pools which sequester and release CO_2. In the context of climate change mitigation an increased understanding of spatial patterns and dynamics of SOC stocks and their contribution to regional, national and global cycles is required (IPCC 2007).

Studies on SOC stock assessment (Homann et al. 1995, Kutsch et al. 2009, Mishra 2009, Mishra et al. 2009) demonstrate the need to calculate SOC stocks at regional levels based on local environmental data due to differences in soil-forming factors such as time, parent material, topography, climate, vegetation and organisms and site management/land use. Particularly in arid environments the spatial variability of soil forming factors affects the formation and degradation of organic carbon in soils (Lieb et al. 2011). Although arid environments and especially their soils are considered to be highly sensitive to climate change and changing environmental conditions (IPCC 2007), spatial patterns and dynamics of SOC regarding the contribution to global SOC storage and the response to global change has been insufficiently investigated (Kutsch et al. 2009, Mishra 2009, Mishra et al. 2009). The net effect of soils regarding SOC sequestration and release is still unclear (Budge et al. 2011, Kirschbaum 2000). There is a lack of detailed understanding due to the major challenges and uncertainties associated with the assessment of SOC stocks in drylands (Rotenberg & Yakir 2010, Schimel 2010). Uncertainties are mainly linked to the high spatial variability of soil forming factors and soil properties (Laity 2008, Parsons & Abrahams 2009, Schimel 2010), analytical errors during the measurement of soil properties and uncertainties that arise from the spatial interpolation of local point data with different spatial interpolation techniques (Aufdenkampe et al. 2011, Lettens et al. 2005, Liebens & Van Molle 2003). As demanded by the Kyoto protocol, these uncertainties need to be established and accurate regional predictions of SOC stocks are required.

2.2 SOC stocks and controlling environmental properties in drylands

Drylands are characterized by ephemeral, seasonal or permanent water deficits (Laity 2008). The rainfall regime is determined by a high variability of low precipitation amounts and a discrete number of infrequent rainfall events. The mean temperature in summer is high which can cause drought stress for vegetation. Drylands are complex ecosystems whose characteristics and dynamic properties depend on the relationship between climate, soil, vegetation and water redistribution (Fig.1) (Rodriguez-Iturbe & Porporato 2004). Climate and soil control vegetation dynamics (D'Odorico & Porporato 2006, Jones 1992, Kramer & Boyer 1995, Larcher 1995). In turn vegetation exerts a strong control on the entire water balance and is responsible for many feedbacks to the atmosphere (Kutzbach et al. 1996, Rodriguez-Iturbe & Porporato 2004, Zeng et al. 1999).

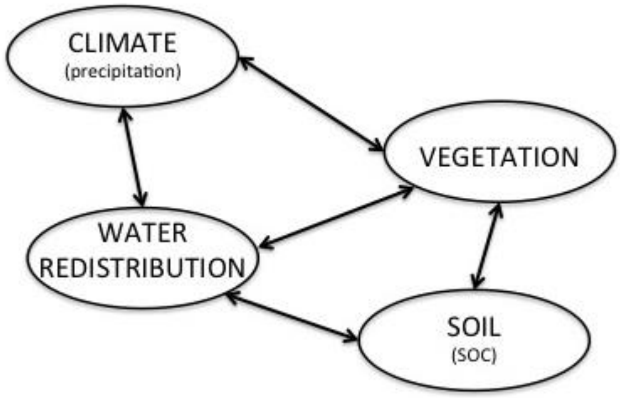

Fig. 1: Schematic representation of the climate – soil – vegetation system (SOC: Soil Organic Carbon) (modified after Rodriguez-Iturbe & Porporato 2004).

About 50% of global drylands are dominated by rocky surfaces where patches of bedrock and shallow soils or pavements prevail, resulting in a high spatial heterogeneity of environmental conditions (Buis & Veldkamp 2008). Several studies have demonstrated that the spatial heterogeneity of surface characteristics has important implications for biological, chemical, hydrological and geomorphological processes (Boeken & Shachak 1994, Li et al. 2010, Yair & Danin 1980, Yair & Raz-Yassif 2004, Zhou et al. 2011).

2.2.1 Soil

Soil formation in arid environments is limited by water availability and by soil and wind erosion processes (Ravi et al. 2010), resulting in poorly developed soils and a significant variability in soil depth (Laity 2008, Parsons & Abrahams 2009, Yair 1990). The spatial heterogeneity of soil formation is furthermore determined by environmental properties such as soil coverage, soil surface permeability, pore volume and rock surface structure (Laity 2008, Parsons & Abrahams 2009). The majority of dryland soils contain small amounts of SOC (0.5-1%) (Lal 2002a, b) and can be considered as far from SOC saturation, suggesting a high potential of SOC uptake (Farage et al. 2003, Lal 2003). The SOC pool tends to decrease exponentially with temperature (Lal 2002a, b). Degradation and desertification of dryland soil also lead to reductions in the SOC pool (Dregne 2002). In general the SOC pool increases with the addition of biomass to soils (Lal 2001). In contrast to soils from humid regions, dryland soils are less likely to lose SOC due to the fact that the limited water availability reduces SOC mineralization (Glenn et al 1993). According to the studies by Farage et al. (2003) and Lal (2001, 2009) the residence time of SOC in desert soils can be much longer than in humid regions. Farage et al. (2003) and Lal (2001, 2009) state that the ratio of the soil to the living biomass SOC pool might be greater in drylands than in tropical forests. However, there is little knowledge regarding the interrelations that take place between soil properties, vegetation and SOC stocks and patterns. This is enforced by insufficient data availability on dryland soils. Literature is still dominated by studies in humid environments and the dynamics of dryland soils regarding SOC sink and source capacity are still not well known (IPCC 2007, Quinton et al. 2010, Seip 2001).

2.2.2 Climate and water redistribution

Dryland ecosystems are characterized by distinctive high physical and low chemical weathering rates determined by significant daily temperature changes and water deficit (FAO 2004, Farage et al. 2003, Lal 2003, Yair 1990). The hot arid climate favours low decomposition rates (due to water deficit) and hence limits vegetation-driven carbon sequestration as well as CO_2 efflux (Fang & Moncrieff 2001, Farage et al. 2003, Qi et al. 2002). Budge et al. (2011) states that the ecosystem response due to rising temperatures remains uncertain, resulting in a significant uncertainty of SOC estimations. As a result of these uncertainties accurate predictions of SOC stocks and their response to changing climate are required as demanded by the Kyoto Protocol. Due to continuous runoff under humid conditions, SOC stocks are generally related to surface morphology, which controls erosion and deposition processes and thus SOC fluxes and sequestration (Egli et al. 2009, Griffiths et al. 2009, Rosenbloom et al. 2006, Tan et al. 2004, Yoo et al. 2006). Topographic parameters (e.g. slope, curvature, relief position) have been shown to correlate with SOC stocks under humid conditions (Berhe et al. 2008, Glatzel & Sommer 2005, Tsui et al. 2004, Yoo et al. 2006). In contrast, arid environments are characterized by a lack of connectivity in runoff due to the spatial heterogeneity of environmental properties and low and erratic precipitation (Laity 2008, Parsons & Abrahams 2009, Yair 1990). However runoff and runoff redistribution exert a strong control on soil formation and soil erosion and deposition and thus on water availability. Topography also plays an important role in water availability. In comparison to flat terrain and hilltops, the hillslopes show lower evaporation rates and hence higher water availability (Kidron & Zohar 2010). The spatial heterogeneity of environmental properties controls water availability and thus vegetation coverage. In turn, vegetation coverage potentially determines SOC concentration and patterns. As a consequence there is a need to understand the ecohydrology of arid environments and its relevance for dryland SOC stocks.

2.2.3 Vegetation

Vegetation needs to be considered as a major factor controlling SOC stocks in arid environments (Zhou et al. 2011). Studies by Jobbágy & Jackson (2000) and Li et al. (2010) show that there is a strong link between aboveground vegetation and SOC. The patchy nature of vegetation distribution is caused by strong variations of soil moisture and therefore exerts a strong control on carbon stocks (Olsvig-Whittaker et al. 1983, Schlesinger et al. 1996). SOC is mostly concentrated beneath shrubs (Burke et al. 1999, Schlesinger 1990, Schlesinger 1995) where in general the organic matter content is higher and the physical soil properties are improved. Drylands are characterized by a low net primary production (NPP) and low decomposition rates, which is in contrast to high NPP and increased organic matter mineralization in humid environments (Lal 2009, Schlesinger 1991). In the context of global warming both CO_2 assimilation by vegetation (net primary production) and CO_2 release by ecosystem respiration will increase, although the relative sensitivity of decomposition and NPP determines the net effect in a warming atmosphere. The direction of the net effect is a controversial subject. Kirschbaum (2000) assumed a decrease of SOC due to the fact that decomposition rates are more affected than primary production. Recent results in Israel show (Rotenberg & Yakir 2010) that the uptake rate of carbon in dryland forests is approximately the same as in more humid regions of continental Europe. This implies that a significant amount of CO_2 (1 Pg out of 3.2 Pg generating the annual increase in atmospheric CO_2 concentration) might be sequestered by reforestation of arid environments (Rotenberg & Yakir 2010).

To conclude, the spatial heterogeneity of surface properties is the main controlling factor of spatial soil moisture distribution. In turn, soil moisture availability determines the spatial heterogeneity of vegetation densities and distribution (Bergkamp et al. 1999, Lavee et al. 1991, Lavee et al. 1998, Olsvig-Whittaket et al. 1983) and therefore the spatial heterogeneity of SOC concentrations and stocks in arid environments.

2.3 Problems with SOC inventory

In recent years the assessment of the spatial characteristics of SOC in the world has gained increasing interest (Burnham et al. 2010, Doetterl et al. 2012a, b, Haynes et al. 2003, Lal 2009, Ping et al. 2008). Several studies show that environmental conditions (Liu et al. 2006, Su et al. 2006, Tan & Lal 2005, Wang et al. 2002) determine the spatial distribution of SOC patterns within an ecosystem (Lal et al. 2011, Yao et al. 2010, Yoo et al. 2006). For the understanding of the role of SOC in the global carbon cycle, detailed knowledge on fluxes, amounts and spatial patterns of SOC is required (Berhe et al. 2008, Doetterl et al. 2012a,b, Mishra et al. 2007). Quinton et al. (2010) and Zhao et al. (2005) therefore state that an accurate quantification of SOC storage and its spatial patterns is of fundamental importance to global climate change modelling. Compared to more humid environments there is only little knowledge about SOC storage in drylands (Lal 2009, Yao et al. 2010) albeit arid environments constitute a significant pool of SOC and are regarded as extremely vulnerable to climate change (Quinton et al. 2010, Seip 2001, Zhao et al. 2005). Particularly in rocky desert environments, soils and vegetation cover are highly discontinuous and soil depth varies significantly (Yair 1999, Yair & Kossovsky 2002). These heterogeneous surface characteristics greatly control surface runoff, the storage potential of fine sediments and the availability of soil moisture (Schreiber et al. 1995, Yair & Raz Yassif 2004) and hence SOC concentrations and spatial patterns of SOC (Jobbàgy & Jackson 2000, Li et al. 2010).

The relationship between soil properties, environmental variables and SOC concentrations are generally derived from local measurements at plot scale. Based on the plot data a precise quantification of SOC stocks considering the required spatial heterogeneity of environmental properties and processes at a local scale is provided (Cerdan et al. 2010, Doetterl et al. 2012b, Wang et al. 2010). Data are extrapolated for the estimation of SOC stocks at coarser scales. The assumption for the extrapolation of plot data to coarser scales is that the local scale conditions are representative for coarser scales (Liu et al. 2006, Meersmann et al. 2008, Mondini 2012). But the extrapolation of local data at a regional scale does not reflect the existing local scale heterogeneous environmental settings at unvisited locations. This leads to large uncertainties in the assessment of SOC stocks (Aufdenkampe et al. 2011, Doetterl et al. 2012a, b, Trumbore 2009). As an alternative for the quantification of SOC stocks at regional scale, datasets (e.g. geological maps, soil maps, digital elevation models) with a typical resolution of 10-50m are utilized (Lal 2005, Leifeld et al. 2005, Stutter et al. 2009). But these datasets do not provide sufficient information regarding the spatial heterogeneity of environmental properties and processes at local scale such as provided by plot or transect datasets (Aufdenkampe et al. 2011, Meersmann et al. 2008). The estimated SOC stocks therefore reflect significant uncertainties associated with data availability at the scale where processes determining SOC concentrations and patterns occur. This is especially true for arid environments where processes and process rates are not investigated in detail (Yair & Kossovsky 2002, Yair & Raz-Yassif 2004). As a consequence, predictions of the response of SOC to global warming are difficult due to the insufficient understanding of the relationship between ecohydrology, vegetation density and SOC related to distinctive environmental properties and their dependency on different scales (Rosenbloom et al. 2006, Wang et al. 2011, Yoo et al. 2006).

For the accurate quantification of SOC stocks and its spatial patterns in drylands it is crucial to (i) identify and understand the relationship between ecohydrological conditions, vegetation density and SOC and (ii) to develop methods for the precise estimation of SOC stocks and patterns at regional scale considering SOC spatial heterogeneity at local scale.

2.4 Remote sensing

Relevant information on different spatial scales is essential to enhance the understanding of the relationship between ecohydrological processes, vegetation coverage and carbon sequestration (Asbjornsen et al. 2011, Doetterl et al. 2012a, b). The first studies on SOC dealt with the estimation of SOC stocks at global scale (Bohn 1982, Bolin 1970, Parton et al. 1987), but these studies emphasize that the great spatial variability of SOC concentrations regarding the different mapping units are the main source of uncertainty (Liebens & Van Molle 2003, Mondini 2012, Wang et al. 2009). In subsequent studies at regional and local scales different data sources, spatial analysis techniques and GIS applications were used (Frogbrook & Oliver 2001, Zhang & McGrath 2004). For the last three decades earth observation systems have been contributing to the assessment and monitoring of dryland ecosystems, environmental properties, vegetation coverage and SOC (Frank & Tweddale 2006, Hein et al. 2011, Mulder et al. 2011, Xiao & Moody 2005). In soils, organic matter content and composition of organic constituents have a strong influence on soil reflectance. Typically soil reflectance decreases with increasing SOC in the wavelength range of 0.4-2.5 µm (Baumgardner et al. 1985, Jarmer et al. 2010). In general, different modelling techniques are used to predict SOC from continuous reflectance spectra (Ben-Dor & Banin 1994, 1995, Reeves et al. 2002, Brown et al. 2006). However the transfer of prediction models to airborne or satellite remote sensing data has only rarely been conducted (Hill & Schuett 2000, Gomez et al. 2008, Jarmer et al. 2010) due to the limited number of satellite bands which necessitates the use of these few spectral bands or parameters derived from them to assess SOC (Jarmer et al. 2010). Several other studies show that the wavelength range that best explains SOC is in the visible spectral domain (Hummel et al. 2001, Brown et al. 2006, Viscarra Rossel et al. 2006). Konen et al. (2003) found significant relationships between SOC and Munsell colour (value / chroma). Wills et al. (2007) showed in his study that horizon matrix colour is a useful parameter to estimate SOC for agricultural and prairie land-use. Jarmer et al. (2010) developed an approach to map SOC in semi-arid and arid ecosystems using soil colour values and Landsat imagery. But there are still some restrictions regarding these approaches. The analysis is limited to (1) soils devoid of any vegetation, due to the fact that vegetation conceals most fertile landscape patches (Schwanghart & Jarmer 2011), (2) the analysis of SOC in the uppermost ~2cm of topsoil and whereas variations of SOC concentrations with depth are not discernible (Stallard 1998) and (3) the spatial resolution of the sensor (Hill & Schuett 2000). Based on the significant spectral properties of vegetation, it can be easily excluded from image analysis (Adams et al. 1989, Roberts et al. 1993). In comparison to the bare interspace, vegetated areas in arid and semi-arid environments are characterized by increased input of carbon and nutrients, higher moisture availability due to higher infiltration rates and reduction of evapotranspiration by the plant canopy layer and protection from water and wind erosion. These “islands of fertility” are hotspots of biotic activity and biogeochemical cycling (Schlesinger et al. 1996, Schlesinger & Pilmanis 1998, Austin et al. 2004, Cánton et al. 2004) and remain hidden from airborne monitoring (Schwanghart & Jarmer 2011). Remote sensing techniques are also used to stratify the area of investigation by its environmental settings (Liu et al. 2006, Wang et al. 2009). In this regard, a bottom up approach is usually implemented to integrate the spatial variability of SOC concentrations. Generally for each class the mean SOC mass is calculated from point SOC measurements (Meersmans et al. 2008). To quantify spatial distribution patterns of SOC, geostatistics and spatial interpolation are used (Liu et al. 2006, Mondini 2012, Wang et al. 2009, Webster & Oliver 2001). Meersmann et al. (2008) developed a multiple regression model to predict a reliable SOC amount based on different land use to soil type combination classes. Furthermore, SOC models are a practical solution for the estimation of SOC stocks due to many different combinations of soil type, environment, land use and climate change scenarios (Kaplan et al. 2010, 2012, Mondini et al. 2012, Sitch et al. 2003). However, studies by Kern (1994), Lettens et al. (2004, 2005) and Ni (2001) indicate that the range of the SOC stock estimation is strongly determined by type and quality of ecosystem data. Both the extrapolation of point measurement data and the determination of classes by environmental settings lead to insufficient consideration of the interrelations between environmental factors and surface processes determining spatial variability of SOC. Combining remote sensing techniques and the dependent relationships of environmental parameters at a local scale seems to provide a methodological approach which compiles the requirements of a precise SOC stock estimation at a regional scale. The extracted information based on remote sensing data analysis serves first to assess the extent and the condition of ecosystems and second to monitor changes of ecosystem conditions and services at different spatial, temporal and spectral resolutions (Foley et al. 2005, Turner et al. 2007). Such information allows for a thorough analysis of ecosystem functionality and is essential to estimate regional SOC stocks concerning local scale heterogeneity. A proxy variable is therefore needed which is detectable by remote sensing techniques and provides information about spatial SOC distribution patterns as well as environmental properties. Vegetation coverage and distribution seem to meet these requirements. The spatial distribution of vegetation patterns provides some key factors for the assessment of SOC stocks and patterns in drylands. First, the mosaic of vegetation coverage and bare areas is related to environmental settings regarding the different EHEs (Lesschen et al. 2008, 2009, Puigdefabregas 2005, Yair & Danin 1980, Yair & Raz-Yassif 2004), second, vegetation coverage seems to be an indicator for the spatial distribution of SOC patterns (Jobbágy & Jackson 2000, Li et al. 2010, Zhou et al. 2011), third, vegetation is detectable by remote sensing techniques due to the strong contrast to bare areas (Qin et al. 2006) and fourth, vegetation is sensitive to changing climate conditions (Laity 2008, Zhou et al 2011).

Remote Sensing techniques were frequently used for the assessment and monitoring of vegetation coverage in arid ecosystems (Barati et al. 2011, Hein et al. 2011, Mulder et al. 2011, Xiao & Moody 2005). Andrew & Ustin (2008) applied aggregated classification and regression tree models (CART) for the spectral analysis of vegetation (*Lepidium*) using 128-band HyMap image data. Lesschen (2008) used QuickBird imagery for the determination of different vegetation indices on fractional vegetation coverage. Qi et al. (2002) developed a modelling approach for the estimation of Leaf Area Index in semiarid regions using measurements, which are available from many sensors (AVHRR, VEGETATION, MODIS). Calvao & Palmeirim (2004) showed in their study that the adaption of dryland vegetation to high temperatures and lower water availability (e.g. strong wax absorptions, reduced leaf absorption) lead to a limited detectability by hyperspectral remote sensing techniques and hence an underestimation of vegetation coverage. The determination of vegetation based on the differences in reflectance between ground and vegetation seems to be more appropriate for the determination of vegetation coverage (Sandholt et al. 2002). Since vegetation absorbs most incoming light at visible wavelength, pixels with low DN-values (Pixel Digital Number) are indicative for vegetation in the photograph (Qin et al. 2006). The determination of vegetation coverage based on these differences in reflectance seems to be applicable for the study area in the Negev Desert due to the strong contrast of dark vegetation to the relatively bright background of the carbonate-rich bare ground.

2.5 Study area and environmental settings

The Sede Boqer (30°52’N, 34°48’E) experimental catchment is located in the Northern Highlands of the Negev Desert, Israel (Olsvig-Whittaker et al. 1983, Schreiber et al. 1995, Yair & Kossovsky 2002) and represents a rocky desert environment (Buis & Veldkamp 2008, Yair & Raz-Yassif 2004).

2.5.1 Climate

The climate in the Northern Negev is arid with a mean annual air temperature of 20°C (Dan et al. 1972). Mean monthly temperatures range from 9°C in January to 25°C in August. The average annual rainfall observed during a 30-year period (Yair, 1994) is 91 mm, with a range from 34 to 167 mm (Kuhn & Yair 2003, Kuhn et al. 2004). The analysis of 784 rainfall events at Sede Boqer (1976-2008) shows that rainfall events up to 10mm represent 91% of the recorded events. Rainfall is concentrated during the winter season between October and April. The potential annual evaporation is high and varies between 2000 and 2600 mm (Evenari et al. 1980, Yair & Kossovsky 2002).

2.5.2 Lithology

The Upper Cretaceous bedrock consists of limestone and dolomite. The local stratigraphy is composed of three lithological formations that are the Netser, Shivta and Drorim formations (Chapter 3, Research Paper, 2, Fig. 2). These three formations are bedded almost horizontally and differ greatly in structural properties, thus creating different surface environments (Yair 1994, Yair & Danin 1980). The Upper Netser formation is characterized by thinly bedded, densely jointed chalky limestone with flint concretions. The surface mainly consists of a rocky substratum (Yair & Danin 1980). The lower part of the Netser formation and the upper part of the Shivta formation could be considered as one structural unit, which is thinly bedded and densely fissured (Olsvig-Whittaker et al. 1983). The lower Shivta formation is a massive unit with a low density of deep cracks. Rock weathers into cobbles and boulders that cover most of the surface, which is almost devoid of any soil (Yair & Shachak 1982). The Drorim formation is densely jointed and covered by an extensive colluvial soil (Dan et al. 1972).

2.5.3 Soil

Soils are very shallow and form patches on the rocky surface (Yair & Danin 1980). Most of the mineral substrate is not derived from the local limestone bedrock, but largely composed of loessial sediments, which were deposited from the early Quaternary Period (Bruins 1986, Reifenberg 1947, Yaalon & Dan 1974). Based on the World Reference Base for Soil Resources (IUSS Working Group WRB 2006), soils are dominantly classified as desert brown Lithosols (Arkin & Braun 1965, Dan et al. 1972). The study site is predominantly characterized by two soil bedding types (Chapter 4, Research Paper, 3, Fig.4): soil is either concentrated in rock fissures (“flower pots”) of the surficial rock strata, or at the base of bedrock steps, soil is accumulated in non-contiguous micro-colluvial deposits (“soil patches”) (Yair & Shachak 1982).

2.5.4 Vegetation

Despite the meteorological aridity, plant communities represent a transition between the Irano-Turanian plant geographical region and the Saharo-Arabian region with some Mediterranean components (Yair & Danin 1980, Yair & Shachak 1982, Zohary 1962). Mediterranean species can be found in most mesic sites where soil patches absorb runoff, generated on rocky surfaces (Olsvig-Whittaker et al. 1983). A transition from semi-desert communities (10-30% perennials vegetation cover) on rocky upper slopes, to patches of true desert communities (less than 10% perennial cover) on the lower colluviums reflects a very narrow ecotone usually found at larger spatial scales.

2.5.5 Ecohydrology

The underlying bedrock consists mainly of limestone rock. The three lithological formations create, due to their structural properties, different environments in terms of their properties (Yair & Danin 1980). According to the studies by Olsvig-Whittaker et al. (1983), Schreiber et al. (1995) and Yair & Raz-Yassif (2004), the following EHEs can be distinguished within the study site (Chapter 4, Research Paper, 3, Table 1): (1) flat desert pavement (FDP), (2) gently sloped desert pavement (SDP), (3) non-fissured bedrock slope (BS), (4) stepped and fissured bedrock slope (FBS) and (5) slope and valley colluvium (SVC). These meso-scale physical environments are linked in regards to hydrology, lithology and water redistribution (Olsvig-Whittaker et al. 1983, Schreiber et al. 1995, Yair & Danin 1980). Despite the low magnitude of rainfall events in the Negev Desert, these events generate runoff and represent an important source of available water for vegetation (Yair 1994, Yair 1999, Yair & Lavee 1985, Yair & Raz-Yassif 2004). Runoff is predominantly generated on non-vegetated patches with low infiltration capacity, leading to run-on infiltration on vegetated patches with higher infiltration capacity. The spatial patterns of infiltration-excess overland flow are controlled by soil and surface properties, soil moisture and precipitation intensity. These patterns are a major control on ecohydrological processes. The microclimatic conditions, litter fall and higher activity of burrowing animals in vegetation patches promote positive feedback between vegetation, surface properties and infiltration (Grayson et al. 1997, Ludwig et al. 2005). Soil moisture variability in the study area is related to the stratigraphic sections and causes a spatial heterogeneity in plant communities (Evenari et al. 1971, Olsvig-Whittaker et al. 1983, Schreiber et al. 1995, Yair & Danin 1980). These meso-scale physical environments influence hydrology, runoff and infiltration, vegetation density and distribution in various ways and therefore potentially the spatial distribution of SOC concentration and SOC stocks (Chapter 4, Research Paper, Figure 3, 4, Table 1).

In general the study site is characterized by a high spatial variability of environmental settings (Schreiber et al. 1995, Yair 1994, Yair & Raz Yassif 2004), which presents a major challenge for the estimation of SOC stocks in arid areas. Lithology, hydrology and vegetation were well studied for the experimental watershed in the Negev Desert by Yair and colleagues (Boeken & Shachak 1994, Olsvig-Whittaker et al. 1983, Schreiber et al. 1995, Yair & Raz-Yassif 2004, Yair & Shachak 1982), although the interrelations between ecohydrology, vegetation distribution and SOC were not studied in detail. But for the precise quantification of SOC stocks at regional scale it is essential to understand the relationship between hydrology, soil, vegetation and SOC stocks at local scale. The Negev Highlands were chosen as an ideal study site because they represent a characteristic desert rocky environment (Olsvig-Whittaker et al. 1983, Yair 1994, Yair & Danin 1980). Due to the fact that 50% of global drylands are dominated by rocky surfaces where patches of bedrock and shallow soils or pavements prevail (Buis & Veldkamp 2008) these environments play a significant role in the global carbon cycle. Methods for a precise estimation of SOC stocks and spatial patterns are still missing. Hence there is a strong need to quantify the SOC source and sink capacity in these environments regarding the prognosticated changing climate conditions (Aufdenkampe et al. 2011, Smith et al. 2003, Trumbore 2009).

Based on the previous findings regarding lithology, hydrology and vegetation and the significant role of rocky desert environments in the global carbon cycle, the study site was ideally suited to answer the remaining global questions regarding the precise quantification of SOC stocks and patterns in such an environment: (i) How are environmental properties, vegetation density and SOC concentrations related? (ii) How are ecohydrological settings vegetation density and SOC concentrations related to different EHEs? (iii) Is it possible to map automatically EHEs using vegetation indices? (iv) How to use proxy indicators for SOC concentrations and patterns for the precise quantification of SOC inventories?

2.6 Methods

According to the aim of study to quantify SOC stocks and patterns at regional scale considering SOC spatial heterogeneity at local scale, methods have to be developed and adapted to the environmental settings of the study area.

First, for the study area the relationships between environmental properties, vegetation coverage, SOC concentrations and SOC stocks were identified at local scale. Therefore several slope sections with different ecohydrological characteristics (e.g. aspect, vegetation coverage, soil depth) were sampled and SOC stocks were calculated. To identify controlling factors of SOC stocks, soil properties, vegetation coverage and SOC concentrations were statistically compared between the different EHEs (Chapter 3, Research Paper, 3; Chapter 4, Research Paper, 4).In addition, rock-soil interactions and the relevance of soil volume for storing plant available water were studied. Rainfall simulation experiments were therefore conducted to determine the amount of rainfall required to fill the available soil water storage capacity and hence the water supply for vegetation coverage determining SOC concentrations and stocks. The design of the rainfall simulator and the selection of the plots were aimed specifically at observing infiltration into small soil patches on a micro-scale relevant for the prevalent vegetation cover (Chapter 4, Research Paper, 4). The rainfall experiments were also conducted to determine the relationship between ecohydrological settings, vegetation density and SOC concentrations and stocks related to the different EHEs. The distinctive EHEs reflect the spatial variability of environmental and ecohydrological conditions within the study site. Vegetation density and patterns, soil properties and SOC concentrations and stocks are related to the distinctive EHEs. In each EHE, micro-scale water supply and soil volume determine vegetation density and spatial distribution and hence SOC concentrations and stocks. Therefore we hypothesize that these relationships could be utilized to support mapping of EHEs using GIS-based aerial image analysis in arid environments. Due to the fact that vegetation coverage is easily detectable at different scales by remote sensing techniques and the relationship between vegetation densities and patterns and the distinctive EHEs, the aim of the third study was to develop an approach towards automated mapping of EHEs supported by vegetation detection. A ground based hyperspectral camera was used to record a north facing and a south facing transect with a spatial resolution of 0.05m. Vegetation coverage was subsequently determined by an unsupervised classification. An aerial image with a spatial resolution of 0.5m was utilized to map vegetation coverage at coarser spatial extent (regional scale). Vegetation coverage was determined by digital image processing. Spatial vegetation pattern indices (vegetation density, lacunarity, bare area fragmentation index, patch upslope side length/area ratio) were calculated for both datasets. The vegetation indices were subsequently investigated regarding their dependence on the spatial resolution of the two different remote sensing datasets. Indices with a high degree of explanatory power and scale independence were then used as variables in a decision tree model for automated mapping of EHEs (Chapter 5, Research Paper, 3). Finally, SOC stock and patterns were calculated at regional scale. To cope with the aim of study to consider local scale spatial heterogeneity of SOC concentrations and patterns for the calculation of SOC stocks at a regional scale, vegetation densities and the distinctive EHEs were implemented as proxy indicators for SOC concentrations and spatial distribution. The applied relationships and methods were derived from the investigations of the previous studies of this thesis using field sampling, remote sensing and digital image processing (Chapter 6, Research Paper, 3). The combination of remote sensing techniques and the understanding of ecohydrological conditions and processes in one method is suggested to precisely quantify SOC stocks and patterns at a regional scale considering SOC spatial heterogeneity at a local scale in arid environments. The potential of the implemented method for the quantification of SOC inventories as well as the contribution to reducing the uncertainties of SOC inventories in heterogeneous arid environments is discussed in the last chapter (Chapter 7) of this thesis.

3. Soil organic carbon in the rocky desert of northern Negev (Israel)

This chapter has been published in the Journal of Soils and Sediments as: Hoffmann U., Yair A., Hikel H., Kuhn N.J. (2012): Soil organic carbon in the rocky desert of northern Negev (Israel). Journal of Soils and Sediments (12), 811-825.

J Soils Sediments (2012) 12:811–825
DOI 10.1007/s11368-012-0499-8

SOILS, SEC 1 • SOIL ORGANIC MATTER DYNAMICS AND NUTRIENT CYCLING • RESEARCH ARTICLE

Soil organic carbon in the rocky desert of northern Negev (Israel)

Ulrike Hoffmann · Aaron Yair · Harald Hikel · Nikolaus J. Kuhn

Received: 24 July 2011 / Accepted: 2 March 2012 / Published online: 5 April 2012

Abstract

Purpose So far, the soil organic carbon (SOC) literature is dominated by studies in the humid environments with huge stocks of vulnerable carbon. Limited attention has been given to dryland ecosystems despite being often considered to be highly sensitive to environmental change. Thus, there is insufficient research about the spatial patterns of SOC stocks and the interaction between soil depth, ecohydrology, geomorphic processes, and SOC stocks. This study aimed at identifying the relationship between surface characteristics, vegetation coverage, SOC, and SOC stocks in the arid northern Negev in Israel.

Materials and methods The study site Sede Boker is ideally suited because of well-researched but variable ecohydrology. For this purpose, we sampled five slope sections with different ecohydrologic characteristics (e.g., soil and vegetation) and calculate SOC stocks. To identify controlling factors of SOC stocks on rocky desert slopes, we compared soil properties, vegetation coverage, SOC concentration, and stocks between the five ecohydrologic units.

Results and discussion The results show that in Sede Boker, rocky desert slopes represent a significant SOC pool with a mean SOC stock of 0.58 kg C m^{-2} averaged over the entire study area. The spatial variability of the soil coverage represents a strong control on SOC stocks, which varies between zero in uncovered areas and 1.54 kg C m^{-2} on average in the soil-covered areas. Aspect-driven changes of solar radiation and thus of water availability are the dominant control of vegetation coverage and SOC stock in the study area.

Conclusions The data indicate that dryland soils contain a significant amount of SOC. The SOC varies between the ecohydrologic units, which reflect (1) aspect-driven differences, (2) microscale topography, (3) soil formation, and (4) vegetation coverage, which are of greatest importance for estimating SOC stocks in drylands.

Keywords Drylands · Ecohydrology · Rocky deserts · SOC stock · Soil organic carbon · Topography

Responsible editor: Zucong Cai

U. Hoffmann (✉) · H. Hikel · N. J. Kuhn
Department of Environmental Science,
Physical Geography and Environmental Change,
University of Basel,
Klingelbergstrasse 27,
4056 Basel, Switzerland
e-mail: ulrike.hoffmann@unibas.ch

A. Yair
Department of Geography, Hebrew University of Jerusalem,
Mount Scopus,
Jerusalem 91905, Israel

1 Introduction

1.1 Soil organic carbon and the global carbon cycle

The global soil system is the largest terrestrial reservoir of organic carbon, which stores approximately 2,400 Pg (Pg=10^{15} g) of soil organic carbon (SOC) in the top 2 m (Amundson 2001; Kirschbaum 2000). Soil and climate systems are closely coupled through the exchange of C between the atmosphere, biosphere, and pedosphere (Berhe et al. 2008). Therefore, there has been increasing international interest in the ability of soils to affect atmospheric concentrations of carbon dioxide (CO_2) (Houghton 2007; Mishra et al. 2009; Sarmiento and Gruber 2002; Schlesinger 1977, 1990; Wigley and Schimel 2005). The risk of global warming and the potential to use soils as a carbon sink in the context of the Kyoto Protocol have increased the attention of the scientific community to SOC stocks and fluxes in terrestrial ecosystems, especially in regions sensitive to climatic change (Branchu et al. 1993; IPCC 2007; Mishra et al. 2009; Smith and Heath 2002). However, the size and dynamics of the global SOC pool are still not well known (IPCC 2007; Quinton et al. 2010; Seip 2001). Precise measurements and estimates of the spatial distribution of SOC stocks are necessary to quantify the SOC sink or source capacity of soils in changing environments. The spatial variation of SOC is significantly influenced by environmental factors such as climate, topography, soil and bedrock materials, vegetation, disturbance, and surface processes due to human activity (Tan et al. 2004).

1.2 Carbon stocks in drylands

Even though drylands occupy 47.2 % of the earth's land surface, their importance in the global carbon cycle received limited attention (Asner et al. 2003; Schimel 2010). Global dryland soils contain 15.5 % of the world's total SOC to 1 m depth (IPCC 2007; Lal 2003; Lal et al. 2001; Schimel et al. 2000). This is about 40 times more than what was added during the 1990s into the atmosphere through anthropogenic activities, estimated at 6.3 Pg C year^{-1} (IPCC 2007; Lal 2003; Lal et al. 2001; Schimel et al. 1994, 2000). Dryland ecosystems are often regarded as "hot spots" of climate change, with large, rapid, and variable responses to even the smallest changes of climate conditions (Farage et al. 2003; Lal 2003; Yair 1990). Furthermore, dryland soils are prone to degradation and desertification due to human activities. Consequently, the majority of degraded dryland soils can be considered as far from SOC saturation, suggesting a high potential of SOC uptake (Farage et al. 2003; Lal 2003). Additionally, recent results (Rotenberg and Yakir 2010) show that dryland forests in Israel take up carbon at rates similar to forests in more humid continental Europe. Based on these results, they suggest that 1 Pg out of 3.2 Pg generating the annual increase in atmospheric concentration of CO_2 can be sequestered by reforestation of dryland soils. In contrast to soils from humid regions, dryland soil areas are less likely to lose SOC because the lack of water limits SOC mineralization and therefore the flux of SOC into the atmosphere. Consequently, the residence time of SOC in desert soils can be much longer than in soils of humid regions (Glenn et al. 1993), and the ratio of the soil to living biomass SOC pool might be greater in drylands than in tropical forests (Farage et al. 2003; Lal 2009; Lal et al. 2001).

1.3 SOC-stock calculation and links to soil-forming factors

SOC stocks (kg C m^{-2}) are generally calculated based on the mean soil organic carbon contents SOC_c (g 100 g^{-1}) of the fine soil fraction (<2 mm), the mean bulk density BD (in grams per cubic centimeter), the mean mass ratio of coarse soil fragments (>2 mm) CF_i (g 100 g^{-1}), and the soil thickness d_{soil} (centimeters):

$$SOC_{stock} = 0.1 \times d_{soil} \times BD \times SOC_c \times (1 - CF/100) \quad (1)$$

In humid environments, which are characterized by strong agricultural activity, human-controlled land cover generally exerts a strong variability on SOC concentration that in turn dominates the spatial variability of SOC stock (Goidts and van Wesemael 2007; Grieve 2001; Lal 2005; Leifeld et al. 2005; van Wesemael et al. 2010). In arid environments, however, the link between SOC stocks and soil-forming factors (such as climate, vegetation, and bedrock material) is much more complex than in humid agricultural landscapes. Significant diurnal temperature changes and the water deficit result in high physical and low chemical weathering rates (FAO 2004). The strong disintegration of rocks and the low chemical transformation therefore suggest a strong control of properties of the parent material (e.g., given by soil thickness, BD, and CF in Eq. (1)) on SOC stocks. Parent material in arid environments is often transported during severe soil erosion caused by extreme precipitation events (Yair 1990). Wash processes, however, are not continuous but disconnected, and sediment is generally transported only over short distances due to the disconnectivity of overland flows (Michaelides and Chappell 2009; Yair 1992). Thus soils, especially in arid environments, need to be "considered as mobile systems, which has major consequences for terrestrial biogeochemical cycles" (Quinton et al. 2010). Furthermore, arid environments lack a continuous vegetation coverage but are dominated by shrub vegetation that concentrates the biogeochemical activity in "islands of fertility" (Schlesinger and Pilmanis 1998; Schlesinger et al. 1996). Therefore, the shift from continuous grassland to patchy shrub vegetation with increasing aridity introduces a further element of complexity in the distribution of SOC stocks.

1.4 Estimation of dryland SOC stocks

Due to continuous runoff under humid conditions, SOC stocks are generally related to the surface morphology, which controls processes such as erosion and deposition and thus SOC fluxes and sequestration (Egli et al. 2009; Griffiths et al. 2009; Rosenbloom et al. 2006; Tan et al. 2004; Yoo et al. 2006). Topographic parameters, such as slope (Berhe et al. 2008; Tsui et al. 2004), curvature (Rosenbloom et al. 2006; Yoo et al. 2006), and relief position (Glatzel and Sommer 2005), have been shown to correlate with SOC stock under humid conditions. In contrast to humid environments with well-developed soils, arid environments with shallow soils are characterized by a lack of connectivity in runoff causing in turn an exceedingly high spatial variability of soil depth (Laity 2008; Parsons and Abrahams 2009; Yair 1990;

Yair and Danin 1980). Since runoff exerts a strong control over water availability, soil formation, and soil erosion and deposition, simple relationships of topographic parameters (such as slope, curvature, and wetness index) and soil properties and SOC stocks are not expected in arid environments.

Vegetation needs to be considered as a major factor controlling SOC stocks in arid environments (FAO 2004; Zhou et al. 2011). First, strong variations of soil moisture availability cause a patchy vegetation distribution, which in turn may exert a strong control on carbon stocks (Olsvig-Whittaker et al. 1983; Schlesinger et al. 1996). Second, in contrast to humid environments, which are characterized by high net primary production (NPP) and increased organic matter mineralization, dry environments have lower NPP, but also lower decomposition rates (Lal 2009; Schlesinger 1991). Third, while high temperatures favor high CO_2 efflux, low decomposition rates (due to water deficit) limit vegetation-driven carbon sequestration in hot arid climates (Fang and Moncrieff 2001; Farage et al. 2003; Qi et al. 2002) and thus may limit the impact of vegetation on SOC stocks. Thus, the link between soil moisture, vegetation coverage, and soil properties to SOC stocks and their relative importance for the spatial patterns of SOC stock in arid environments are much less clear than under humid conditions.

The spatial variability of relevant soil properties (Eq. (1)) presents a major challenge to the establishment of SOC stocks in arid and semi-arid environments. Despite the apparent significance of the dryland SOC pool, systematic studies on the spatial variability and the effects of environmental factors (such as soil moisture and vegetation coverage) in rocky desert soils are still missing. Thus, there is a strong need to estimate SOC stocks in arid soils and to evaluate their importance under a changing climate (Rotenberg and Yakir 2010; Schimel 2010). This need provides the major motivation of our study, which aims (1) to determine SOC stocks in a range of ecohydrologically different slope environments, (2) to identify soil properties relevant for the SOC stocks in each ecohydrologic setting, and (3) to assess the effects of NPP (represented by vegetation coverage) on SOC stocks.

The study was conducted in the northern highlands of the Negev desert in Israel near the town of Sede Boker, which is ideally suited because of well-researched ecohydrology. The influence of surface properties and patches of rock and soil on ecohydrology and vegetation has been intensely investigated in this area (e.g., Evenari et al. 1980; Olsvig-Whittaker et al. 1983; Yair 1990; Yair and Danin 1980). Based on this research, it was possible to determine SOC stocks in a range of ecohydrologically different slope environments and to identify soil properties relevant for SOC concentration and stock. The established link between vegetation coverage and water supply at Sede Boker also offers the opportunity to test the effects of ecohydrology on SOC, especially the balance between NPP (indicated by vegetation coverage) and SOC-stock development.

2 Study site

The Sede Boker research area is located in a second-order drainage basin (4.5 ha) about 40 km south of Beersheva (30° 52′ N, 34°48′ E) in the northern Negev Desert of Israel (Fig. 1). The elevation ranges between 485 and 535 m above sea level. The mean annual air temperature in Sede Boker is 20 °C (Dan et al. 1972), and mean monthly temperatures vary from 9 °C in January to 25 °C in August. The average annual rainfall, observed during a 30-year period (Yair 1994), ranges from 34 to 167 mm, with an average of 91 mm (Kuhn and Yair 2004). Rainfall is concentrated during the winter season between October and April. Potential evaporation rates are approximately 2,500 mm, generating an arid climate (Evenari et al. 1980; Olsvig-Whittaker et al. 1983; Yair and Danin 1980).

The Upper Cretaceous bedrock stratigraphy is composed of three limestone formations that are the Netser, Shivta, and Drorim formation (Fig. 2). Based on Yair and Danin (1980), Olsvig-Whittaker et al. (1983), and Schreiber et al. (1995), the formations can be classified in four meso-scale surface structural units (Upper Netser, Lower Netser/Upper Shivta, Lower Shivta, colluvium above Drorim). The upper part of the slope is characterized by the Upper Netser formation with thinly bedded limestones and flint concretions. The lower part of the Netser and the Upper Shivta formation is a thinly bedded and densely fissured formation and could be considered as one structural unit according to Olsvig-Whittaker et al. (1983). The Lower Shivta formation is a massive unit with a low density of deep cracks. The Drorim formation represents the lowest unit, which is densely jointed and covered with an extensive colluvial mantle (Yair and Shachak 1982) (see Fig. 2). These bedrock formations provide distinctive surface properties influencing hydrology, plant communities, and therefore potentially the spatial distribution of SOC concentration and SOC stock.

In situ chemical weathering of bedrock is of minor importance for soil formation. Most of the substrate is not derived from the local limestone, but composed of aeolian loess-like sediments, which were deposited since the early Quaternary (Bruins 1986; Reifenberg 1947; Yaalon and Dan 1974). Based on the World Reference Base for Soil Resources (IUSS Working Group WRB 2006), the soil is dominantly classified as a desert brown Lithosol (Arkin and Braun 1965; Dan et al. 1972) with patchy and thin soil cover. Generally, the study area is characterized by three soil bedding types: (1) soil patches, which are mainly located at the base of rock steps, (2) soil material filling crevices

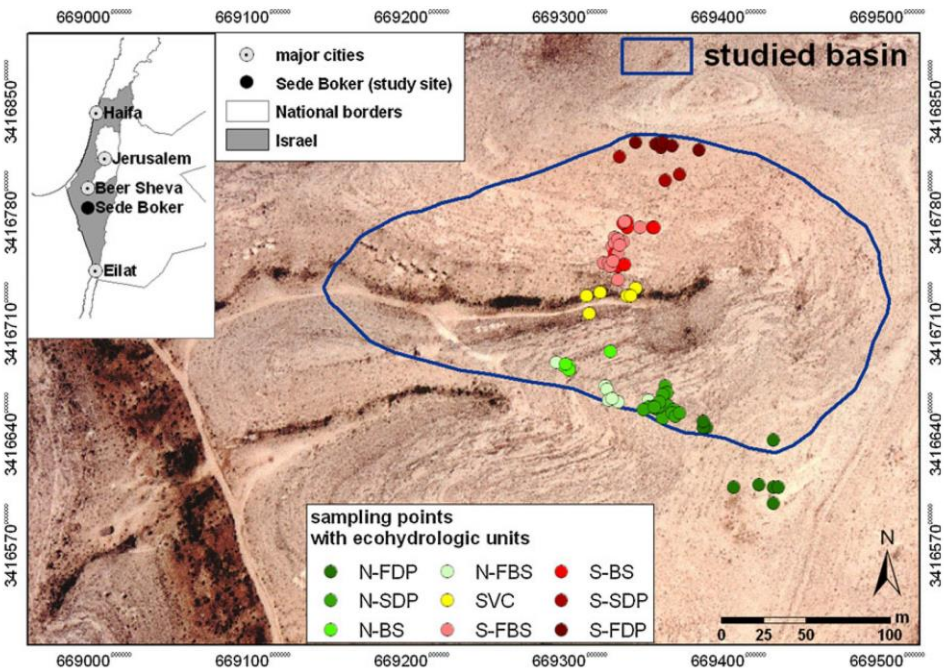

Fig. 1 Location of the study site and sampling points with respect to aspect and ecohydrologic units. *N* and *S* indicated northern and southern aspects, respectively. *FDP* flat desert pavement, *SDP* gently sloped desert pavement, *FBS* stepped and fissured bedrock slope, *BS* non-fissured bedrock slope, *SVC* slope and valley colluvium. Coordinates are given by projection system UTM longitude zone 36, latitude zone R, ellipsoid WGS 84

and fissures generated by rock shattering, and (3) colluvial soil sheets on bedding planes of the near surface rock strata. The loessic substrate is high in sand and silt (85–95 %), while clay content varies between 14.5 % in joints and crevices and 7–10 % in soil patches covering bedding planes (Olsvig-Whittaker et al. 1983; Yair and Danin 1980). Due to the arid conditions, with low vegetation coverage and high wind speeds and surface runoff, the soil genesis is

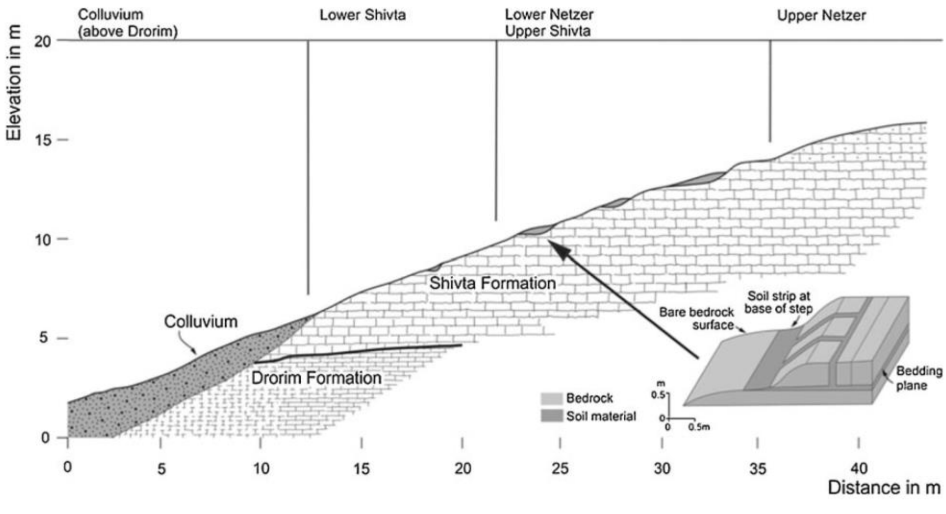

Fig. 2 Geological cross section with lithological formations of the study site modified after Olsvig-Whittaker et al. (1983)

strongly controlled by the erosion and deposition caused by wind and surface runoff (Olsvig-Whittaker et al. 1983).

Despite the meteorologic aridity, the vegetation of this region is considered to be at the transition of the Irano-Turanian plant geographical region and the Saharo-Arabian region with some Mediterranean components (Danin et al. 1975; Olsvig-Whittaker et al. 1983; Yair and Danin 1980; Yair and Shachak 1982; Zohary 1962). The study area has a range of communities from semi-desert (10–30 % perennial shrubs and semi-shrubs) on the rocky upper north exposed slopes, which are characterized by an unfavorable water regime (Yair and Danin 1980), to some patches of true desert vegetation (less than 10 % perennial cover) on the lower colluvium and southerly exposed slopes. The most favorable water regime prevails in soil pockets and crevices; therefore, vegetation is more or less concentrated along the soil patches and bedrock joints filled with soil. Hence, the study site is very well suited to determine the role of surface ecohydrology for SOC stocks.

3 Methods

Based on the aims of the study, the following objectives for field sampling and data analysis are derived: (1) to sample slope sections with different ecohydrologic characteristics (soil and vegetation) to calculate SOC stocks; (2) to compare soil properties, vegetation, SOC concentrations, and SOC stocks for the different ecohydrologic units; and (3) to identify the factors which determine SOC stocks on rocky desert slopes.

3.1 Ecohydrologic units along rocky desert slopes at Sede Boker

The study site was mapped based on differences in surface conditions (such as geology, rock/soil ratio, soil distribution, soil bedding, soil depth), microclimate (as indicated by slope gradient and aspect), and vegetation according to Olsvig-Whittaker et al. (1983), Schreiber et al. (1995), and Yair and Raz-Yassif (2004). These factors control the water availability for vegetation and thus determine the ecohydrologic units (EHUs) along the rocky desert slopes. The following units were distinguished for soil sampling and vegetation mapping (Table 1): (1) flat desert pavement (FDP), (2) gently sloped desert pavement (SDP), (3) non-fissured bedrock slope (BS), (4) stepped and fissured bedrock slope (FBS), and (5) slope and valley colluvium (SVC). A detailed description of each unit is given in Table 1. The FDP represents the uppermost unit in the study site, which represents the flat plateau in which the basin is incised. It is characterized by a medium soil and vegetation coverage (~30 %). The SDP forms the transition from the FDP to the incised valley. It has a higher soil and vegetation coverage, which is conditioned through the accumulation of aeolian deposits. The bedrock slope, which is located below the SDP, is subdivided into stepped fissured (FBS) and non-fissured bedrock (BS). The FBS shows a characteristic stepped topography with a localized soil cover in small soil pockets and noncontinuous soil strips. The former forms in zones of structural weakness in the Shivta formation and the latter are deposits of fine sediment at the base of the bedrock step below the soil pockets (Yair and Shachak 1982). The vegetation coverage in this unit is generally high. The BS is a massive unit of bedrock with a low density of deep cracks. Soil cover in this unit is generally very shallow and covers only 5–10 %. The colluvium, at the base of the slope, can be distinguished in slope colluvium and valley colluvium (SVC). This unit is characterized by a continuous deposition of colluvial sediments, which provide the parent material for the formation of soil. However, soil coverage is still limited due to the presence of large rocks, which cover a significant portion of the surface and inhibit the growth of vegetation and soil formation.

The ecohydrology of these units is strongly influenced by their surface characteristics. Therefore, the soil coverage was classified for each ecohydrologic unit using six soil-cover classes (I: <1 %; II: 1–2 %; III: 2–5 %; IV: 5–10 %; V: 10–30 %; and VI: >30 %) in the field (compare AG Bodenkunde 2005) and by visual interpretation of photos taken normal to the surface. Rocks larger than 20 cm, which cover the surface and prevent the growth of vegetation, were considered as "bedrock" and were excluded from soil coverage.

Vegetation was mapped and estimated for each ecohydrological unit based on the Braun-Blanquet (McAuliffe 1990) method as well as the plant guide of Zohary (1962) (see Table 1). The vegetation coverage was calculated on total surface (including rock and soils). Larger vegetation coverage than soil coverage is possible due to the canopy effect of the vegetation. Furthermore, we differentiated between the northwest and south exposed slopes, because according to Olsvig-Whittaker et al. (1983), an effect of solar radiation on soil moisture and vegetation and thus on evaporation can be expected on these slopes (Table 2).

3.2 Soil sampling and data analysis

To estimate SOC stocks, we took 82 soil samples covering all ecohydrologic units described above at the northeast and south-facing slopes. The number of samples per ecohydrologic unit was arranged to ensure a sufficient amount of samples for each set of relevant ecohydrologic surface properties along a slope (see Table 2). Soil sampling was conducted along a N–S transect through the studied valley at sampling sites across each ecohydrologic unit (see Fig. 1) in regular depth intervals (0–5, 5–15, 15–20 cm), continuing in

Table 1 Observed and mapped properties of the ecohydrologic units in the study area Sede Boker according to the findings of Olsvig-Whittaker et al. (1983), Schreiber et al. (1995), and Yair and Shachak (1982). Mean soil depth refers to areas covered by soil, and the rock/soil ratio is calculated as (100−soil cover)/soil cover

Ecohydrologic unit / general characteristics	Ecohydrologic unit	Mapped characteristics
Flat desert pavement (FDP) Uppermost unit with thinly bedded limestone and flint concretions Very shallow patchy soil and low vegetation coverage Dominant lithology: upper Netser formation		Slope: 6 % Soil cover: 30 % Soil depth: 15.76 cm Vegetation coverage: 10 % Rock/soil ratio: 2.33 pH (H_2O): 8.19 SOC_c (g 100 g^{-1}): 0.46 SIC (g 100 g^{-1}): 6.29
Gently sloped desert pavement (SDP) Forms the transition zone from the flat desert pavement to the incised valley Higher soil and vegetation coverage than FDP, accumulation of aeolian deposits Dominant lithology: upper Netser formation		Slope: 15 % Soil cover: 27.5 Soil depth: 18.75 cm Vegetation coverage: 22 % Rock/soil ratio: 2.63 pH (H_2O): 7.76 SOC_c (g 100 g^{-1}): 1.08 SIC (g 100 g^{-1}): 4.33
Stepped and fissured bedrock slope (FBS) Thinly bedded and densely fissured formation with stepped topography Soil accumulated in two different environments: (1) concentrated in crevices and fissures (2) accumulated in non-contiguous soil patches (Yair and Shachak 1982) Dominant lithology: lower Netser and upper Shivta formation	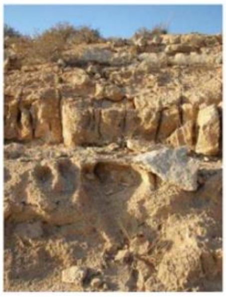	Slope: 20 % Soil cover: 45 % Soil depth: 20.52 cm Vegetation coverage: 32 % Rock/soil ratio: 1.22 pH (H_2O): 7.95 SOC_c (g 100 g^{-1}): 1.09 SIC (g 100 g^{-1}): 4.73

intervals of 20 cm where possible until the profile met bedrock). In addition to SOC concentrations, information of corresponding soil depth, bulk density, and coarse fraction are necessary to estimate SOC stocks (Eq. 1). Soil was sampled with a soil core sampler with a given volume (100 cm^3), which allowed the estimation of the soil bulk density BD (g cm^{-3}) based on the total soil weight (in grams) and the volume of the cylinder (in cubic centimeters) (Ravindranath and Ostwald 2008; Rodeghiero et al. 2009). The coarse fraction CF (g 100 g^{-1}) was calculated by the weight of coarse grains (>2 mm) divided by the total weight of the sample. At sampling sites with very shallow soils, such as weathering planes or depositional patches at the base of the steps, a mixed bag sample of 150 g was collected for a certain sampling area. In this case, the bulk density was estimated by multiplying the sampling area with the mean soil thickness of the sample.

3.3 Laboratory and statistical SOC analysis

Soil analysis was conducted in the laboratories of the University of Basel, Switzerland. The samples were

Table 1 (continued)

Ecohydrologic unit / general characteristics	Ecohydrologic unit	mapped characteristics
Non-fissured bedrock slope (BS) Extensive bedrock outcrops of massive limestone with low density of deep cracks Bedrock weathers into cobbles and boulders Soil shallowly accumulated as small soil patches Dominant lithology: upper Drorim formation		Slope: 21 % Soil cover: 7.5 % Soil depth: 10 cm Vegetation coverage: 9 % Rock/soil ratio: 12.33 pH (H_2O): 8.14
		SOC_c (g 100 g^{-1}): 0.61 SIC (g 100 g^{-1}): 4.37
Slope and valley colluvium (SVC) Soil bedding can be described as a colluvial mantle Densely jointed and covered with an colluvial mantle (Dan et al., 1972) Dominant lithology: lower Drorim formation		Slope: 18 % Soil cover: 45 % Soil depth: 28.66 cm Vegetation coverage: 23 % Rock/soil ratio: 1.22 pH (H_2O): 8.23 SOC_c (g 100 g^{-1}): 0.72 SIC (g 100 g^{-1}): 5.26

Table 2 Mean soil depth (related to soil-covered areas), median soil, and vegetation coverage and minimum, median, mean, max, and standard deviation of SOC stocks with respect to aspect and ecohydrologic units. The ecohydrological units in the table are ordered according to their sequence along the studied transect (compare Fig. 1). *N* northern aspect, *S* southern aspect, *FDP* flat desert pavement, *SDP* gently sloped desert pavement, *FBS* stepped and fissured bedrock slope, *BS* non-fissured bedrock slope, *SVC* slope and valley colluvium

Aspect	Ecohydrologic unit	No. of samples	Soil depth (cm)	Soil coverage (%)	Vegetation coverage (%)	$SOC_{stock,ehu}$ (kg C m^{-2})				
						Min	Median	Mean	Max	STD
N	FDP	9	15.3	30	10.5	0.13	0.26	0.28	0.74	0.18
N	SDP	23	12	40	21	0.06	0.56	0.72	1.90	0.55
N	FBS	7	17	45	35	0.68	1.21	1.42	3.04	0.78
N	BS	5	12	5	–	0.08	0.09	0.12	0.25	0.07
–	SVC	6	28.7	45	23	0.07	0.85	0.93	1.81	0.72
S	BS	8	14	10	–	0.03	0.07	0.07	0.13	0.04
S	FBS	14	19	45	12	0	0.59	0.71	2.37	0.63
S	SDP	3	23.1	15	5	0.02	0.22	0.17	0.26	0.13
S	FDP	7	24.7	30	–	0.05	0.15	0.21	0.39	0.13
	Total	82	18.7	29.4	24	0	0.31	0.58	3.03	0.61

initially dried at 40 °C and afterwards sieved using a stack of sieves to separate the coarse fraction (>2 mm), the fine fraction (<2 mm), and the fraction smaller than 0.032 mm. The latter was subject to further particle size analyses carried out with a SediGraph (SediGraph 5100, Micromeritics). That way, information about the clay fraction was obtained to test its influence on SOC stocks. SOC concentrations were measured using a LECO 100 CHN analyzer. First, total C content was measured with the untreated samples. Second, we estimated the SOC content based on the loss of ignition with 500 °C. Third, we calculated the soil inorganic carbon content for the same sample (without organic matter after burning) using again the CHN analyzer. For each representative layer i of a soil sample with thickness $d_{soil,\ i}$ (in centimeters), SOC stock ($SOC_{stock,\ i}$, in kilograms of carbon per square meter) was estimated based on Eq. (2):

$$SOC_{stock,\ i} = 0.1 \times d_{soil,\ i} \times BD \times SOC_{ci} \times (1 - CF_i/100) \quad (2)$$

SOC stocks (SOC_{stock}) per sampling site were then calculated by summarizing the SOC stock of each layer i at the corresponding sampling site:

$$SOC_{stock} = \sum SOC_{stock,\ i} \quad (3)$$

Based on Eq. (3), SOC stocks are not integrated over a certain reference depth, but for the entire soil column. To consider the limited soil coverage in each ecohydrological unit, we multiplied the stocks given in Eq. (3) with the mean soil coverage of each unit:

$$SOC_{stock,\ ehu} = SOC_{stock} \times soilcoverage \quad (4)$$

To test the influence of the ecohydrologic units on SOC storage, the factors in the SOC-stock equation (Eq. (3) and the $SOC_{stock,\ ehu}$ (Eq. (4) estimates for each ecohydrologic unit were compared using box–whisker plots. The Kruskal–Wallis test was used to compare the variability of soil properties between ecohydrologic units with the variability within the units. The non-parametric Wilcoxon test for non-normally distributed variables was additionally used to test for differences of SOC stocks between pairs of ecohydrologic units. In the case of significant difference between the ecohydrological units (e.g., higher variability between the units than within the units), calculated p values are lower than 0.05 (equal to a level of significance of 5 %). For each ecohydrological unit, averages and standard deviation for each soil property were calculated. The spatial variations were evaluated by the coefficient of variation CV, which is given by the ratio of the standard deviation to the mean value of each soil property. The CV therefore allows the comparison of the variations of each soil property in different ecohydrologic units through the normalization of the standard deviation.

4 Results

4.1 Variability of SOC stocks and controlling soil properties

The results regarding the minima, mean, median, maxima, and standard deviations of the measured soil properties (BD, CF, SOC_c, and d_{soil}) and the calculated SOC stocks are summarized in Tables 2 and 3. The largest variability of all SOC-stock controlling variables is displayed by the coarse fraction (CF factor in Eq. (1)), which ranges between 0 and 45.4 g 100 g^{-1} with a mean of 12.0 g 100 g^{-1} and a coefficient of variation of 81 %. SOC_c shows the second largest variability of the independent variables in Eq. (1), ranging from 0 to 4.48 g 100 g^{-1}, with a mean value of 0.86 g 100 g^{-1} and a coefficient of variation of 78.8 %. Soil depths range between 5 and 60 cm with a CV of 59.5 %. The lowest variability of the independent variables in Eq. (1) is shown by BD ranging between 0.56 and 1.90 g cm^{-3}, with a mean of 1.30 g cm^{-3} and a CV of only 20.7 % (see Table 3).

The large variability associated with the independent variables of BD, CF, SOC_c, and d_{soil} is propagated through the calculation of the carbon stocks (Eqs. 1, 2, 3, and 4). Calculated SOC stocks show a wide variability ranging from 0 up to 3.03 kg C m^{-2}, with a mean of 0.58 kg C m^{-2} and a standard deviation of 0.61 kg C m^{-2}. The estimated CV of 105 %, which is the largest of the soil properties presented in Table 3, is mainly a result of the large spatial variability associated with the coarse fraction and the SOC concentration.

4.2 SOC stocks, soil properties, and ecohydrology

The median SOC concentration shows strong differences between the north- and the south-facing slopes (Fig. 3) and a tendency of increasing concentration downslope from the N-FDP to the N-FBS (Fig. 4a). As a combination of differences in aspect and the downslope increase, the greatest SOC concentrations are shown in the north-facing FBS (see Fig. 4q). Soil depths are higher on the S-facing slope and lowest on the N-facing slope (see Figs. 3c and 4b). Maximum soil depths and variability are observed in unit SVC, which is generally covered by a layer of colluvial deposits (up to 50 cm). Somewhat lower soil depths are observed at unit FDP of the northern exposed slope, while at the southern slope, this unit is characterized by higher values. As suggested by the Kruskal–Wallis test (p value= 0.19), differences of soil depth between ecohydrological units are not significant (see Fig. 4b). In contrast, significant

Table 3 Minima, median, mean, maxima, and standard deviation of measured soil properties relevant for the calculation of the SOC stock

Parameter	Min	Median	Mean	Max	STD	STD/mean (%)
BD (g cm^{-3})	0.56	1.30	1.30	1.90	0.27	20.7
CF (g 100 g^{-1})	0	10.38	12.02	45.42	9.74	81.0
SOC_c (g 100 g^{-1})	0	0.67	0.86	4.48	0.68	78.8
$SOC_{stock,\ ehu}$ (kg C m^{-2})	0	0.31	0.58	3.03	0.61	105.17
Soil depth (cm)	5	15	18.7	60	11.12	59.46

Values are calculated using the entire dataset (n=82). Mean soil depth refers to areas covered by soils. According to Eq. 4, SOC stocks refer to the entire area of the study site

differences of the $SOC_{stock,\ ehu}$ between the ecohydrologic units are confirmed by the p values derived from the Kruskal–Wallis test and the non-parametric Wilcoxon test (see Fig. 4c). The Wilcoxon test indicates that the EHUs cannot be stratified into clearly defined statistical groups according to their SOC stock. SOC stocks of the N-FBS unit are significantly higher than the other EHUs (expect for the SVC), but other EHUs do not classify into groups that are defined by major gaps of SOC stock in between. The trend along the transect (from N-FDP to S-FDP) is similar to the SOC concentration (see Fig. 4a) and dissimilar to the soil depths given in Fig. 4b. The mean vegetation coverage (see Fig. 4d and Table 2) is characterized by the largest differences between the aspect and the ecohydrologic units. The trend of the vegetation coverage along the different ecohydrologic units (see Fig. 4d) is similar to the trend of the SOC concentration and stock (see Fig. 4a, c). The lowest median vegetation coverage is observed at the southern SDP (5 %) and the highest median coverage at the northern exposed FBS (35 %) (see Fig. 4d and Table 2).

The clay fraction in all soil samples ranged from 9.05 to 16.61 %, with a mean of 13.23 % and a standard deviation of 2.32. No significant differences in average clay content between ecohydrologic units were identified, which suggests that clay content had only a minor effect on SOC stocks.

Measured SOC contents do not exhibit a notable vertical gradient at a point (Fig. 5). The SOC concentrations in the upper 40 cm of the soil are characterized by a strong variability, without any detectable trend. Below 40 cm, SOC concentrations are somewhat lower, with a smaller variability.

5 Discussion

5.1 SOC stock, surface characteristics, and vegetation

The very strong control of vegetation on the SOC concentration and $SOC_{stock,\ ehu}$ is revealed by their similar pattern on different aspects (see Fig. 3) and in the ecohydrologic units (see Fig. 4). Mean SOC concentrations and stocks strongly correlate with vegetation coverage in each ecohydrologic unit (R^2=0.8 and 0.9, respectively, Fig. 6a and b). The highest SOC concentration and $SOC_{stocks,\ ehu}$ are found at slope exposures that favor high soil moisture and thus

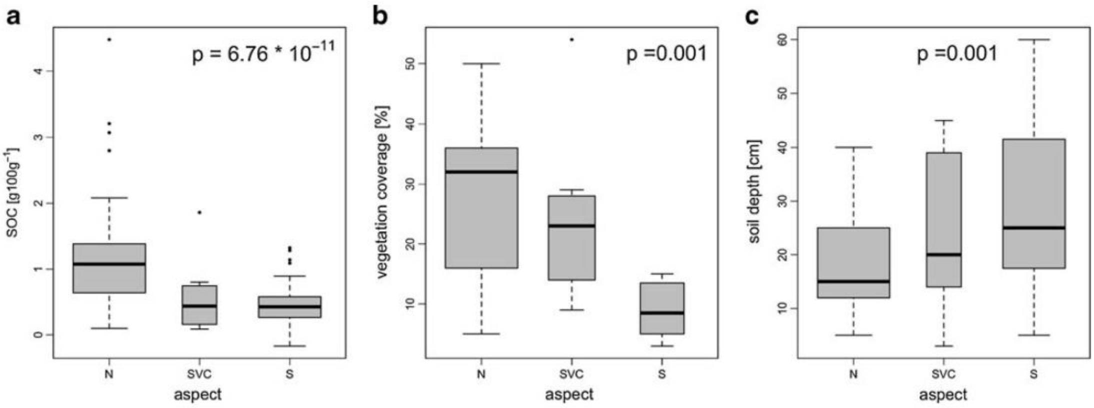

Fig. 3 SOC concentration (g 100 g^{-1}) (**a**), vegetation coverage (in percent) (**b**), and soil depth (in centimeters) (**c**) with respect to aspect from the whole investigation area. N and S indicated northern and southern aspects, respectively. The *boxes* have widths proportional to the number of sampling points in each box (number of total measurements, 82)

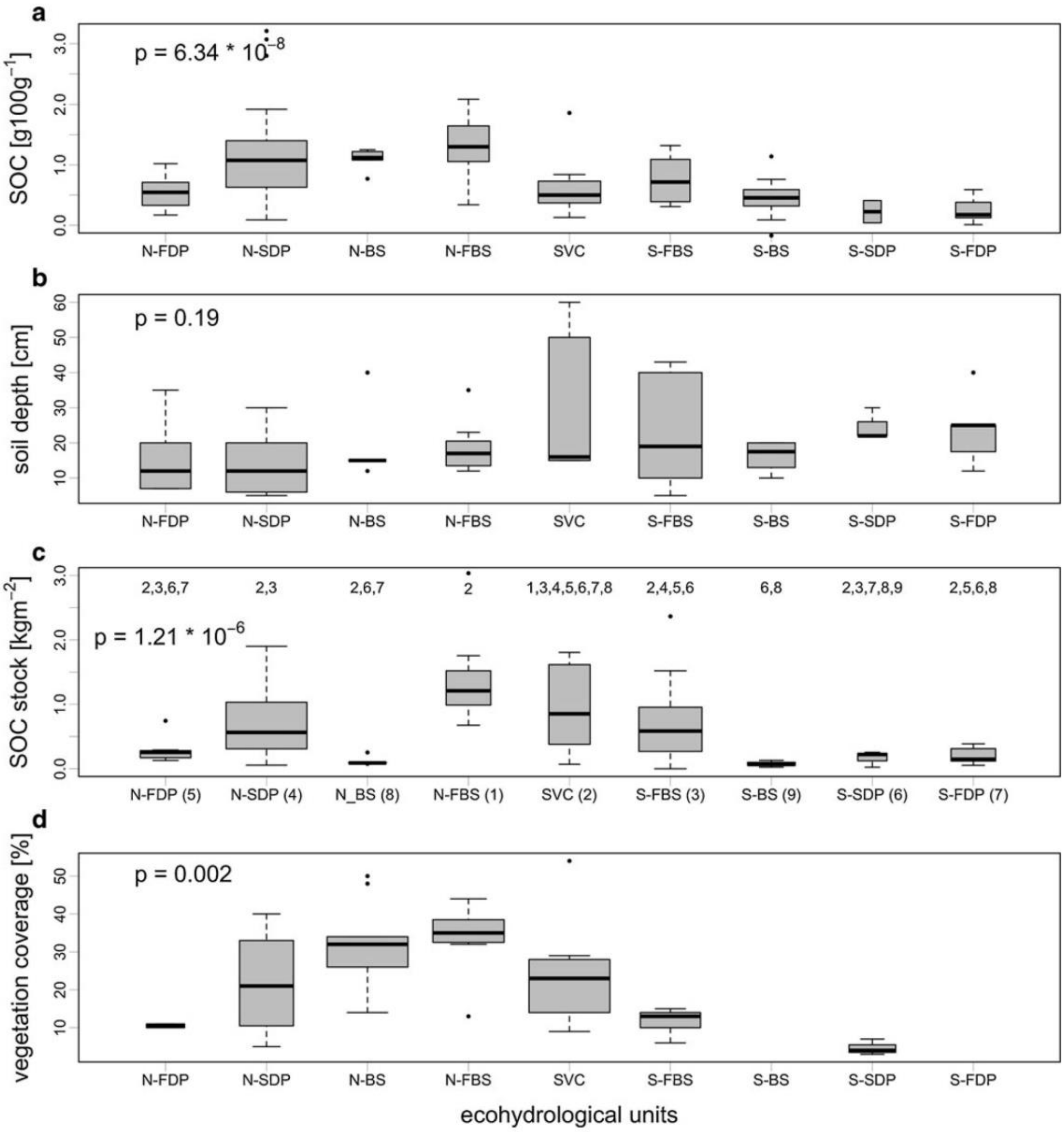

Fig. 4 **a** SOC concentration, **b** soil depths, **c** $SOC_{stock,\ ehu}$, and **d** vegetation coverage, **d** with respect to correspondence ecohydrologic unit and aspect. *N* and *S* indicated northern and southern aspect, respectively. *FDP* flat desert pavement with significant higher soil cover and depth due to minor slope gradient, *SDP* gently sloped desert pavement with lower soil depth due to higher slope gradient, *FBS* stepped and fissured bedrock slope, *BS* non-fissured bedrock slope, *SVC* slope and valley colluvium. Ecohydrologic units are ordered in correspondence to their locations from N to S along the transect. The *numbers* in brackets following the EHU names of Fig. 4c denote the rank of the EHU (e.g., the highest median of N-FBS is given by *(1)*, the lowest for S-BS given by *(9)*). The *numbers* above the *boxes* denote EHUs (according to their rank) with a similar SOC-stock distribution (as given by $p>0.05$ using the non-parametric Wilcoxon test). The *boxes* have widths proportional to the number of sampling points in each box (number of total measurements, 82). The *p* values are derived using the Kruskal–Wallis test and give significant differences between EHUs in case $p<0.05$

high vegetation densities (e.g., northern exposed slopes and lower slope positions, Figs. 3 and 4). In contrast, the mean soil depth of the ecohydrologic units correlates only very weakly with SOC concentration (see Fig. 6c), and no

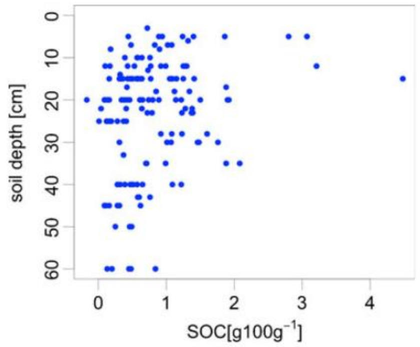

Fig. 5 SOC concentration as a function of depth below surface, plotted for every sample (n=82)

correlation is found between soil depth and $SOC_{stock,\ ehu}$ (see Fig. 6d). Thus, aspect-driven microclimatic effects that control soil moisture and vegetation coverage appear to affect SOC stocks more strongly than soil depth. The lacking relevance of soil thickness on rocky desert slopes is in strong contrast to its importance for SOC stocks in more humid areas (Berhe et al. 2008; Yoo et al. 2006). The positive relationship between vegetation coverage and SOC stocks at Sede Boker shows that the findings of Olsvig-Whittaker et al. (1983), who studied the effects of surface properties on vegetation, can also be applied to SOC stocks. Our results suggest that the different ecohydrologic conditions along rocky desert slopes near Sede Boker identified by Olsvig-Whittaker et al. (1983), Schreiber et al.

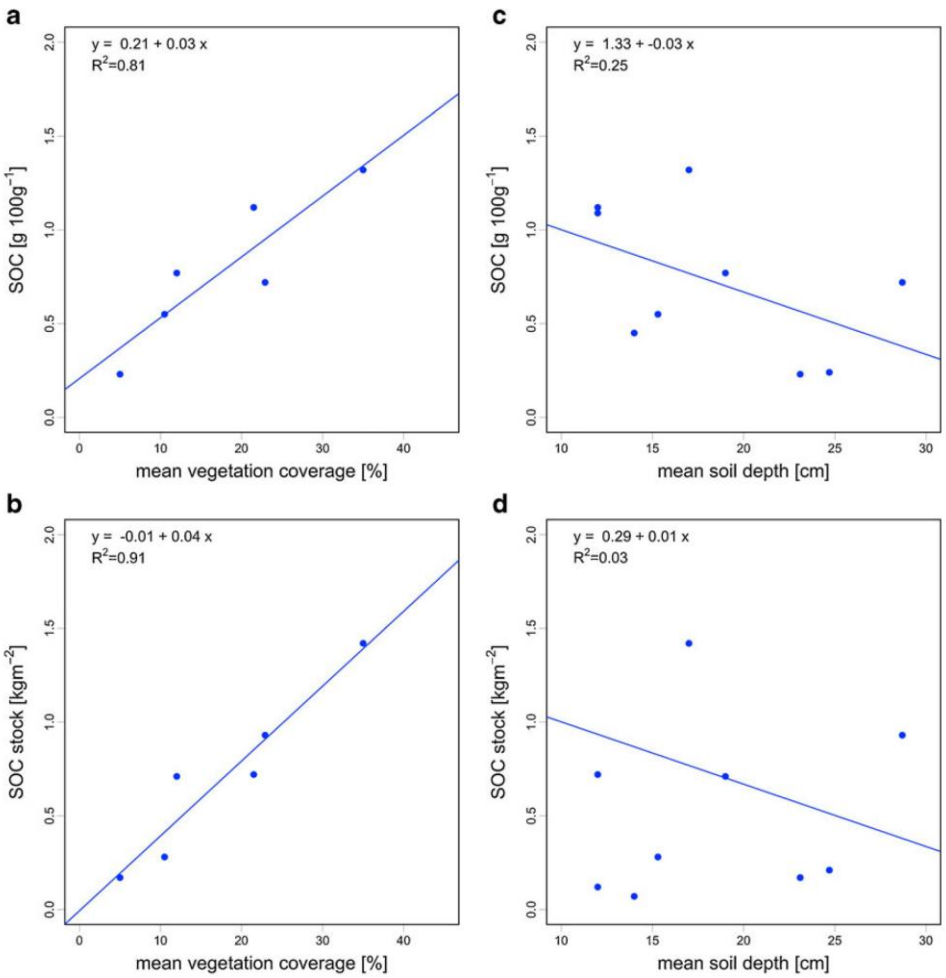

Fig. 6 Scatterplot of SOC concentration (**a**, **c**) and $SOC_{stock,\ ehu}$ (**b**, **d**) of sampled soils versus vegetation coverage and soil depth. Values are mean values obtained for each ecohydrologic unit

(1995), and Yair and Raz-Yassif (2004) also affect the SOC stocks on the different units. A similar effect is reported by Li et al. (2010) and Jobbágy and Jackson (2000) who both found a strong link between aboveground vegetation properties (e.g., density, type, stand age) and SOC. Our results also suggest that vegetation coverage provides a direct index for the spatial pattern of SOC stocks in drylands.

5.2 Surface processes and SOC stocks

The variability of the soil properties and the SOC stocks at Sede Boker is associated with differences in slope aspect (see Fig. 3) and NPP of the ecohydrologic units along the rocky desert slopes (see Fig. 4, Tables 2 and 3). In accordance with Olsvig-Whittaker et al. (1983), these results imply a positive dependency of SOC stocks on the relative moisture supply, which is given by surface runoff and aspect-driven differences of evaporation. The discontinuity of runoff associated with the patchwork of water sources and sinks also affects the distribution of SOC in the soil profile. In undisturbed soils, a strong vertical SOC gradient between topsoil and bottom soil is common (Arrouays and Pelissier 1994; Mishra et al. 2009; Wang et al. 2004). At Sede Boker, fine sediments provide the bulk substrate for soil formation and are preferentially deposited in small depressions and bedrock fissures, which act as local sediment sinks (see Figs. 1 and 2) (Olsvig-Whittaker et al. 1983; Yair and Danin 1980). Soil depth therefore varies on a centimeter to meter scale due to the spatial pattern of bedrock surface morphology. Eroded topsoils, which are generally enriched in SOC, are deposited in these fissures and may be stored over a long period of time. The limited change of SOC concentration with depth (see Fig. 5) at our sampling sites is in agreement with strong SOC redistribution and deposition at Sede Boker. Thus, the relationship of SOC content and soil depth appears to be strongly influenced by lateral soil movement, highlighting the need to consider soil as a mobile layer, formed by selective erosion and deposition (Hoffmann et al. 2009; Kuhn et al. 2009), which varies in time through changing source areas and/or the changing soil conditions in the source area (Dotterweich 2008).

5.3 SOC-stock comparison with other drylands

Table 4 summarizes results of SOC studies in arid and semi-arid areas, regarding the measured SOC concentrations and stocks. The estimated $SOC_{stocks,\ ehu}$ of the Sede Boker study area are in a similar range, while SOC concentrations are generally greater than those in other arid environments (see Table 4). Because $SOC_{stocks,\ ehu}$ refer to the entire study site and SOC concentrations to places in which soils are developed, the similar spatial pattern of $SOC_{stocks,\ ehu}$ and

Table 4 Global comparison of SOC and SOC stocks in different arid environments

Reference	Region	Environment	MAP (mm $year^{-1}$)	Area (km^2)	Reference depth (cm)	SOC stock (kg C m^{-2})	SOC_c (g 100 g^{-1})
Schlesinger (1977)	Global	World desert soils		1.83×10^9	Not specified	0.023–0.055	
Amundson (2001)	Global	Warm desert		14×10^6	Not specified	1.4	
Watson et al. (2000)	Global	Deserts and semi-deserts		45.5×10^6	0–100	4.37	
Feng et al. (2002)	Land regions of China	Different desert types	46–800	Variable	0–100	0.02–12.52 (mean, 2.32)	
Feng et al. (2002)	Land regions of China	Different desert types	46–800	Variable	0–20	0.02–4.97 (mean, 1.12)	
Balpande et al. (1996)	Central India	Vertisols	877–975	Profile measurement	Not specified		0.1–0.4
Zak et al. (1994)	Mexico, S-USA	Chihuahuan desert	240	Point measurement	Not specified		0.16
Bolton et al. (1993)	SE Washington, USA	Sagebrush steppe	100–250	Point measurement	Not specified		0.08
Perkins and Thomas (1993)	Kalahari, Botswana	Kalahari desert	150–600	Point measurement	Not specified		0.2–0.6
Ardö (2003)	Sudan	Semi-arid Sudan	200–800	2.62×10^6	0–20	0.06	
Zaady et al. (1996)	Negev, Isreal	Negev desert	200	Point measurement	Not specified		0.45–0.56
Fliessbach et al. (1994)	Negev, Israel	Negev desert	90 (19.5–180)	Point measurement	Not specified		0.03
This study	Sede Boker Negev, Israel	Rocky desert	91 (34–167)	0.045	Variable	0.31 (0.0–3.03)	0.67 (0.0–4.48)

MAP mean annual precipitation

increased SOC concentrations are attributed to the patchiness of soil cover in our study area compared to other areas cited in Table 4. While large fractions of our study area have rocky surfaces, sites with soil cover also carry vegetation and thus increased SOC concentrations. This is in accordance to the "islands of fertility" (Schlesinger and Pilmanis 1998) with increased biogeochemical processes, NPP, and SOC concentrations. Furthermore, higher concentrations in our study site might be attributed to the reduced mineralization of SOC, due to the lack of water in the Negev desert (Yao et al. 2010) and/or the degradation of soil due to overgrazing (compare for instance Bolton et al. 1993) in some of the other sites mentioned in Table 4. The comparison of our study to those presented in Table 4 remains limited. The studies presented in Table 4 rely on different measurement techniques of the SOC, different upscaling approaches, and variable reference soil depths taken into account. Unfortunately, reference soil depths are only given for 4 of the 13 case studies. Differences in SOC stocks may thus not represent environmental conditions, but simply the different methodologies applied for inventorying. The comparison indicates that the number of high-resolution SOC inventories in arid environments is very limited, and more case studies using a comparable methodology are necessary to evaluate the importance and potential changes of SOC in arid environments. In any case, on a global scale, the relatively large $SOC_{stocks,\ ehu}$ in our study area indicates that soils in arid environments, especially in rocky deserts associated with hardly any soil cover, may comprise a significant SOC pool that is sensitive to NPP. Even the admittedly somewhat arbitrarily calculated average soil depth of 18 cm is also in contrast to the notion that rocky deserts do not contain significant soil cover and thus SOC.

6 Conclusions

This study aimed at identifying the relationship between surface characteristics, vegetation coverage, and SOC concentration and stocks in the arid northern Negev in Israel. Soils cover 30 % of the study area, and the soil-covered areas are on average 18 cm deep and contained similar concentrations of SOC than soils from more humid drylands. However, the results show a large spatial variability of SOC, soil bulk density, and soil thickness. Consequently, the estimated SOC stock ranges between 0 and 3.03 kg C m^{-2} with a mean of 0.58 kg C m^{-2} (median, 0.31 kg C m^{-2}) and a standard deviation of 0.61 kg C m^{-2}. The differences in SOC stocks between ecohydrologic units on the north- and south-facing slopes indicate the relevance of eco-climate and thus the potential impact of climate change on rocky desert SOC stocks. They confirm that conceptual approaches, which explain the spatial patterns of vegetation cover on rocky desert slopes in the Negev, can also be applied to SOC stocks. In addition to climate-driven differences between aspect and slope position, the ecohydrologic units take changes of small-scale surface properties into account. The small-scale variability is mainly caused by lithology-driven differences of the microtopography, which provides accommodation space in fissures and on bedrock steps, for fine sediment accumulation and soil formation. Thus, significant differences of SOC stocks as well as vegetation densities between ecohydrologic units demonstrate that small-scale surface properties modulate climate-driven differences and provide a further control on the presence or absence of soils and thus on the amount of SOC storage.

In more general terms, our results show that dryland soils contain a significant amount of SOC even in arid regions. Even this amount is smaller than in more humid environments; it is of major importance for the functioning and thus conservation of arid ecosystem. Differences in eco-climate, microtopography, surface processes, soil formation and properties, and vegetation between the ecohydrologic units are apparently of greatest importance for SOC stocks in drylands. The results strongly suggest that the microscale (decimeter to meter) water supply and NPP, as indicated by the vegetation coverage, determine SOC stocks on rocky desert slopes. The variability of SOC stocks, driven by aspect, soil moisture availability, and vegetation coverage, also implies that SOC stocks in arid environments are highly sensitive to climate change and thus represent a major unstable C pool within the global carbon cycle of the twenty-first century.

Acknowledgments We owe our gratitude to the Freiwillige Akademische Gesellschaft (FAG) Basel and the University of Basel for funding the field work in Sede Boker.

References

Amundson R (2001) The carbon budget in soils. Ann Rev Earth Planet Sci 29:535–562

Ardö JLO (2003) Assessment of soil organic carbon in semi-arid Sudan using GIS and the CENTURY model. J Arid Environ 54:633–651

Arkin Y, Braun M (1965) Type sections of upper cretaceous formations in the northern Negev (southern Israel). Israel Geol. Survey Stratigraphic Section, No.2a, Jerusalem, pp 1–19

Arrouays D, Pelissier P (1994) Modeling carbon storage profiles in temperate forest humic loamy soils of France. Soil Sci 157:185–192

Asner GP, Borghi CE, Ojeda RA (2003) Desertification in Central Argentina: changes in ecosystem carbon and nitrogen from imaging spectroscopy. Ecol Appl 13:629–648

Balpande SS, Deshpande SB, Pal DK (1996) Factors and processes of soil degradation in Vertisols of the Purna Valley, Maharashtra, India. Land Degrad Dev 7:313–324

Berhe AA, Harden JW, Torn MS, Harte J (2008) Linking soil organic matter dynamics and erosion-induced terrestrial carbon sequestration at different landform positions. J Geophys Res 113:1–12

AG Bodenkunde (2005) Bodenkundliche Kartieranleitung KA 5 (German Soil Mapping Guide, 5th edition), Bundesanstalt für Geowissenschaften und Rohstoffe und Geologische Landesämter der Bundesrepublik Deutschland (Federal Institute for Geosciences and Natural Resources and Geological Survey offices of the Federal Republic of Germany) (eds.), Hannover, pp. 438

Bolton H, Smith JL, Link SO (1993) Soil microbial biomass and activity of a disturbed and undisturbed shrub-steppe ecosystem. Soil Biol Biochem 25:545–552

Branchu P, Faure H, Ambrost JP, Bakker EMV, Fauredenard L (1993) Africa as source and sink for atmospheric carbon dioxide. Glob Planet Chang 7:41–49

Bruins HJ (1986) Desert environment and agriculture in the Central Negev and Kadesh-Barnea during historical times. Ph.D. thesis, Agricultural University Wageningen. Midbur Foundation, Nijkerk, the Netherlands

Dan J, Yaalon DH, Koyumdjiski H, Raz Z (1972) The soil association map of Israel. Israel J Earth Sci 21:29–49

Danin A, Orshan G, Zohary M (1975) The vegetation of the northern Negev and the Judean Desert of Israel. Israel J Bot Basic Appl Plant Sci 24:118–172

Dotterweich M (2008) The history of soil erosion and fluvial deposits in small catchments of Central Europe: deciphering the long term interaction between human and the environment—a review. Geomorphology 101:192–208

Egli M, Sartori G, Mirabella A, Favilli F, Giaccai D, Delbos E (2009) Effect of north and south exposure on organic matter in high Alpine soils. Geoderma 149:124–136

Evenari M, Masig D, Rogel A (1980) Runoff-farming in the Negev Desert of Israel (VI). Jacob Blaustein Institute for Desert Research, Sede Boker

Fang C, Moncrieff JB (2001) The dependence of soil CO_2 efflux on temperature. Soil Biol Biochem 33:155–165

FAO (ed) (2004) Carbon sequestration in dryland soil. World soil resources reports 102, Rome. Available at: http://www.fao.org/docrep/007/y5738e/y5738e00.htm. Accessed Febuary 2012

Farage P, Pretty J, Ball A (2003) Biophysical aspects of carbon sequestration in drylands. Seminar paper presented at University of Essex, Feb 3, 1–25 pp

Feng Q, Endo KN, Guodong C (2002) Soil carbon in desertified land in relation to site characteristics. Geoderma 106:21–43

Fliessbach A, Sarig S, Steinberger Y (1994) Effects of water pulses and climate conditions on microbial biomass kinetics and microbial activity in yermosol of Central Negev. Arid Soil Res Rehab 8:353–362

Glatzel S, Sommer M (2005) Colluvial soils and landscape position: field studies on greenhouse gas exchange and related ecological characteristics. Z Geomorphol 139:87–99

Glenn E, Squired V, Olson M, Frye R (1993) Potential for carbon sequestration in the drylands. Water Air Soil Pollut 70:341–355

Goidts E, van Wesemael B (2007) Regional assessment of soil organic carbon changes under agriculture in Southern Belgium (1955–2005). Geoderma 141:341–354

Grieve IC (2001) Human impacts on soil properties and their implications for the sensitivity of soil systems in Scotland. Catena 42:361–374

Griffiths RP, Madritch MD, Swanson AK (2009) The effects of topography on forest soil characteristics in the Oregon Cascade Mountains (USA): implications for the effects of climate change on soil properties. For Ecol Manag 257:1–7

Hoffmann T, Glatzel S, Dikau R (2009) A carbon storage perspective on alluvial sediment storage in the Rhine catchment. Geomorphology 108:127–137

Houghton RA (2007) Balancing the global carbon budget. Ann Rev Earth Planet Sci 35:313–347

IPCC (2007) Chapter 7: Couplings between changes in the climate system and biogeochemistry. In: Climate Change 2007: The physical science basis. Contribution of Working Group I to the Fourth Assessment Report of the Intergovernmental Panel on Climate Change. Cambridge University Press, Cambridge

IUSS Working Group WRB (2006) World reference base for soil resources 2006. World soil resources reports no. 103. FAO, Rome

Jobbágy EG, Jackson RB (2000) The vertical distribution of soil organic carbon and its relation to climate and vegetation. Ecol Appl 10:423–436

Kirschbaum MUF (2000) Will changes in soil organic carbon act as a positive or negative feedback on global warming? Biogeochemistry 48:21–51

Kuhn NJ, Yair A (2004) Spatial distribution of surface conditions and runoff generation in small arid watersheds, Zin Valley Badlands, Israel. Geomorphology 57:183–200

Kuhn NJ, Hoffmann T, Schwanghart W, Dotterweich M (2009) Agricultural soil erosion and global carbon cycle: controversy over? Earth Surf Proc Land 34:1033–1038

Laity J (2008) Deserts and desert environments. Wiley-Blackwell, Singapore, p 342

Lal R (2003) Carbon sequestration in dryland ecosystems. Environ Manage 33:528–544

Lal R (2005) Soil erosion and carbon dynamics. Soil Tillage Res 81:137–142

Lal R (2009) Sequestering carbon in soils of arid ecosystems. Land Degrad Dev 20:441–454

Lal R, Kimble JM, Stewart BA (2001) Importance of soil bulk density and methods of its measurement. In: Kimble JM, Follett RF, Stewart BA (eds) Assessment methods for soil carbon. CRC Press, Boca Raton, pp 31–44

Leifeld J, Bassin S, Fuhrer J (2005) Carbon stocks in Swiss agricultural soils predicted by land-use, soil characteristics, and altitude. Agr Ecosyst Environ 105:255–266

Li P, Wang Q, Endo T, Zhao X, Kakubari Y (2010) Soil organic carbon stock is closely related to aboveground vegetation properties in cold-temperate mountainous forests. Geoderma 154:407–441

McAuliffe JR (1990) A rapid survey method for the estimation of denisty and cover in desert plant communities. J Veg Sci 1:653–656

Michaelides K, Chappell A (2009) Connectivity as a concept for characterising hydrological behaviour. Hydrol Process 23:517–522

Mishra U, Lal R, Slater BK, Calhoun F, Liu D, Van Meirvenne M (2009) Predicting soil organic carbon stock using profile depth distribution functions and ordinary kriging. Soil Sci Soc Am J 73:614–621

Olsvig-Whittaker L, Shachak M, Yair A (1983) Vegetation patterns related to environmental factors in a Negev Desert watershed. Vegetation 54:153–165

Parsons AJ, Abrahams AD (eds) (2009) Geomorphology of desert environments, 2nd edn. Springer, New York

Perkins JS, Thomas DSG (1993) Spreading deserts or spatially confined environments? Land degradation and cattle ranching in the Kalahari Desert of Botswana. Land Degrad Rehabil 4:179–194

Qi Y, Xu M, Wu J (2002) Temperature sensitivity of soil respiration and its effects on ecosystem carbon budget: nonlinearity begets surprises. Ecol Model 153:131–142

Quinton JN, Govers G, Van Oost K, Bardgett RD (2010) The impact of agricultural soil erosion on biogeochemical cycling. Nat Geosci 3:311–314

Ravindranath NH, Ostwald M (2008) Carbon inventory methods. Handbook for greenhouse gas inventory, carbon mitigation and roundwood production projects. Advances in global change research 29. Springer Science + Business Media B.V, Dordrecht, 308 pp

Reifenberg A (1947) The soils of Palestine. Murby, London, p 106

Rodeghiero M, Heinemeyer A, Schrumpf M, Bellamy P (2009) Determination of soil carbon stocks and changes. In: Kutsch WLB,

Heinemeyer A (eds) Soil carbon dynamics. An integrated methodology. Cambridge University Press, New York, pp 49–75
Rosenbloom NA, Harden JW, Neff JC, Schimel DS (2006) Geomorphic control of landscape carbon accumulation. J Geophys Res 111:1–10
Rotenberg E, Yakir D (2010) Contribution of semi-arid forests to the climate system. Science 327:451
Sarmiento JL, Gruber N (2002) Sinks for anthropogenic carbon. American Institute of Physics
Schimel DS (2010) Drylands in the earth system. Science 327 (5964):418–419
Schimel D, Enting IG, Heimann M, Wigley TML, Raynaud D, Alves D, Siegenthaler U (1994) CO_2 and the carbon cycle. Extracted from the Intergovernmental Panel on Climate Change (IPCC Report, "Climate Change, 1994"). In: Wigley TMLS (ed) The carbon cycle. Cambridge University Press, New York, pp 7–36
Schimel D, Melillo J, Tian H (2000) Contribution of increasing CO_2 and climate to carbon storage by ecosystems in the United States. Science 287:2004–2006
Schlesinger WH (1977) Carbon balance in terrestrial detritus. Annu Rev Ecol Syst 8:51–81
Schlesinger WH (1990) Evidence from chronosequence studies for a low carbon-storage potential of soils. Nature 348:232–234
Schlesinger WH (1991) Biogeochemistry: an analysis of global change. Academic, San Diego, p 588
Schlesinger WH, Pilmanis AM (1998) Plant–soil interactions in deserts. Biogeochemistry 42:169–187
Schlesinger WH, Raikes JA, Hartley AE, Cross AF (1996) On the spatial pattern of soil nutrients in desert. Ecosyst Ecol 77:364–374
Schreiber KF, Yair A, Shachak M (1995) Ecological gradients along slopes of the Northern Negev Highlands, Israel. Catena Adv Geoecol 28:209–229
Seip HM (2001) We know too little about the carbon cycle. Cicerone (1), Oslo, p 6
Smith JE, Heath LS (2002) A model of forest floor carbon mass for United States forest types. Newtown Square, PA: U.S. Department of Agriculture, Forest Service, Northeastern Research Station, Newtown Square PA. Research Paper NE-722, 37 pp
Tan ZX, Lal R, Smeck NE, Calhoun FG (2004) Relationships between surface organic carbon pool and site variables. Geoderma 121:187–195
Tsui C-C, Chen Z-S, Hsieh C-F (2004) Relationships between soil properties and slope position in a lowland rain forest of southern Taiwan. Geoderma 123:131–142
van Wesemael B, Paustian K, Meersmans J, Goidts E, Barancikova G, Easter M (2010) Agricultural management explains historic changes in regional soil carbon stocks. Proc Natl Acad Sci 107:14926–14930
Wang S, Huang M, Shao X, Mickler RA, Li K, Ji J (2004) Vertical distribution of soil organic carbon in China. Environ Manage 33:200–209
Watson RT, Noble IR, Bolin B, Ravindranath NH, Verardo DJ, Dokken DJ (eds) (2000) Land use, land-use change, and forestry. A special report of the IPCC. Cambridge University Press, Cambridge
Wigley TML, Schimel DF (eds) (2005) The carbon cycle. Cambridge University Press, Cambridge. 312 pp
Yaalon DH, Dan J (1974) Accumulation and distribution of loess-derived deposits in the semi-desert and desert fringe areas of Israel. Z Geomorphol 20:91–105
Yair A (1990) The role of topography and surface cover upon soil formation along hillslopes in arid climates. Geomorphology 3:287–299
Yair A (1992) The control of headwater area on channel runoff in a small arid watershed. In: Parsons AJ, Abrahams AD (eds) Overland flow: hydraulics and erosion mechanics. UCL Press, London, pp 53–68
Yair A (1994) The ambiguous impact of climate change at a desert fringe: Northern Negev, Israel, A.C. In: Millington AC, Pye K (eds) Environmental change in drylands: biogeographical and geomorphological perspectives. Wiley, Chichester, pp 199–227
Yair A, Danin A (1980) Spatial variations in vegetation as related to the soil moisture regime over an arid limestone hillside, Northern Negev Israel. Oecologia 47:83–88
Yair A, Raz-Yassif N (2004) Hydrological processes in a small arid catchment: scale effects of rainfall and slope length. Geomorpholohgy 61:155–169
Yair A, Shachak M (1982) A case study of energy water and soil flow chains in an arid ecosystem. Oecologia 54:389–397
Yao S-H, Zhang B, Hu F (2010) Biophysical controls over mineralization and sequestration of amended organic carbon in soil: effects of intensity and frequency of drying and wetting cycles. World Congress of Soil Science: Soil solutions for a changing world. Brisbane, Australia
Yoo K, Amundson R, Heimsath AM, Dietrich WE (2006) Spatial patterns of soil organic carbon on hillslopes: integrating geomorphic processes and the biological C cycle. Geoderma 130:47–65
Zaady E, Groffman P, Shachak M (1996) Litter as a regulator of N and C dynamics in macrophytic patches in Negev Desert soils. Soil Biol Biochem 28:39–46
Zak JC, Willig MR, Moorhead DL, Wildman HG (1994) Functional diversity of microbial communities: a quantitative approach. Soil Biol Biochem 26:1101–1108
Zhou ZY, Li FR, Chen SK, Zhang HR, Li G (2011) Dynamics of vegetation and soil carbon and nitrogen accumulation over 26 years under controlled grazing in a desert shrubland. Plant Soil 341:257–268
Zohary M (1962) Plant life in Palestine, Israel and Jordan. The Roland Press Co., New York, p 262

4. Experimental investigation of soil ecohydrology on rocky desert slopes in the Negev Highlands, Israel

This chapter has been published in Zeitschrift für Geomorphologie as: Hikel H., Yair A., Schwanghart W., Hoffmann U., Straehl S., Kuhn N.J. (2012): Experimental investigation of soil ecohydrology on rocky desert slopes in the Negev Highlands, Israel. Zeitschrift für Geomorphologie 57, Suppl.1, 039-058.

Zeitschrift für Geomorphologie, Vol. 57, Suppl. 1, 039–058 **Article**
Published online October 2012

Experimental investigation of soil ecohydrology on rocky desert slopes in the Negev Highlands, Israel

Harald Hikel, Aaron Yair, Wolfgang Schwanghart, Ulrike Hoffmann, Sarah Straehl and Nikolaus J. Kuhn

with 11 figures and 3 tables

Abstract. *Purpose:* Dryland vegetation is expected to respond sensitively to climate change and the projected variability of rainfall events. Rainfall as a water source is an obvious factor for the water supply of vegetation. However, the interaction of water and surface on rocky desert slopes with a patchy soil cover is also vital for vegetation in drylands. In particular, runoff on rocky surfaces and infiltration capacity of soil patches determine plant available water. Process-based studies into rock-soil interaction benefit from rainfall simulation, but require an approach accounting for the micro-scale heterogeneity of the slope surfaces. This study therefore aims at developing a suitable procedure for examining rock-soil interaction and the relevance of soil volume for storing plant available water in the northern Negev, Israel.

Materials and methods: To determine the amount of rainfall required to fill the available soil water storage capacity rainfall simulation experiments were conducted. The design of the rainfall-simulator and the selection of the plots aimed specifically at observing infiltration into small soil patches on a micro-scale relevant for the prevalent vegetation cover.

Results and discussion: The preliminary results of the study in the Negev Desert indicate that the ratio between soil volume and frequency of rainfall events determine the effect of climate change on plant available water and thus ultimately vegetation cover.

Conclusions: Based on the experiments examining runoff and soil moisture the qualitative understanding of hillslope ecohydrology in a rocky desert environment can be expanded into a quantitative assessment of the potential impact of varying rainfall conditions. The study also illustrates the contribution of rainfall simulation experiments for studies on the impact of climate change.

Keywords: Drylands, Ecohydrology, Rocky deserts, Rainfall simulation

1 *Introduction*

Deserts and semi-deserts occupy more than one-third of the Earth's land surface (Laity 2008). About 50 % of these arid regions are dominated by rocky surfaces, where patches of bedrock and shallow soil or pavements prevail (Buis & Veldkamp 2008, Walker 1986). The heterogeneity of surface characteristics has important implications for biological, chemical, hydrological and geomorphological processes (Boeken & Shachak 1994, Yair & Danin 1980, Yair & Raz-Yassif 2004, Yair & Shachak 1982, Yair et al. 1980, Lavee et al. 1991, 1998, Del Barrio et al. 1997). The spatial variations of the ratio of rock and soil covered surfaces; soil properties and water distribution often coincide with the distribution of vegetation patterns (Barth & Klemmedson 1978, Cantón et al. 2004, Garner & Steinberger 1989, Schlesinger et al. 1996). In arid areas vegetation patterns constitute hotspots of biological productivity and diversity of herbaceous plants (Boeken & Shachak 1994, Zaady et al. 1996, Golodets & Boeken 2006). The mosaic of vegetated and non-vegetated patches is dynamically interdependent. Bare ground acts as a source of water and

www.borntraeger-cramer.de
DOI: 10.1127/0372-8854/2012/S-00116 0372-8854/12/S-00116 $ 2.50

sediments, vegetated patches act as sinks where water and sediments are trapped (PUIGDEFABREGAS 2005, PARIENTE 2002). Vegetated patches absorb more water due to higher soil porosity, infiltration capacity, water holding capacity, hydraulic conductivity, structural stability, organic matter content and lower bulk density (STAVI et al. 2009, PUIGDEFABREGAS 2005, CAMMERAAT 2002).

Understanding the dynamic interactions and feedback mechanisms between the formation of vegetation patches and their hydrological and geomorphological controls is in the focus of the rising field of ecohydrology (BRADFORD et al. 2003). The self-organized spatial mosaic of banded, dashed and spotted vegetation cover is an adaptation of the ecosystem characterized by limited water availability (LOIK et al. 2004, VON HARDENBERG et al. 2001, LUDWIG et al. 2005, STAVI et al. 2009). The limited water supply can be caused by low and erratic precipitation (BROMLEY et al. 1997, SHNERB et al. 2003, VAN DE KOPPEL & RIETKERK 2004) and/or the capacity of the soil to absorb and/or store water (VON HARDENBERG et al. 2001, RIETKERK et al. 2004, YIZHAQ et al. 2005). Water availability is therefore not purely limited by climate conditions, but also by the surface properties, such as the extent, volume and pattern of rock and soil covered surfaces (CANTÓN et al. 2011, CANTÓN et al. 2002, YAIR & KOSSOVSKY 2002).

Various studies at the hillslope scale have demonstrated the importance of the ratio between rock and soil covered surfaces controlling the spatial distribution of soil moisture (CANTÓN et al. 2011, CANTÓN et al. 2002, YAIR et al. 1980, YAIR & KOSSOVSKY 2002, BUIS & VELDKAMP 2008, BUIS et al. 2009). Studies by YAIR & DANIN (1980) and OLSVIG-WHITTAKER et al. (1983) in the Negev Desert, Israel, qualitatively describe the water regime of an arid rocky slope environment. In such conditions, soil moisture and water availability is strongly influenced by the ratio of runoff generating rocky surfaces and soil patches, which act as sinks for water. OLSVIG-WHITTAKER et al. (1983) developed a semi-quantitative relationship (equation 1) linking soil and rock cover for this environment. The distribution of potential soil moisture is expressed by equation 1 which involves the rock-soil ratio and soil depth,

$$M \sim \frac{A_{rock}}{A_{soil}} \frac{1}{d_{soil}} \quad (1)$$

where M is potential soil moisture, A denotes the surface area of rock and soil, respectively and d is soil depth. OLSVIG-WHITTAKER et al. (1983) state that the rock-soil ratio can serve as a simple guide to predict soil moisture variability within a catchment and hence the spatial distribution of vegetation growth. According to equation 1, the potential soil moisture increases by increasing rock surface area, resulting in a positive relationship between rock-soil ratio and potential soil moisture. Increasing rock surfaces provide more water for infiltration and hence higher values for potential soil moisture. Small soil volumes are not considered to affect the potential soil moisture. This contradicts with the necessity to store water for plant consumption between rainfall events. Hence, the semi-quantitative relationship does not reflect the effect of soil volume on plant available water because for a micro-catchment with a given rock-soil ratio the amount of plant available water will depend on the soil volume available for water storage. Extreme values of the rock-soil ratio such as close to 100 % rock cover or minimal soil volume within a micro-catchment generate no or only very limited plant available water due to the lack of storage capacity. The equation does not describe the plant available water (M) for such a situation appropriately because the amount of plant available water is determined by both the extent of the contributing rocky area (rock-soil ratio) and by the volume of soil storing runon and rainfall for subsequent plant consumption. This ability of the hillslope surface to store water is of particular importance in drylands, where soil water storage capacity acts as a buffer to compensate for the temporal variability of rainfall and high evapotranspiration throughout a growing season. We therefore hypothesize that soil volume shows a positive relationship with plant available water on rocky dryland slopes. Testing this hypothesis in a feasible and controlled way requires rainfall simulation on a series of plots with different rock-soil ratio and soil volume. In this study, preliminary results, aimed at developing a suitable method for examining the interaction between rainfall and surface characteristics of rocky desert slopes are presented.

2 *Rainfall simulation as a tool for runoff measurements on rocky desert slopes*

Measuring runoff and infiltration in a rocky desert environment has, due to the sparse and variable rainfall, often been done using rainfall simulation (e.g. Salomon & Schick 1980, Greenbaum et al. 2003, Greenbaum 1986, Poesen & Lavee 1997, Lavee et al. 1991, Lavee & Poesen 1991, Renard 1979, Stone & Paige 2003). Using rainfall simulation offers not only control over the time of the event, but also control rainfall intensity and duration and preceding soil conditions. Rainfall simulation studies are typically conducted over a rectangular plot with a surrounding barrier to control the direction of the runoff. This design generates appropriate runoff and infiltration data only on straight slopes where all runoff flows into one downhill direction. Barriers surrounding a plot causing a deviation from the natural flow geometry can affect the observed runoff and infiltration rates, e.g. by increasing flow depth, wetted surface and thus infiltration along the edges of a plot (Dunne et al. 1991). Significant distortion of results due to the plot design can only be avoided by having large plots compared to the possible side effects. However, the patchy nature of rocky desert slopes often inhibits the use of large square plots with barriers due to the arbitrary delineation of the catchment they generate. Large plots also generate an integrated response, which cannot be easily separated into the infiltration on surface patches with different properties. Rainfall simulation on rocky-desert slopes therefore requires a different approach to account for the micro-scale heterogeneity. Specifically, the effect of topography on runoff routing and the different types of surface cover on infiltration have to be accounted for. The generally non-square nature of the micro-catchments can be addressed by limiting the use of artificial barriers than interfere with natural runoff routing. Such a "not-bounded" approach was used e.g. by Kuhn & Yair (2003). In their study, a collecting trough was installed in a naturally formed rill. The extent of the micro-catchment was identified by applying dye tracers to the rained-on surface and mapping the area that contributed runoff to the sampled rill. The heterogeneity of the surface cover can be addressed by designing the test plots in such a way that the hydrological response is determined by one dominant type of cover in each tested plot.

In this study, we present results of a series of rainfall simulation tests conducted on rocky surface slopes in the Negev desert. The aim of the presented study is to develop a suitable rainfall simulation procedure for testing the relevance of soil volume and rock-soil interaction for plant available water. The specific objectives are to measure infiltration during a "typical" rainfall event on micro-plots with different soil volumes and rock-soil ratios to determine their infiltration capacity. Based on this data, a preliminary analysis of rainfall and soil conditions relevant for plant water supply is conducted.

3 *Study area*

The study was conducted near Sede Boqer (30° 52′ N, 34° 48′ E) in the Northern Highlands of the Negev Desert at an altitude of 510 m a.s.l. (Fig. 1). The test plots (1 m²) are situated in a second-order drainage basin (0.05 km²) on rocky desert slopes with patchy soil and vegetation cover (Schreiber et al. 1995, Olsvig-Whittaker et al. 1983). The hydrology and vegetation of this area are well studied (Olsvig-Whittaker et al. 1983, Schreiber et al. 1995, Yair & Raz-Yassif 2004, Boeken & Shachak 1994, Yair & Shachak 1982). The semi-quantitative relationship (equation 1) indicates that soil moisture (M) increases with increasing rock-soil ratio. Hence vegetation density would also increase with increasing soil moisture. Linking rock and soil cover and vegetation density within the catchment (Fig. 2) the different bedding types, which are a combination of different values of rock and soil are associated with an increasing rock-soil ratio, but a declining vegetation density, which indicates that the interaction of runoff and surface is more complex than equation 1 suggest.

Bedrock consists of limestone and dolomite of Turonian age. The local stratigraphy is composed of three lithological units: the Drorim, Shivta and Netser formations (Fig. 3). The three formations are bedded almost horizontally and differ greatly in surface properties (Schreiber et al. 1995, Olsvig-Whittaker et al. 1983, Yair & Shachak 1982). Based on Schreiber et al. (1995),

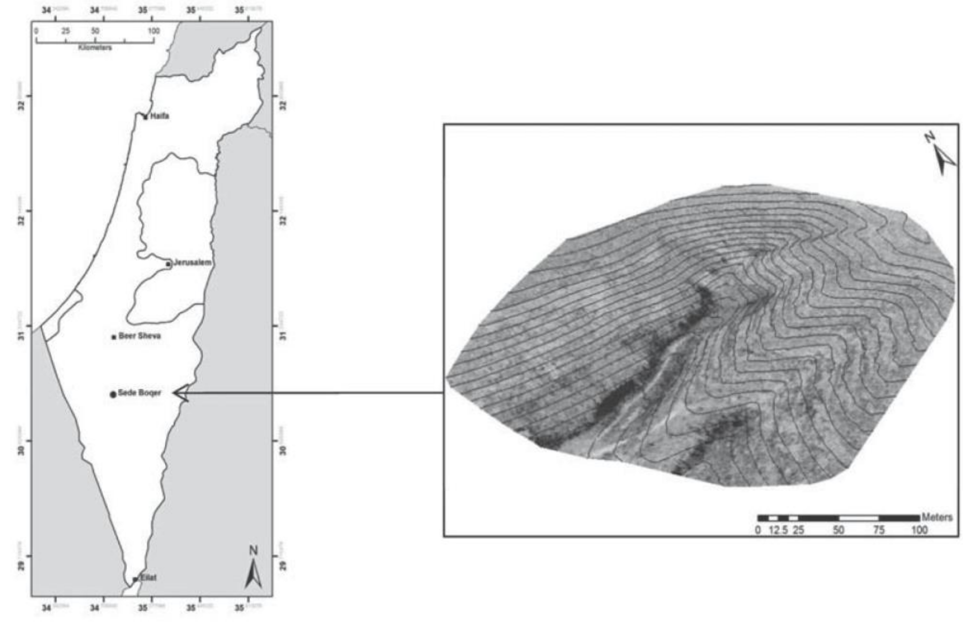

Fig. 1. Map of Israel and location of the study site (Sede Boqer) in the Negev Highlands, Israel.

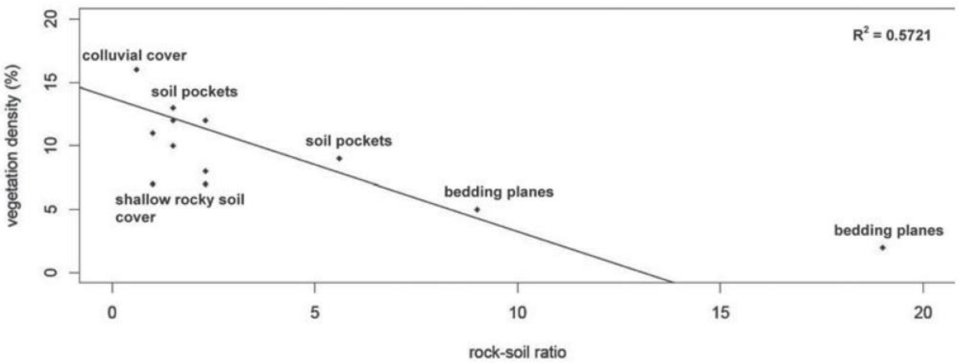

Fig. 2: Relationship between rock-soil ratio and vegetation density in the Sede Boqer study area (based on Hoffmann et al. 2011 and Straehl & Kuhn 2012, in prep.). For a description of the different types of bedding, see Fig. 4 and Table 1

Olsvig-Whittaker et al. (1983) and Yair & Danin (1980) the formations can be classified in four meso-scale surface structural units (Upper Netser, Lower Netser / Upper Shivta, Lower Shivta, Colluvium above Drorim). These formations create four different environments with distinctive surface properties influencing hydrology and plant communities. The Upper Netzer formation is characterized by thinly bedded densely jointed chalky limestone with flint concretions. The surface mainly consists of a rocky substratum (Yair & Danin 1980). According to the findings of Olsvig-Whittaker et al. (1983) the lower part of the Netser formation and the upper Shivta formation could be considered as one structural unit, which is thinly bedded and densely fissured.

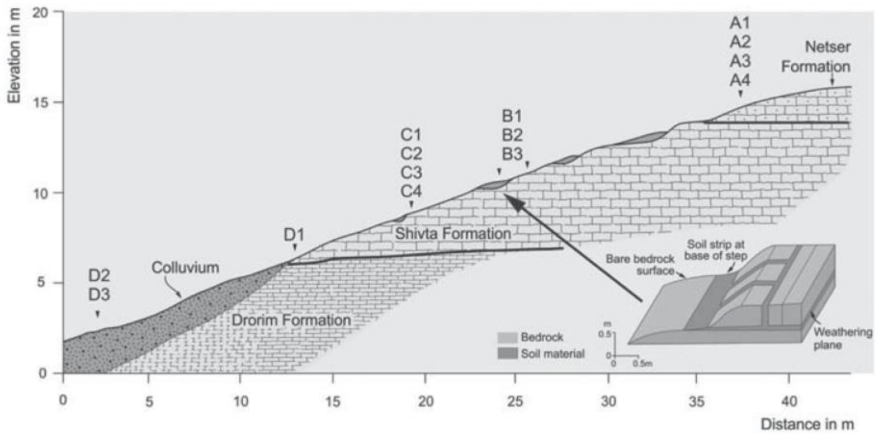

Fig. 3. Lithological formations within the studied catchment (modified after Yair & Shachak 1982, Olsvig-Whittaker et al. 1983 and Schreiber et al. 1995) and the location of the naturally sized micro-catchments and rainfall simulation plots (A1–D3).

shallow rocky soil cover | rock fissures (flower pots) | bedding planes | colluvial cover

Fig. 4. Overview of the different bedding types within the catchment.

The lower Shivta formation is a massive unit with a low density of deep cracks. Rock weathers into cobbles and boulders that cover most of the surface which is almost devoid of any soil (Yair & Shachak 1982). The Drorim formation is densely jointed and covered by an extensive colluvial soil (Dan et al. 1972).

Soils are very shallow and, with the exception of the colluvium on the Drorim formation, only form patches on the rocky surface (Yair & Danin 1980). Their mineral substrate is not solely derived from the local limestone bedrock, but largely composed of loessial sediments deposited since the early Quaternary (Reifenberg 1947, Bruins 1986, Yaalon & Dan 1974). Two different types of bedding can be distinguished (Fig. 4): soil is either concentrated in rock fissures ("flower pots") of the surficial rock strata, or at the base of the bedrock steps soil is accumulated in non-contiguous micro-colluvial deposits ("bedding planes") (Yair & Shachak 1982). The soils are classified according to the FAO-classification (FAO 2006) as desert brown lithosols (Arkin & Braun 1965, Dan et al. 1972, Yaalon & Dan 1974). The soils are rich in sand and silt (85–93 %) while clay content varies between 14.5 % in joints and 7 %–10 % in bedding planes covering bedrock (Yair & Danin 1980). An overview of the different ecohydrological units and the nature of their soil cover are presented in Table 1.

The climate in the study area is hot and arid (Laity 2008) and characterized by large seasonal contrasts in rainfall. The annual mean air temperature is 19.2 °C. Mean monthly temperatures range from 9 °C in January to 25 °C in August. Average annual rainfall at the study site is 90 mm characterized by high interannual variability with extreme values between 34 mm and 167 mm (Yair & Kossovsky 2002, Evenari et al. 1971, Evenari et al. 1980, Kuhn et al. 2004). 70 % of the annual rainfall occurs between December and February (Orni & Efrat 1966). Most of the total annual rainfall volume is usually provided by 10–20 individual events with duration of up to 8 hours (Shanan et al. 1967). Yair & Raz-Yassif (2004) showed that rainfall events of low magnitude (5 mm) have a frequency of 80 % in this region (for a detailed description of rainfall characteristics see section on rainfall simulation below). The observed potential annual evaporation varies between 2000 mm and 2600 mm (Kidron & Zohar 2010, Rosenan & Gilad 1985, Nativ et al. 1997). In comparison to flat terrain and hilltops, the slopes show lower evaporation rates (~14 %) and higher water availability (Kidron & Zohar 2010).

Plant communities in the study area represent a transition between the Irano-Turanian plant geographical region and the Saharo-Arabian region (Zohary 1962, Danin et al. 1975, Yair & Danin 1980). The catchment slope has a range of communities from semi-desert (10–30 % peren-

Table 1. Properties of the ecohydrologic units in the study area Sede Boker according to the findings of Yair & Shachak 1982, Olsvig-Whittaker et al. 1983, Schreiber et al. 1995.

Ecohydrologic Unit / General Characteristics	Ecohydrologic Unit	Mapped Characteristics
Flat Desert Pavement (FDP) Uppermost unit with thinly bedded limestone and flint concretions Very shallow patchy soil & low vegetation coverage Lithology: upper Netser formation	 Ridge	Slope: 6% Soil cover: 35% Soil depth: 15 cm Vegetation coverage: 10% Rock/soil ratio: 1.8
Gently Sloped Desert Pavement (SDP) Forms the transition zone from the flat desert pavement to the incised valley Higher soil and vegetation coverage than FDP, accumulation of aeolian deposits Lithology: upper Netser formation		Slope: 15% Soil cover: 30% Soil depth: 20 cm Vegetation coverage: 15% Rock/soil ratio: 2.3
Stepped and Fissured Bedrock Slope (FBS) Thinly bedded & densely fissured formation with stepped topography Soil accumulated in two different environments: (1) concentrated in rock fissures (flower pots) (2) accumulated in non-contiguous soil patches (bedding planes) (Yair & Shachak 1982) Lithology: lower Netser and upper Shivta formation	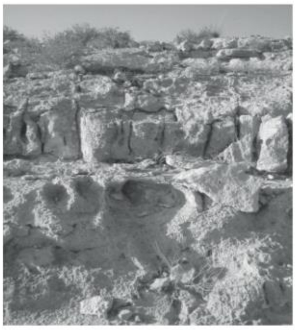	Slope: 20% Soil cover: 40% Soil depth: 20 cm Vegetation coverage: 30% Rock/soil ratio: 1.5
Non-Fissured Bedrock Slope (BS) Extensive bedrock outcrops of massive limestone with low density of deep cracks Bedrock weathers into cobbles and boulders Soil shallowly accumulated as small soil patches Lithology: upper Drorim formation		Slope: 21% Soil cover: 25% Soil depth: 5 cm Vegetation coverage: 5% Rock/soil ratio: 3
Slope and Valley Colluvium (SVC) Soil bedding can be described as a colluvial mantle Densely jointed and covered with an colluvial mantle (Dan et al. 1972) Lithology: lower Drorim formation	 Colluvium	Slope: 18% Soil cover: 60% Soil depth: 60 cm Vegetation coverage: 25% Rock/soil ratio: 0.6

nials vegetation cover) on the rocky upper slopes, to some patches of true desert (less than 10 % perennial cover) on the lower colluviums. Mediterranean species can be found in most mesic sites where soil patches absorb runoff, generated on rocky surfaces (Olsvig-Whittaker et al. 1983). Dominant species of the perennials are shrubs and semi-shrubs *Artemisia herba-alba*, *Gymnocarpos decander*, *Hammada scoparia*, *Noaea mucronata*, *Reamuria negevensis* and *Zygophyllum dumosum*. An assortment of annuals, geophytes and hemicryptophytes can be identified especially during the rainy winter season (Olsvig-Whittaker et al. 1983, Schreiber et al. 1995).

4 *Material and Methods*

4.1 *Plot selection and description*

To accommodate the particular hydrologic conditions of rocky desert slopes a rainfall simulator and experimental procedures were designed and used. Rainfall simulation was conducted on 14 non-rectangular open plots with a size of 1 m². Each plot represents a micro-catchment with different values for rock-soil ratio, soil volume and soil bedding (Table 2) across the second-order catchment. Micro-catchments of approximately 1 m² were chosen for the tests. The size of each plot was then limited to 1 m² by barriers placed to guide the runoff to a terminal weir at the lower end of the soil patch. Apart from identical plot size this ensured that the plots were completely covered by the simulated rainfall. The selection of the plots is based on relevant characteristics (such as geology, rock-soil ratio, soil distribution, soil depth) observed in earlier studies in this area (Yair & Raz-Yassif 2004, Schreiber et al. 1995, Olsvig-Whittaker et al. 1983). These factors control the water availability for vegetation and thus determine the ecohydrological units along the rocky desert slopes. For this initial study, micro-catchments with a range of rock-soil ratios, soil volumes and the type of bedding were selected to develop a procedure for measuring their respective soil water storage capacity. Digital photographs were taken for each plot normal to the surface. To quantify the rock-soil ratio for each plot rock and soil covered surfaces were digitized from the photographs in ArcGIS 10 and then the areas were measured using the *Spatial Analyst Tool*. To calculate the total soil volume, two different methods were used. Shallow soil patches were laser-scanned prior to and after soil excavation. DEMs (resolution ~2 cm) were created from the data and soil volume was estimated calculating the difference between both DEMs. This method was technically not feasible in areas with many fissures owing to shadowing effects. For these soil pockets bulk density was measured using 100 cm³ ring samplers. Subsequently, all soil was excavated and the total soil volume was measured. The soil mass was calculated by multiplying bulk density and measured excavated soil volume. Soil water storage capacity was calculated as the difference between solid soil volume and soil volume, the volumetric water content by dividing total infiltration by pore volume. Based on measured evaporation values in this area by Kidron & Zohar (2010) and Hillel & Tadmor (1962) and the water amount stored in the soil volume after a rainfall experiment, the period of time could be calculated until the infiltrated water is evaporated. Therefore 784 rainfall events (1976–2008) were analyzed regarding the period of time between single rainfall events.

Table 2. Values for soil volume (l), rock-soil ratio, bulk density (g/cm³) and porosity and soil covered area (m²) were calculated for 14 plots installed at different bedding types.

ID Plot	Bedding Type	Code	Soil volume (l)	Rock/Soil Ratio	Bulk Density (g/cm³)	Porosity	Soil Covered Area (m²)
1	Shallow rocky soil cover	A1	40	2.3	1.60	0.40	0.30
2	Shallow rocky soil cover	A2	45	2.3	1.62	0.39	0.30
3	Shallow rocky soil cover	A3	40	1.8	1.50	0.43	0.35
4	Shallow rocky soil cover	A4	40	1.8	1.53	0.42	0.35
5	Soil pockets	B1	15	1.5	1.52	0.43	0.40
6	Soil pockets	B2	20	1.5	1.38	0.48	0.40
7	Soil pockets	B3	35	1.5	1.49	0.44	0.40
8	Bedding planes	C1	25	3.0	1.23	0.54	0.25
9	Bedding planes	C2	10	5.6	1.23	0.54	0.15
10	Bedding planes	C3	5	5.6	1.23	0.54	0.15
11	Bedding planes	C4	30	4	1.23	0.54	0.20
12	Colluvial cover	D1	55	0.6	1.26	0.52	0.60
13	Colluvial cover	D2	60	0.6	0.83	0.69	0.60
14	Colluvial cover	D3	70	0.6	1.23	0.54	0.60

4.2 *Rainfall simulation and infiltration measurements*

The nature of the rocky desert slopes regarding the spatial variability of rock-soil ratio and soil volume required some specific design criteria for the rainfall simulator. First, rainfall roughly had to cover the natural micro-catchment supplying a soil patch with runon. Second, the simulated rainfall should fall within the envelope of frequently occurring natural events to ensure that the results can be used for an analysis of observed rainfall and plant water supply. Finally, the simulator had to be feasibly transported and run at the field sites. To meet these criteria, a portable nozzle simulator (Fig. 5) was built (Iserloh et al. 2012). The simulated rainfall was produced by a commercial full cone nozzle (Lechler, 1/8 inch, 460.408.30 CA) fed with a pressure of 1 bar. A fall height of 1.1 m was chosen to ensure that the plots (1 m^2) are completely covered by the simulated rainfall. The rainfall intensity applied was 18 mm h^{-1} for 20 min (i.e. a shower of 6 mm or rather 0.3 mm h^{-1}). This type of event falls well within range of intensities and durations of the natural rainfall in the study area (Yair 1994, 1999, Yair & Lavee 1985, Yair & Shachak 1982, Yair & Raz-Yassif 2004, Kuhn et al. 2004). The analysis of 784 rainfall events recorded at Sede Boqer between 1976–2008 shows that rain events up to 5 mm represent some 78 % of the rain recorded in the area (Fig. 6), rainfall up to 10 mm represent 91 % of recorded events. Events of this magnitude generate runoff over the rocky surfaces and represent an important source of plant available water (Yair & Lavee 1985). Drop size distribution and fall velocities of the simulated rainfall were measured using a Thies Laser Distrometer (see Fister & Ries 2009, Ries et al. 2009). The D_{50} value of raindrop diameter size ranges between 0.375 mm –0.5 mm, while the average fall velocity was 2.1 m s^{-1} (mean) and 2.4 m s^{-1} (median), respectively; 90 % of the velocities range between 0.2 m s^{-1} and 4.2 m s^{-1}. Based on these data, rainfall kinetic energy (J m^{-2} mm^{-1}) was calculated by using equations from Fornis et al. (2005). Fall velocity and thus kinetic energy of the drops (0.8 J m^{-2} mm^{-1}) are lower than for natural rainfall conditions of similar intensity (22.0 J m^{-2} mm^{-1}, Morgan et al. 1998). However, for our simulation such differences can be ignored when studying vegetation covered plots where the kinetic energy of the rainfall is absorbed by plants and litter. For the simulation tap water was used. According to the findings of Borselli et al. (2001) the impact of water

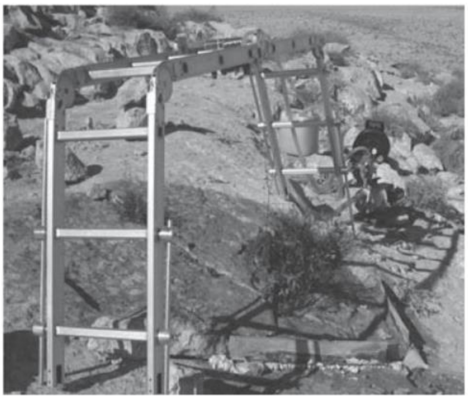

Fig. 5. Portable nozzle simulator during rainfall simulation test.

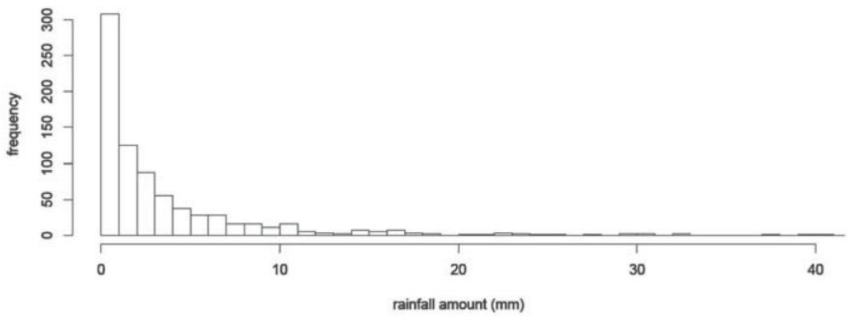

Fig. 6. Frequency analysis of the magnitude of rainfall events calculated for 784 rainfall events during the period of 1976–2008 (data source: http://bidr.bgu.ac.il/bidr/research/phys/meteorology/index.html).

Fig. 7. Naturally crusted soil patch in the Sede Boqer catchment.

Fig. 8. Naturally sized micro-catchment with installed metal sheets to guide runoff.

quality regarding hydrological and soil degradation processes depends on the soil's sensitivity to solutes in water. The topsoil has already developed an intense crust (Fig. 7) and is characterized by high concentrations of ions (mean electrical conductivity: 0.675 mS cm^{-1}, pH-value: 7.4-8.6). Due to the alkaline nature of the tap water and the crusted soil surface the quality of the used water is not considered to affect the results of the rainfall experiments.

The non-rectangular open nature of the micro-catchments avoided the installation of artificial barriers to guide runoff and limited hence negative side effects such as runoff concentration and an increase of infiltration along entrenched metal sheets. Artificial barriers were only installed at the outlet of each micro-catchment to collect runoff (Fig. 8) and ensure an identical size of 1 m^2 for each plot. Runoff volume was measured in intervals of 30 seconds. Infiltration was calculated as the difference between rainfall (moistened area * duration * intensity) and runoff. To keep the effect of evaporation at a minimum, the sprinkling experiments were conducted in the early morning hours. The depth of wetting front was recorded immediately after the rainfall experiments by excavating unconsolidated material at several locations in each plot. The depth of the wetting front can be used as an index for the degree of soil water storage capacity that is actually filled during a rainfall event.

5 *Results and Discussion*

Values of total infiltration (l), wetting depth (cm), runoff ratio, volumetric water content (%) and the ratio of total infiltration and direct rainfall are shown for each plot in Table 3. On all plots near constant runoff was reached during the tests (Fig. 9). Runoff ratio was high ranging from 0.28 to 0.60, which indicates that only a limited amount of water entered the soil, despite the short duration and low magnitude of the simulated event. This observation is confirmed by the low total infiltration, compared to the available pore space, i.e. the potentially maximum volume of plant available water per micro-plot and the low depth of the wetting front (values range between 2 cm and 17 cm; the average wetting front depth is 7 cm). While preliminary, the infiltration data observed during the rainfall simulations indicate that a rainfall event with a moderate magnitude and intensity leads only to a partial filling of the plant available water in the soil cover. This is attributed to the relatively high runoff ratios and low infiltration rates. According to the review of runoff generation and soil erosion by Cantón et al. (2011) soil patches acting as sinks only become saturated during high rainfall events. Saturation also enhances the connectivity of runoff pathways. In turn, the spatial distribution of water and sediment sink and source areas is affected by their spatial configurations and runoff connectivity (Puigdefabregas 2005). It is noteworthy that the volume of water that infiltrated into the flower pots is relatively low compared to the evaporation rates. According to the studies by Kidron & Zohar (2010) and Hillel & Tadmor (1962) daily winter evaporation values range in this area between 4–6 mm. On average, the soils would therefore dry completely within 1–3 days.

The results of the rainfall simulation tests can also be used to assess the proposed hypothesis on the effects of soil volume on plant available water. The relationship between soil volume (l) and total infiltration (l), rock-soil ratio and total infiltration (l) and soil volume (l) and rock-soil ratio are shown in Figure 10. The calculated p-value for all regressions is less than 0.05, which indicates a statistically significant relationship. Soil volume and total infiltration (Fig. 10a) show a

Table 3. Values for total infiltration (l), wetting depth (cm), runoff ratio, volumetric water content and the ratio of total infiltration and direct rainfall were calculated for 14 plots installed at different bedding types.

ID Plot	Bedding Type	Code	Total Infiltration (l)	Wetting Front Depth (cm)	Runoff Ratio	Volumetric Water Content (%)	Ratio Total Infiltration-Direct Rainfall
1	Shallow rocky soil cover	A1	5.5	2.5	0.60	35	3.06
2	Shallow rocky soil cover	A2	5.6	4.5	0.41	32	3.11
3	Shallow rocky soil cover	A3	4.4	3.5	0.37	25	2.10
4	Shallow rocky soil cover	A4	5.3	4.5	0.33	31	2.52
5	Soil pockets	B1	4.6	14.0	0.28	72	1.92
6	Soil pockets	B2	5.2	10.0	0.28	54	2.17
7	Soil pockets	B3	5.2	17.0	0.33	34	2.17
8	Bedding planes	C1	2.5	5.0	0.51	19	1.67
9	Bedding planes	C2	2.1	2.0	0.46	39	2.33
10	Bedding planes	C3	1.6	4.0	0.50	60	1.78
11	Bedding planes	C4	3.0	8.0	0.41	19	2.50
12	Colluvial cover	D1	5.2	7.0	0.56	18	1.44
13	Colluvial cover	D2	5.3	6.5	0.47	13	1.47
14	Colluvial cover	D3	5.7	10.0	0.42	15	1.58

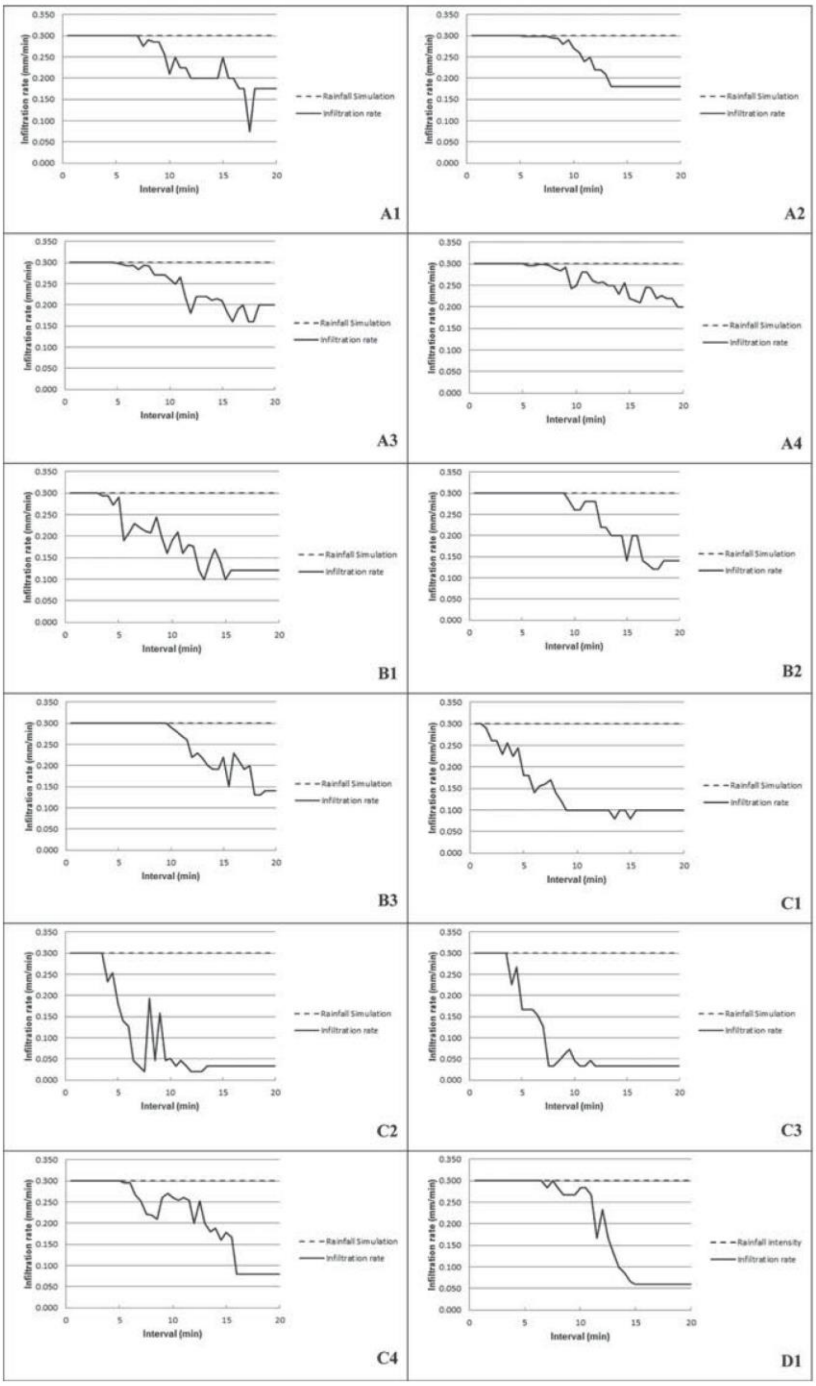
Infiltration rate (mm/min)
Interval (min)
Rainfall Simulation
Infiltration rate
Rainfall intensity
A1
A2
A3
A4
B1
B2
B3
C1
C2
C3
C4
D1

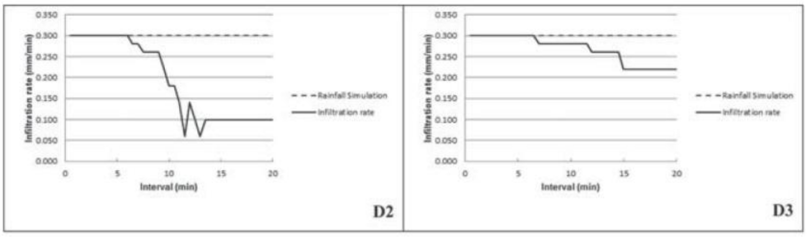

Fig. 9. Infiltration observed on plots during rainfall simulation tests.

moderate positive ($R^2 = 0.54$) relationship, confirming the a priori reasoning that soil volume has a positive effect on plant available water. Rock-soil ratio and total infiltration (Fig. 10b) are stronger, but *negatively*, correlated ($R^2 = -0.8$), i.e. plots with a high rock-soil ratio experienced lower total infiltration. This is in contrast to the positive relationship that can be expected from equation 1, but also confirms that at similar plot area the soil volume (negatively related to soil covered area $R^2 = -0.56$, Fig. 10c) affects the amount of infiltration. The results confirm that rock cover has an ambivalent effect on infiltration (Poesen & Lavee 1994). Rock cover can prevent direct infiltration and increase runoff generation. The generated runoff is then concentrated at the downslope side of the non-permeable rock surfaces. There, infiltration may increase due to greater water supply. As a consequence, deep infiltration of runoff develops at the upslope side of the soil patches (Olsvig-Whittaker et al. 1983). At the same time, rock-soil ratio declines with soil volume (Fig. 10c), indicating that flower pots and bedding planes with greater soil volume receive their water supply from a proportionally smaller rock surface than those micro-catchments with a small soil volume. Analyzing the degree of water saturation (Fig. 11a and b) offers an explanation for the apparent contradiction between Figure 2, equation 1 and Figure 10 b. The two regressions (Fig. 11), soil volume (l) and volumetric water content (%) and rock-soil ratio and volumetric water content (%) show p-values less than 0.05, which indicates a statistically significant relationship. For both 14 experiments were conducted. Low soil volume limits plant available water. Soil volume displays a moderate negative relationship ($R^2 = -0.56$) with volumetric water content, which illustrates that flower pots and bedding planes with a small volume filled up closer to their maximum water storage capacity than the larger ones during the simulated rainfall. At the same time, no relationship between rock-soil ratio and volumetric water content is visible ($R^2 = 0.09$). These two relationships (or the lack thereof) indicate that while runon is of critical importance for supplying water for vegetation growth (increasing the amount of infiltrated water by 40 to 300 %, see Table 3), the volume of the flower pots determines the plant available water and thus the risk of drought stress. The apparent relevance of soil volume and bedding also offers an explanation for the negative relationship between rock-soil ratio and vegetation density illustrated in Figure 2. Bedding planes and flower pots with a small volume, i.e. limited capacity to store water, tend to have a large rock-soil ratio. The reason for this trend is probably the structure of the rock surface, which generates predominantly shallow soil patches and deeper flower pots on the FBS.

The relevance of the soil volume observed during our experiments confirms the a priori reasoning conducted in the Introduction. Basically, the size of the flower pot determines the volume of water it can hold and thus the frequency and amount of watering (= rainfall) that is required to

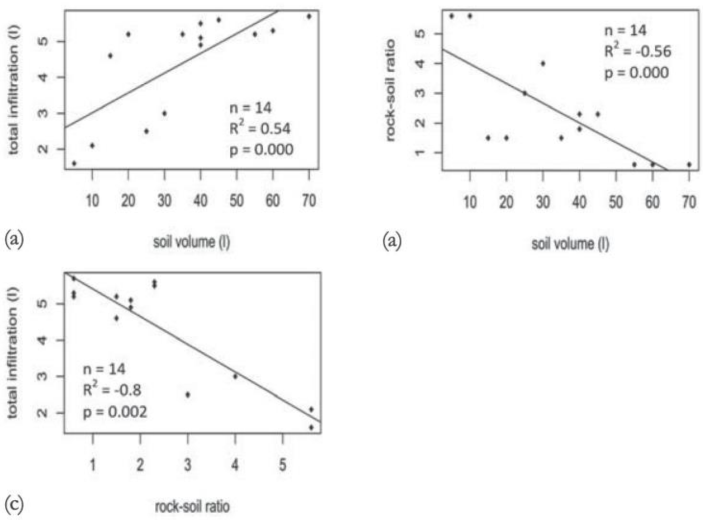

Fig. 10. Relationship between (a) soil volume (l) and total infiltration (l), (b) rock-soil ratio and total infiltration (l), (c) and soil volume (l) and rock-soil ratio. Values were measured for each plot.

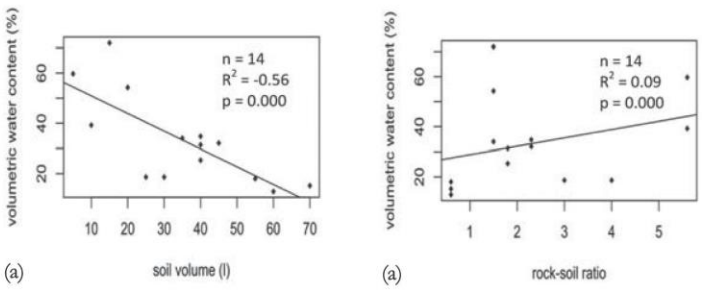

Fig. 11. Relationship between soil volume (l) and volumetric water content (%) and rock-soil ratio and volumetric water content (%).

maintain vegetation. In conjunction with the analysis of the rainfall magnitude and frequency in the region the results show that the amount of rainfall required to potentially deeply wet the soil is achieved frequently. The soil storage capacity is not filled until saturation, but low magnitude rainfall events are sufficient enough to deeply wet the soil. The degree of wetting is not linear correlated with the rainfall amount, but with rock-soil ratio and soil volume. At this, soil volume plays not a decisive role determining water saturation but larger soil volumes are characterized by higher total infiltration and lower volumetric water content. This implicates that for a given rainfall event and surface runoff the soil moisture tension based on a larger soil volume transfers more water into the soil resulting in an improved water supply. The critical role of soil volume and infiltration rate indicates that the duration of periods without rainfall seem to be more important for vegetation growth than the absolute event or annual rainfall amount because they determine whether drought stress occurs once the water in the flower pot has evaporated. The latter result is of critical relevance when assessing the potential impact of climate change on the vegetation in the region. Highlighting the relevance of rainfall frequency also illustrates that common climate models, which mostly focus on seasonal temperature and precipitation differences, do not provide the information required for conducting a proper impact assessment.

6 *Conclusion*

This study aimed at developing an experimental approach to identify the relevance of soil volume and rock-soil interaction for plant available water in a rocky desert environment. Runoff from non-permeable surfaces surrounding pockets of soil is of critical importance for the plant water supply, increasing the amount of infiltrated water into the flower pots during rainfall. A rainfall simulation procedure was developed to determine soil – rainfall interaction, specifically the relevance of soil volume for plant available water. The results show that during the simulated low magnitude rainfall events, which occur at a high frequency in the study area, only a limited amount of rainfall and runoff (i.e. runon from surrounding rock surfaces) infiltrated into the soil, resulting in a partial wetting of the soil profile. The degree of wetting increased with soil volume. This indicates that soil volume potentially affects plant water supply when the infiltration capacity of the soil body is smaller than the amount of water required by the vegetation until the next rainfall. The frequency-magnitude analysis of 784 rainfall events during the past 30 years and an estimation of the period of time until the infiltrated water is evapotranspirated again indicate that soil volume, in conjunction with rainfall frequency, may indeed have an important effect on plant water supply on rocky desert slopes. Overall, rainfall frequency rather than magnitude or annual precipitation amount appear to determine plant available water on a slope with a given pattern of rock-soil cover and soil volumes. To confirm these findings, a much larger number of rainfall tests, covering the full range of surface conditions would be necessary. But while preliminary, the study showed that a rainfall simulation test can be used to assess the effects of rainfall-surface interaction on rocky desert slopes and generate valuable information to gain an understanding of the effect of climate change on dryland ecohydrology.

Acknowledgements

Support for this research was provided by the Freiwillige Akademische Gesellschaft (FAG) Basel, and the project PilotHydroSurf, financed by the Seed Money fund, which is highly acknowledged by the authors.

References

ARKIN, Y. & BRAUN, M. (1965): Type sections of Upper Cretaceous formations in the northern Negev, Israel. – Geol. Surv. Stratigraph. Sec. **2** a, Jerusalem.

BARTH, R. & KLEMMEDSON, J. (1978): Shrub-induced spatial patterns of dry matter, nitrogen, and organic carbon. – Soil Sci. Soc. Amer. J. **42:** 804–809.

BOEKEN, B. & SHACHAK, M. (1994): Desert plant communities in human-made patches-implications for management. – Ecol. Appl. **4:** 702–716.

Borselli, L., Torri, D., Poesen, J. & Sanchis-Sanchis, P (2001): Effects of water quality on infiltration, runoff and interrill erosion processes during simulated rainfall. – Earth Surf. Proc. and Landf. **26:** 329–342.

Bradford, P., Wilcox, P., Breshears, D. D. & Allen, C. D. (2003): Ecohydrology of a resource-conserving semiarid woodland: effects of scale and disturbance. – Ecohydrol. Monogr. **73** (2): 223–239.

Bromley, J., Brouwer, J., Barker, A. P., Gaze, S. R. & Valentin, C. (1997): The role of surface water redistribution in an area of patterned vegetation in a semi-arid environment, south-west Niger. – J. Hydrol. **198:** 1–29.

Bruins, H. (1986): Desert Environment and Agriculture in the Central Negev and Kadesh Barnea During Historical Times. – PhD-Thesis, Wageningen Agricult. Univ., Nijkerk, The Netherlands.

Buis, E. & Veldkamp, A. (2008): Modelling dynamic water redistribution patterns in arid catchments in the Negev Desert of Israel. – Earth Surf. Proc. and Landf. **33:** 107–122.

Buis, E., Veldkamp, A., Boeken, B. & Van Breemen N. (2009): Controls on plant functional surface cover types along a precipitation gradient in the Negev Desert Israel. – J. Arid Environ. **73:** 82–90.

Cammeraat, L. H. (2002): A review of two strongly contrasting geomorphological systems within the context of scale. – Earth Surf. Proc. and Landf. **27:** 1201–1222.

Cantón, Y., Solé-Benet, A., de Vente, J., Boix-Fayos, C., Calvo-Cases, A., Asensio, C. & Puigdefábregas, J. (2011): A review of runoff generation and soil erosion across scales in semiarid south-eastern Spain. – J. Arid Environ. **75:** 1254–1261.

Cantón, Y., Del Barrio, G., Sole-Benet, A. & Lazaro, R. (2004): Topographic control on the spatial distribution of ground cover in the Tabernas badlands of SE Spain. – Catena **53:** 341–365.

Cantón, Y., Domingo, F., Sole-Benet, A. & Puigdefábregas, J. (2002): Influence of soil-surface types on the overall runoff of the Tabernas badlands: south-east Spain: field data and model approaches. – Hydrol. Proc. **16:** 2621–2643.

Dan, J., Yaalon, D. H., Koyumdjiski, H. & Raz, Z. (1972): The soil association map of Israel. – Israel J. Earth Sci. **21:** 29–49.

Danin, A., Orsham, G. & Zohary, M. (1975): The vegetation of the northern Negev and the Judean Desert of Israel. – Israel J. Bot. Bas. and Appl. Plant Sci. **24:** 118–172.

Del Barrio, G., Alvera, B., Puigdefabregas, J. & Diez, C. (1997): Response of high mountain landscape to topographic variables: Central Pyrenees. – Landsc. Ecol. **12:** 95–115.

Dunne, T., Zhang, W. & Aubry, B. F. (1991): Effects of rainfall, vegetation, and microtopography on infiltration and runoff. – Water Resour. Res. **27** (9): 2271–2285.

Evenari, M., Masig, D. & Rogel, A. (1980): Runoff-Farming in the Negev Desert of Israel VI. – Jacob Blaustein Institute for Desert research: Sede Boker, Israel.

Evenari, M., Shanan, L. & Tadmor N. H. (1971): The Negev. The challenge of a desert. – Harvard Univ. Press, Cambridge, Massachusetts, 344 pp.

FAO (2006): World reference base for soil resources. Rome.

Fister, W. & Ries, J. B. (2009): Wind erosion in the central Ebro Basin under changing land use management. Field experiments with a portable wind tunnel. – J. .Arid Environ. **73:** 996–1004.

Fornis, R. L., Vermeulen, H. R. & Niewenhuis, J. D. (2005): Kinetic energy-rainfall intensity relationship for central Cebu, Philippines for soil erosion studies. – J. Hydrol. **300:** 20–32.

Garner, W. & Steinberger, Y. (1989): A proposed mechanism for the formation of “fertile islands” in the desert ecosystem. – J. Arid Environ. **16:** 257–262.

Golodets, C. & Boeken, B. (2006): Moderate sheep grazing in semiarid shrubland alters small scale soil surface structure and patch properties. – Catena **65:** 285–291.

Greenbaum, N., Salmon, O. & Schick, A. P. (2003): Geomorphological implications and hydrological applications of infiltration tests in a hyperarid region. – In: Greenbaum, N., Lekach, J. & Inbar, M. (eds.): Current Aspects of Rainfall-Runoff-Sediment Relations in Israel: 44–69.

Greenbaum, N. (1986): Runoff in an extremely arid region. Infiltration-runoff tests on small plots in the Southern Arava and their hydrological and pedological implications. – M. Sc. Thesis, Hebrew University of Jerusalem, Israel.

Hillel, D. & Tadmor, N. (1962): Water Regime and vegetation in the Central Nebev Highlands of Israel. – Ecology **43** (1): 33–41.

Hoffmann, U., Yair, A., Hikel, H. & Kuhn, N. J. (2012): Soil organic carbon in the rocky desert of northern Negev (Israel). – J. Soils and Sedim. **12:** 811–825.
Iserloh, T., Ries, J. B., Cerdá, A., Echeverría, M. T., Fister, W., Geissler, C., Kuhn, N. J., León, F.,J., Peters, P., Schindewolf, M., Schmidt, J., Scholten, T. & Seeger, M. (2012): Comparative measurements with seven rainfall simulators on uniform bare fallow land. – Z. Geomorph. (same issue).
Kidron, G. J. & Zohar, M. (2010): Spatial evaporation patterns within a small drainage basin in the Negev Desert. – J. Hydrol. **380:** 376–385.
Kuhn, N. J. & Yair, A. (2003): Spatial distribution of surface conditions and runoff generation in small arid watersheds, Zin Valley Badlands, Israel. – Geomorphology **57:** 183–200.
Kuhn, N. J., Yair, A. & Kasanin-Grubin, M. (2004): Spatial distribution of surface properties, runoff generation and landscape development in the Zin Valley Badlands, northern Negev, Israel. – Earth Surf. Proc. and Landf. **29:** 1417–1430.
Laity, J. (2008): Deserts and desert environments. – Wiley-Blackwell, Chichester, 342 pp.
Lavee, H., Imeson, A. C., Pariente, S. & Benjamini, Y. (1991): The response of soils to simulated rainfall along a climatological gradient in an arid and semi-arid region. – Catena Suppl. **19:** 19–37.
Lavee, H., Imeson, A. C. & Pariente, S. (1998): The impact of climate change on geomorphology and desertification along Mediterranean – arid transect. – Land Degrad. and Develop. **9:** 407–422.
Lavee, H. & Poesen, J. (1991): Overland flow generation and conductivity on stone-covered soil surfaces. – Hydrol. Proc. **5:** 345–360.
Loik, M. E., Breshears, D. D., Lauenroth, W. K. & Belnap, J. (2004): A multi-scale perspective of water pulses in dryland ecosystems: climatology and ecohydrology of the western USA. – Oecologia **141:** 269–281.
Ludwig, J. A., Wilcox, B., Breshears, D., Tongway, D. J. & Imeson, A. (2005): Vegetation patches and runoff-erosion as interacting ecohydrological processes in semiarid landscapes. – Ecology **86:** 288–297.
Morgan, R. P. C., Quinton, J. N., Smith, R. E., Govers, G., Poesen, J. W. A., Auerswald, K., Chisci, G., Torri, D., Styczen, M. E. & Folley, A. J. V. (1998): The European Soil Erosion Model (EUROSEM): Documentation and User Guide. – Silsoe Colege, Cranfield University, Silsoe, Bedford.
Nativ, R., Adar, E., Dahan, O. & Nissim, I. (1997): Water salinization in arid regions – observations from the Negev desert, Israel. – J. Hydrol. **196:** 271–296.
Olsvig-Whittaker, L., Shachak, M. & Yair, A. (1983): Vegetation patterns related to environmental factors in a Negev Desert watershed. – Plant Ecol. **54:** 153–165.
Orni, E. & Efrat, E. (1966): Geographie Israels, Jerusalem.
Pariente, S. (2002): Spatial patterns of soil moisture as affected by shrubs in different climatic conditions. – Environ. Monitor. and Assess. **73:** 237–251.
Poesen, J. & Lavee, H. (1994): Rock fragments in top soils: significance and processes. – Catena **23:** 1–28.
Poesen, J. & Lavee, H. (1997): How efficient were ancient harvesting systems in the Negev desert, Israel? – Bull. Seanc. – Acad. Roy. Sci. d'Outre-Mer Mededelingen der Zittingen – Konin. Acad. Overzeese Wetenschappen **43:** 405–419.
Puigdefabregas, J. (2005): The role of vegetation patterns in structuring runoff and sediment fluxes in drylands. – Earth Surf. Proc. and Landf. **30:** 133–147.
Reifenberg, A. (1947): The Soils of Palestine. – Murby, London.
Renard, K. G. (1979): Rainfall simulation as a research tool. – Proc. Rainf. Simulat. Worksh., Tucson, AZ, USDA-SEA, ARM-W-**10:** 60–64.
Ries, J. B., Seeger, M., Iserloh, T., Wistorf, S. & Fister, W. (2009): Calibration of simulated rainfall characteristics for the study of soil erosion on agricultural land. – Soil and Till. Res. **106:** 109–116.
Rietkerk, M., Dekker, S. C., De Ruiter, P. C. & Van De Koppel, J. (2004): Self-organized patchiness and catastrophic shifts in ecosystems. – Science **305:** 1926–1929.
Rosenan, N. & Gilad, M. (1985): Atlas of Israel, Meteorological data, sheet IV/2, Carta, Jerusalem.
Salomon, O. & Schick, A. P. (1980): Infiltration tests. – Arid Zone Geosys., Res. Rep., Hebrew Univ. Jerusalem: 55–115.
Schlesinger, W., Raikes, J., Hartley, A. & Cross, A. (1996): On the spatial pattern of soil nutrients in desert ecosystems. – Ecology **77:** 364–374.
Schreiber, K. F., Yair, A. & Shachak, M. (1995): Ecological Gradients Along Slopes of the Northern Negev Highlands, Israel. – Adv. GeoEcol. **28:** 209–229.

SHANAN, L., EVENARI, M. & TADMOR, N. H. (1967): Rainfall patterns in the Central Negev desert. – Israel Explor. J. **17:** 163–184.
SHNERB, N. M., SARAH, P., LAVEE, H. & SOLOMON, S. (2003): Reactive grass and vegetation patterns. – Phys. Rev. Lett. **90:** 038101-1–038101-4.
STAVI, I., LAVEE, H., UNGAR, E. D. & SARAH, P. (2009): Ecogeomorphic feedbacks in semiarid rangelands: a review. – Pedosphere **19** (2): 217–229.
STONE, J. J. & PAIGE, G. B. (2003): Variable rainfall intensity rainfall simulator experiments on semi-arid rangelands. – In: RENARD, K. G., MCELROY, S., GBUREK, W., CANFIELD, E. & SCOTT, R. L. (eds.): Proc. 1st Interagency Conference on Research in the Watersheds: 83–88.
STRAEHL, S. (2012): Reaktion der Vegetation auf Trockenstress im nördlichen Teil der Negev. – Regio Basilensis **53** (1/2): 87–93.
VAN DE KOPPEL, J. & RIETKERK, M. (2004): Spatial interactions and resilience in arid ecosystems. – Amer. Natural. **163:** 113–121.
VON HARDENBERG, J., MERON, E., SHACHAK, M. & ZARMI, Y. (2001): Diversity of vegetation patterns and desertification. – Phys. Rev. Lett. **87** (9): 198101-1–198101-4.
WALKER, A. S. (1986): Eolian landforms. – In: BLAIR JR., R. W. (eds.): Geomorphology from Space: a Global Overview of Regional Landforms. – Spec. Publ. **486:** 447–520, NASA Sci. and Techn. Branch, Washington DC.
YAALON, D. H. & DAN, J. (1974): Accumulation and distribution of loess-derived deposits in the semi-desert and desert fringe areas of Israel. – Z. Geomorph. **20:** 91–105.
YAIR, A. & DANIN, A. (1980): Spatial variations in vegetation as related to the soil moisture regime over an arid limestone hillside, Northern Negev Israel. – Oecologia **47:** 83–88.
YAIR, A., SHARON, D. & LAVEE, H. (1980): Trends in runoff and erosion processes over an arid limestone hillside, northern Negev, Israel. – Hydrol. Sci. **25** (3): 243–255.
YAIR, A. & SHACHAK, M. (1982): A case study of energy, water and soil flow chains in an arid ecosystem. – Oecologia **54** (3): 389–397.
YAIR, A. & LAVEE, H. (1985): Runoff generation in arid and semi-arid areas. – In: ANDERSON, M. G. & BURT, T. P. (eds.): Hydrological Forecasting: 183–220, Wiley, Chichester.
YAIR, A. (1994): The ambiguous impact of climate change at a desert fringe: Northern Negev, Israel. – In: PYE, K. (eds.): Effects of Environmental Change in Drylands: 199–227.
YAIR, A. (1999): Spatial variability in the runoff generated in small arid watersheds: implications for water harvesting. – In: HOEKSTRA, T. M. & SHACHAK, M. (eds.): Arid Land Management, toward Ecological Sustainability: 212–222.
YAIR, A. & RAZ-YASSIF, N. (2004): Hydrological processes in a small arid catchment: scale effects of rainfall and slope length. – Geomorpholohgy **61:** 155–169.
YAIR, A. & KOSSOVSKY, A. (2002): Climate and surface properties: hydrological response of small arid and semi-arid watersheds. – Geomorphology **42** (1/2): 43–57.
YIZHAQ, H., GILAD, E. & MERON, E. (2005): Banded vegetation: biological productivity and resilience. – Physica A **356:** 139–144.
ZAADY, E., GROFFMAN, P., SHACHAK, M. (1996): Litter as a regulator of N and C dynamics in macrophytic patches in Negev desert soils. – Soil Biol. and Biochem. **28** (1): 39–46.
ZOHARY, M. (1962): Plant life of Palestine. – The Roland Press Company, New York.

Addresses of the authors:

H. Hikel (corresponding author), N. J. Kuhn, U. Hoffmann and S. Straehl, Department of Environmental Science, Physical Geography and Environmental Change, University of Basel Klingelbergstrasse 27, 4056 Basel, Switzerland; e-mail: Harald.Hikel@unibas.ch, phone: + 41-61-2670733

W. Schwanghart, Institute of Earth and Environmental Science, University of Potsdam, 14476 Potsdam-Golm, Germany.

A. Yair, Department of Geography at the Hebrew University of Jerusalem, Mount Scopus Jerusalem, 91905 Israel.

F-GEO_57-1_S001-201.indb 58 16.02.2013 16:36:15

5. Combining remote sensing and spatial statistics for the analysis of shrub patterns in arid regions

Hikel H., Jarmer T., Kuhn N.J., Shoshany M., Schwanghart W. (in prep.): Combining remote sensing and spatial statistics for the analysis of shrub patterns in arid regions.

Combining remote sensing and spatial statistics for the analysis of shrub patterns in arid regions

Harald Hikel[1], Thomas Jarmer[2, 3], Nikolaus J. Kuhn[1], Maxim Shoshany[2], Wolfgang Schwanghart[1, 4]

Affiliations

1 Department of Environmental Science, Physical Geography and Environmental Change, University of Basel, Klingelbergstrasse 27, 4056 Basel, Switzerland

2 Mapping and GeoInformation Engineering, Faculty of Civil and Environmental Engineering, Technion – Israel Institute of Technology, Haifa 32000, Israel

3 Institute for Geoinformatics and Remote Sensing, University of Osnabrueck, Barbarastrasse 22b, 49076 Osnabrueck

4 Institute of Earth and Environmental Science, University of Potsdam, Karl-Liebknecht-Strasse 24-25, 14476 Potsdam-Golm, Germany

(🖂) **Corresponding author:**
Harald Hikel
Tel: 0041-61-267 07 33
Fax: 0041-61-267 0740
e-mail: Harald.Hikel@unibas.ch

Abstract

Arid and semi-arid areas are often covered by sparse and patchy vegetation. The spatial patterns are related to water scarcity, topography and substrate that in turn reflect prevalent geomorphological and hydrological processes. We hypothesize that this relation can be applied to support mapping of ecohydrological environments in dryland areas. The aim of this study is to develop an approach towards automated mapping of ecohydrological environments in drylands. Mapping was carried out at the experimental catchment site nearby Sede Boqer, Israel, along two hillslope transects. Twenty rectangular plots were surveyed to determine the percent vegetation cover. A ground based hyperspectral camera was used to image transects with a spatial resolution of 0.05 m. Plant canopy was obtained using an unsupervised classification. In addition, an aerial photo with a spatial resolution of 0.5 m was utilized to map plants at a larger spatial extent. Both datasets were used to calculate spatial vegetation pattern indices such as vegetation density, lacunarity, bare area fragmentation index and patch upslope side length/area ratio. The indices were investigated regarding their dependence on the spatial resolution of the datasets. Indices with a high degree of explanatory power and scale independence were then used as variables in a decision tree model for automated mapping of ecohydrological environments. The results indicate that the spatial pattern indices can be used as an identification tool of ecohydrological environments. The result suggests that mapping of ecohydrological environments in arid and semi-arid areas can be supported by vegetation detection using remote sensing and digital image processing.

Keywords

Automated mapping, vegetation patterns, ecohydrology, remote sensing

1. Introduction

Arid and semi-arid areas are often covered by sparse and patchy vegetation. The spatial patterns of vegetation are related to water scarcity and reflect the feedback mechanisms with geomorphological and hydrological processes (Boer & Puigdefabregas 2005). Understanding these patterns and feedback mechanisms is within the research scope of the rising field of ecohydrology (Cammeraat & Imeson 1999, Imeson & Prinsen 2004).

The Negev Desert in Israel is characterised by a mosaic of vegetated patches within a matrix of bare ground. Essential ecosystem resources such as soil moisture, sediment, organic matter and nutrients cohere with vegetation patterns as well as plant productivity and diversity (Olsvig-Whittaker et al. 1983). Topography, rainfall intensity, antecedent moisture content, bedrock outcrops, soil depth and soil surface properties affect runoff generation. Water, sediment and nutrients are redistributed from runoff generating source areas to sink areas where water preferentially infiltrates (Shashak et al. 1998). Systems of source and sink areas in dryland regions have been described for different arid and semi-arid regions, such as found in Israel (Yair & Danin 1980), Australia (Ludwig et al. 1999) and Spain (Puigdefabregas & Sanchez 1996). According to Yair and colleagues (Schreiber et al. 1995, Olsvig-Whittaker et al. 1983) the mosaic of vegetated and non-vegetated patches is related to different ecohydrological environments (EHEs). The topology or downward sequence of EHEs determines how water is distributed in the landscape and, thus, the identification of EHEs contributes to a better understanding of dryland hydrological systems and finally, how vegetation responds to rainfall events. This information can further be used for the up- and down-scaling and is required to link remotely sensed and ground based studies (Shoshany 2012, Shoshany et al. 1995).

Vegetation studies in arid regions have largely focused on species abundances measured at plot scale or along transects (e.g. Pariente 2002, Boeken & Shashak 1994). Catchment wide information on plant cover at high spatial resolution is often unavailable due to the large efforts required for detailed mapping (Puigdefabregas 2005) and since extrapolations from plots and long transects to larger areas are problematic (Hill & Schuett 2000). Wu (2004) emphasized the need to quantify spatial heterogeneity and its scale dependency (i.e. how patterns change with spatial scale) to understand, characterize and monitor landscape patterns. This scale problem constitutes a major challenge for ecohydrological studies. Remote sensing is a practical method of catchment-wide data collection with spatial resolution being a limiting factor for describing vegetation patterns. Downscaling methods provide ways to obtain information on subgrid-scale but require parameterization schemes of fine-scale heterogeneity (Zhang et al. 1998). In addition, vegetation patches are often too small and most of the required information on different vegetation structures is lost (Puigdefabregas 2005).

In this study we address the problem of scale dependency in vegetation pattern analysis using ground based imaging with very high spatial resolution (0.05 m) and investigate how these patterns are represented in a coarser resolved (0.5 m) orthophoto obtained from airborne imaging. Our aim is to find scale-independent pattern indices operating at both spatial scales that support mapping EHEs in areas where very high spatial resolution data is unavailable. We hypothesize that different surface conditions can lead to variable vegetation patterns at the hillslope scale and that spatially distributed data on vegetation patterns can support the automated mapping of EHEs. Our objectives are (i) to identify vegetation from ground based hyperspectral imagery, (ii) to characterize vegetation patterns using different vegetation pattern indices, (iii) to test and apply measures that are independent of the spatial resolution of our remotely sensed imagery and (iv) to automatically map EHEs.

2. Study area and environmental settings

The study area is located near Sede Boqer (30°52’N, 34°48’E) in the Northern Highlands of the Negev Desert of Israel, at an altitude of 510 m a.s.l. (Fig.1). The experimental catchment is a second order drainage basin situated in an arid rocky environment (Schreiber et al. 1995, Olsvig-Whittaker et al. 1983) and covers an area of 0.05 km^2.

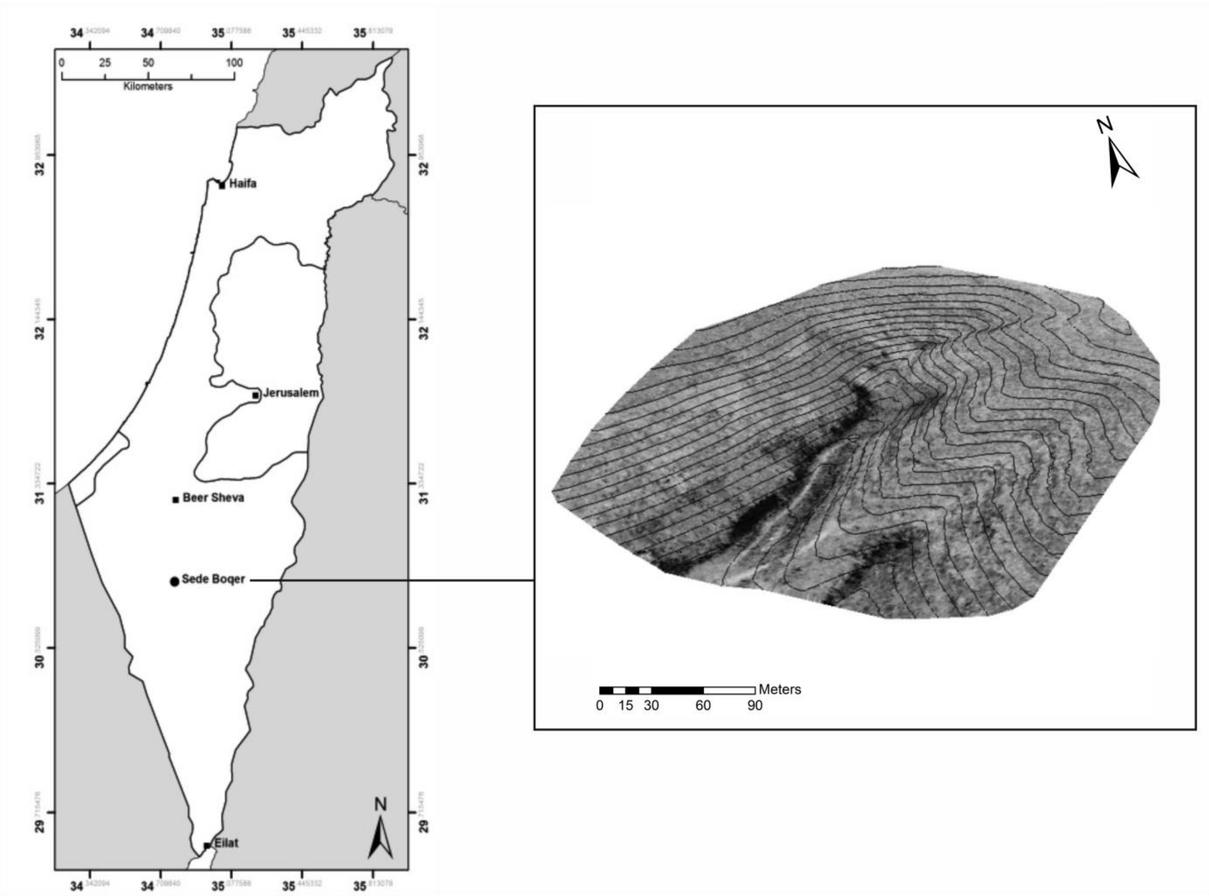

Figure 1: Map of Israel and location of the study site (Sede Boqer) in the Negev Highlands, Israel.

The climate in the Northern Negev is arid and characterized by large seasonal contrasts governed by seasonal shifts of the zonal circulation. The mean annual air temperature is 19.2°C. Mean monthly temperatures range from 9°C in January to 25°C in August. The average annual rainfall is 90mm with the majority of 70 % recorded between December and February. The potential annual evaporation is high and varies between 2000 and 2600 mm (Yair & Kossovsky 2002).

Bedrock consists of limestone and dolomite of Turonian age. The local stratigraphy is composed of three lithological units: the Drorim, Shivta and Netser formations (Fig.2). The three formations are bedded almost horizontally and differ in surface properties (Schreiber et al. 1995, Olsvig-Whittaker et al. 1983, Yair & Shashak 1982).

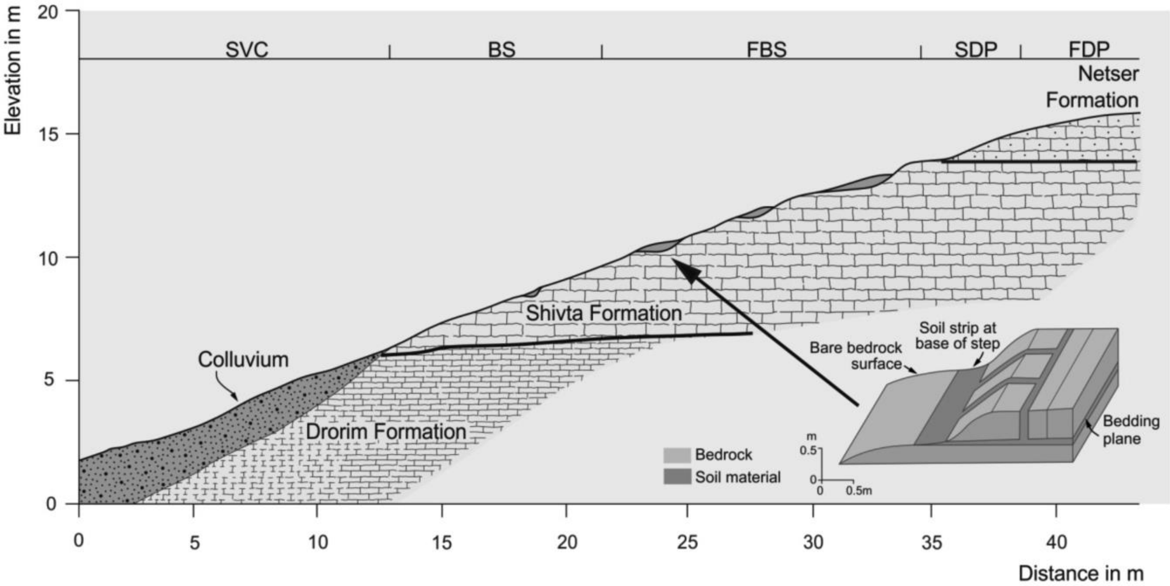

Figure 2: Lithological formations within the studied catchment (modified after Yair & Shachak 1982, Olsvig-Whittaker et al. 1983, Schreiber et al. 1995) and EHEs at the hillslope scale: flat desert pavement (FDP), gently sloped desert pavement (SDP), non-fissured bedrock slope (BS), stepped and fissured bedrock slope (FBS) and slope and valley colluvium (SVC).

The Netser formation is characterized by thinly bedded chalky limestone and flint concretions. Surface substrate mainly consists of a rocky substratum and soils are very shallow and patchy (Yair & Danin 1980). The Shivta formation is a thinly bedded and densely fissured formation and forms a stepped topography, structured in almost horizontal layers. Soils developed as small soil patches in aeolian silts and fine sands deposited either directly by the wind or redeposited by slopewash. At the base of the bedrock steps soils developed in non-contiguous soil strips and rock fissures of the surficial rock strata. The Drorim formation represents the lowest unit, which is densely jointed and covered with an extensive colluvial mantle with downslope increasing thickness (Yair & Shachak 1982).

The lithological formations within the study site provide distinct structural properties creating different surface environments (Yair & Danin 1980). According to the studies by Olsvig-Whittaker et al. (1983) and Schreiber et al. (1995) following EHEs are distinguished along a hillslope (Fig.2): flat desert pavement (FDP), gently sloped desert pavement (SDP), non-fissured bedrock slope (BS), stepped and fissured bedrock slope (FBS) and slope and valley colluvium (SVC). These meso-scale physical environments in various ways act upon water redistribution (Schreiber et al. 1995, Olsvig-Whittaker et al. 1983, Yair & Danin 1980). Runoff is predominantly generated on non-vegetated patches with low infiltration capacity, leading to run-on infiltration on vegetated patches with higher infiltration capacity. The spatial patterns of infiltration-excess overland flow are controlled by soil, surface properties, soil moisture and precipitation intensity.

The catchment hosts plant communities that represent a transition between the Irano-Turanian plant geographical region and the Saharo-Arabian region (Zohary 1962, Yair & Danin 1980). A transition from semi-desert communities (10-30% perennials vegetation cover) on rocky upper slopes, to patches of true desert communities (less than 10% perennial cover) on the lower colluviums reflects a very narrow ecotone usually found at larger spatial scales. Dominant species of the perennials are shrubs and semi-shrubs *Artemisia herba-alba*, *Gymnocarpos decander*, *Hammada* *scoparia*, *Noaea mucronata*, *Reamuria negevensis* and *Zygophyllum dumosum*. An assortment of annuals, geophytes and hemicryptophytes can be identified especially during the rainy winter season (Olsvig-Whittaker et al. 1983).

3. Material and Methods

In order to characterize the small-scale heterogeneity of surface properties of the study site, a north-facing and a south-facing hillslope transect were selected. Both cover (i) the local stratigraphy from the thalweg to the divide of the basin and (ii) the small-scale heterogeneity within each EHE. The EHEs are related to the differences in the local stratigraphy and are easily identified in the field (Fig.3).

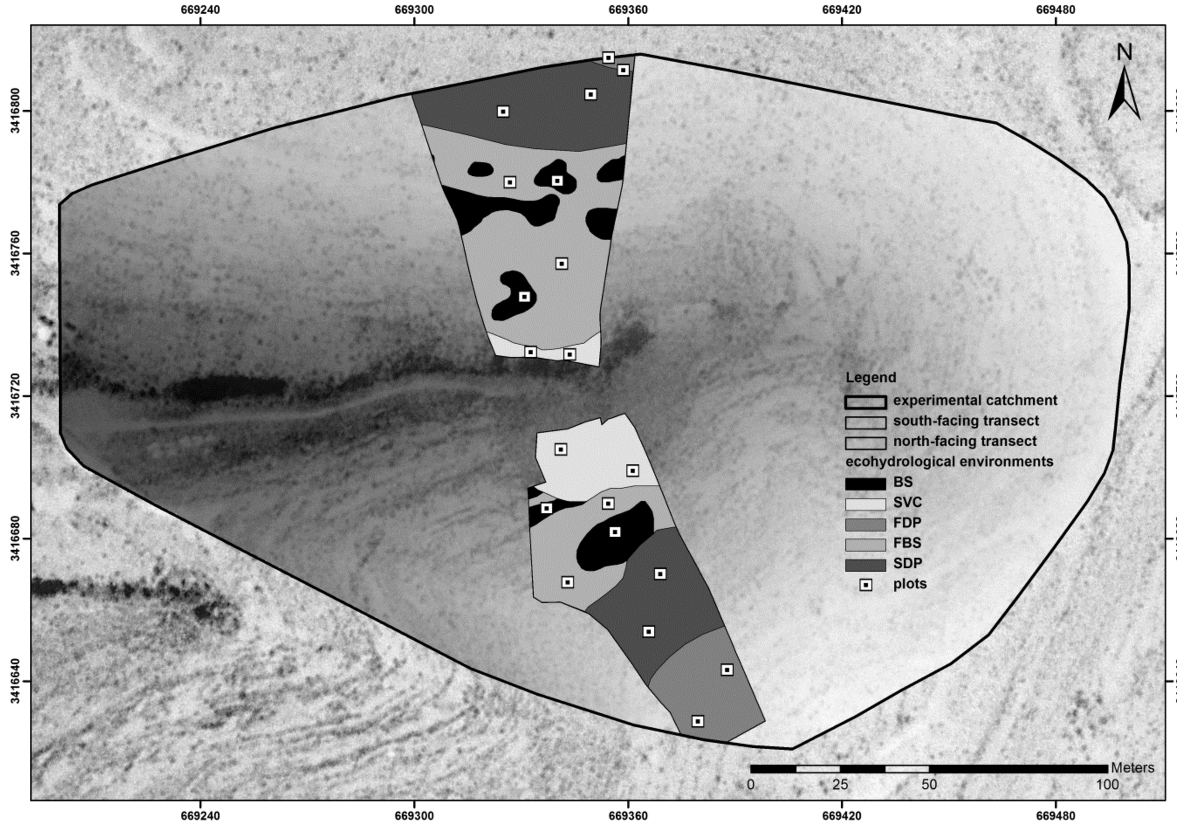

Figure 3: Map of the studied catchment showing the location of the plots and the different EHEs within the two hillslope-transects. EHEs: (FDP) flat desert pavement, (SDP) gently sloped desert pavement, (BS) non-fissured bedrock slope, (FBS) stepped and fissured bedrock slope, (SVC) slope and valley colluvium.

3.1 Available Data

The available data basis for further analysis is an orthorectified aerial photograph. The image was acquired in May 1993 and has three bands in the visible range (RGB). We assume that the temporal gap between field visit and image acquisition only insignificantly affects our results. Tongway & Ludwig (1994) postulated that vegetation pattern and cover is related to long-term average climatic conditions, indicating equilibrium between water availability by rainfall and runoff reallocation and vegetation patterning and density. According to the findings of Littmann & Berkowitz (2008) precipitation in the Negev Desert is characterized by high interannual variability but lacks a longterm trend. Hence, we assume vegetation patterns derived from the aerial photograph to be representative for the findings obtained during our field stay. A pixel size of 0.5 m is sufficiently high to visually distinguish the shrub canopies from their surrounding background.

Since vegetation absorbs most incoming light at visible wavelengths, pixels with low DN-values (Pixel Digital Number) are indicative for desert shrub canopies in the photograph (Qin et al. 2006). Here we adopt this approach since the dark vegetation is in strong contrast to the relatively bright background of the carbonate rich bare ground. We identify vegetation patches using grayscale image morphology. Prior to the analysis a principal component analysis (PCA) was conducted to obtain a grayscale image that best represents the albedo contrasts between vegetation and bare ground. The band with the first principal component scores (PC1) was found to incorporate this information since it represents the brightness of the data set. In a second step, regional minima were extracted from the PC1 using the flood fill operator in ArcGIS. The flooded image was then subtracted from PC1. Thirdly, a threshold was applied to the difference image to obtain a binary image where ones refer to vegetation and zeros to bare ground. A threshold of 40 was identified by visual comparison of the binary image with the RGB imagery and impressions obtained in the field.

3.2 Data acquisition and preparation

3.2.1 Mapping

Field observation was conducted in spring/summer 2008 and 2009. Primary purpose of the observation was to quantify the percent vegetation cover and composition along two hillslope-transects. Ten 3m x 3m plots and ten 10m x 10m plots distributed within the different EHEs were selected for the inventory (Fig. 3). Vegetation density was determined as the ratio of canopy cover to plot size. Canopy cover was calculated by measuring diameter and perimeter of each plant. Vegetation mapping was conducted using the mapping chart of Braun Blanquet and Zohary (Zohary 1962). The anatomy of shrubs is based on the definition by Ferguson (1964). The results of the field observation were used to validate the developed remote sensing approach.

3.2.2 Hyperspectral imaging

Hyperspectral imagery has been acquired by a VDS Vosskühler Cool-1300Q hyperspectral camera in the spectral range 300-1100nm. The camera produces spectral data cubes of 1280x1024 pixels in 91 spectral bands with 12 bit radiometric resolution. A Nikon's NIKKOR 105mm telephoto lens with 23°20' field of view (FOV) was mounted on the camera. The output spectra of the camera are in digital numbers (DN).

In total, a number of 108 images were acquired from the entire valley, from which nine images were used in this study. The images were georeferenced by image-to-image georeferencing based on images pictured by a Totalstation (TOPOCON Imaging Station IS03). Hyperspectral data sets were reduced to 944x768 to cut off outer parts of the images which are blurred and have less light intensity. Additionally, the spectral range was limited to 470-820 nm (37 spectral bands) to exclude noisy parts of the recorded spectra from further analysis. Since hyperspectral data contains redundant information principle components analysis was performed and the first three principle components explaining more than 99 percent of inherent spectral variance were extracted.

Images were classified into five or six (in case of sky included in the image) classes using the k-means algorithm implemented in ENVI of which one class was found to well represent vegetation cover. Further on, classified images were rectified to map coordinates. Since locating ground control points (GCP) on classified images was almost impossible, GCPs were identified on original hyperspectral images and transferred to classified data using pixel coordinates. To validate the high-resolution vegetation canopy data obtained from ground-based imaging the location (XY-coordinates) of 99 single shrubs was determined by using the TOPCON Totalstation. The validation shows an accuracy of 88 percent. After geocoding and validating the classified images were combined to a mosaic of the investigated area.

3.2.3 Laser scanning

We used the automated Totalstation (TOPCON Imaging Station IS03) to acquire 3D point clouds as a basis for a digital elevation model (DEM) of the study site. The study site was scanned from various positions and the pointclouds transformed to a local coordinate system using tie point registration. Pointcloud density varies depending on distance but averages ~25 points m^{-2}. The data were processed with the software IMAGE MASTER (TOPCON). In a second step, a gridded digital surface model with 0.5 m cellsize was obtained using bilinear interpolation and vegetation and erroneous elevation data were filtered out using a bottom-hat filter to obtain a DEM. Subsequent analysis were carried out using TopoToolbox (Schwanghart & Kuhn 2010) and ESRI ArcGIS 9.3 and 10.0.

3.2.4 Derivation of plant canopy from ground based imagery

The high-resolution vegetation canopy data obtained from ground-based imaging was further employed to identify trunk locations of individual plants. Trunk locations were obtained by a procedure that accounts for both the horizontal and vertical viewing angle and overlapping canopies of individual plants.

As a first step, the georeferenced, classified image was transformed from the orthogonal coordinate system to the Θ-D space where Θ is the azimuth angle and D the distance between the imaging station and each pixel center (Fig.4a). A resolution of $2x10^{-4}$ radians for Θ and 0.02 m for D was chosen. Subsequently, the plant height was estimated for each profile (Fig.4b) by identifying the distant boundary of each plant object in the image. From here, the vertical angle between the pixel as derived from the DEM and the horizontal distance were used to calculate the plant height. Closely arranged plants with merged shadows where accounted for by assuming a maximum plant height of 0.4 m. The maximum plant height was observed in our plot data. As soon as this height was reached the height was reset to zero and plant height accumulation was restarted. Subsequently, all local maxima in the plant height map were identified, which were then transformed back into the XY space. Based on our data acquired in the field, the mean width-height ratio of shrubs is 0.8. This value was then taken to calculate the planform extent of the canopy of each individual plant (Fig. 5).

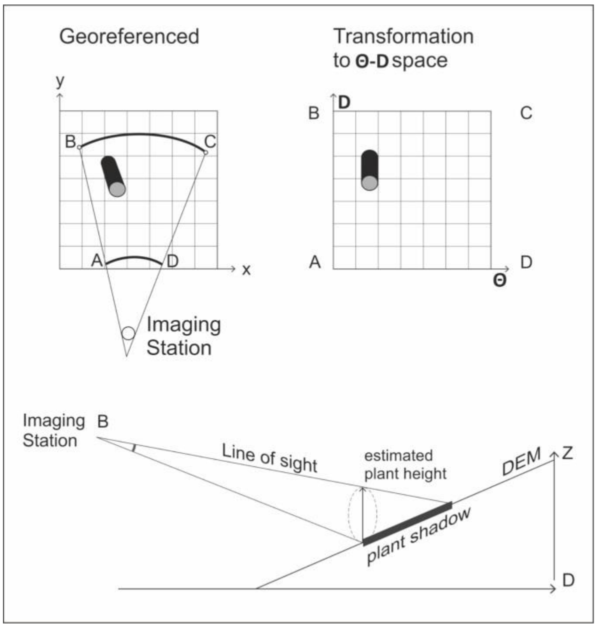

Figure 4a,b: Schematic illustration of the procedure to obtain trunk locations regarding the horizontal and vertical viewing angle of individual plants.

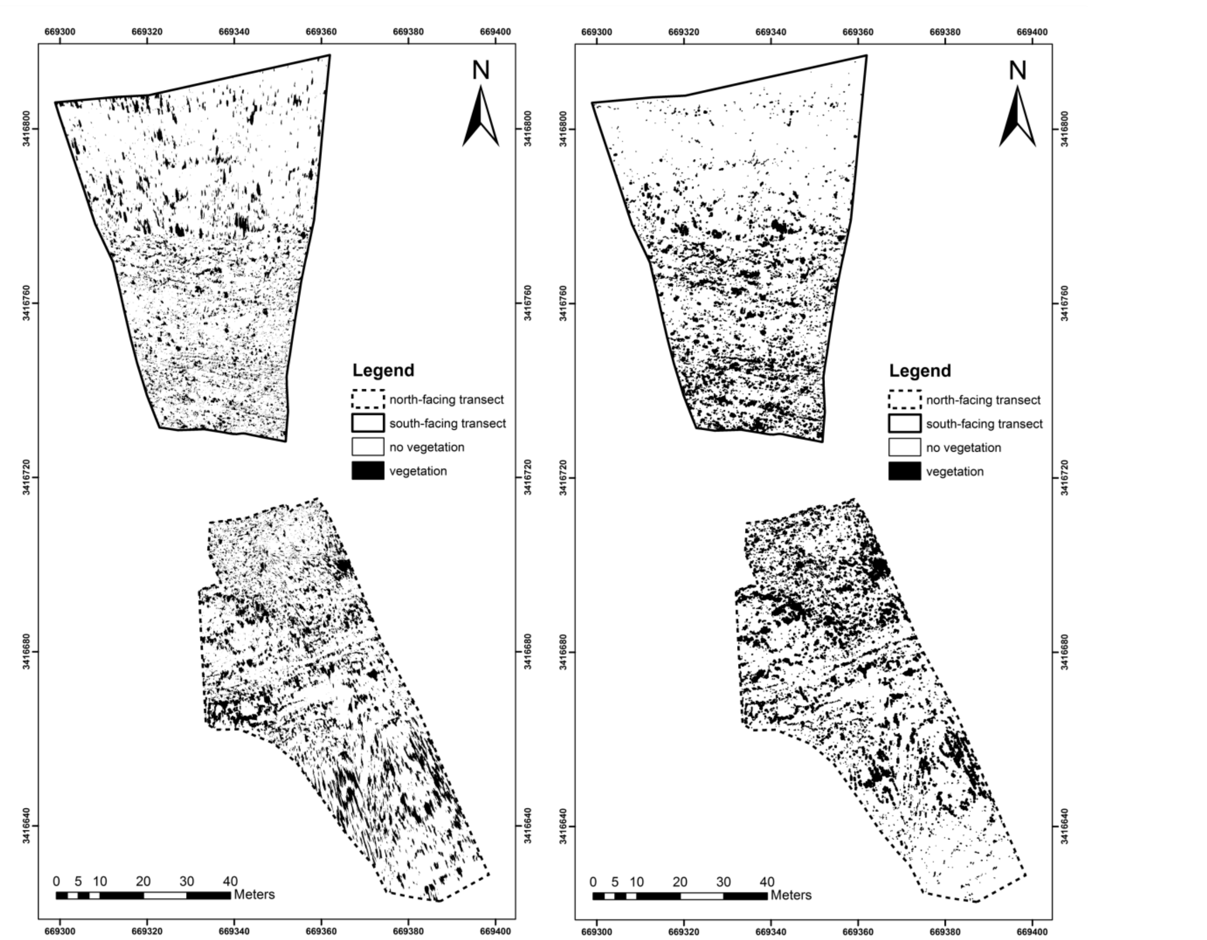

Figure 5: Planform extent of high-resolution vegetation canopy data (Fig.5, right) obtained from ground-based imaging (Fig.5, left).

3.3 Vegetation pattern analysis and explorative data analysis

A number of measures and indices exist to characterize spatial patterns of vegetation (Imeson & Prinsen 2004). Following vegetation pattern indices were used: vegetation density, lacunarity, bare area fragmentation index and patch upslope side length/area ratio (PUSLAR). Two datasets were generated for the vegetation analysis. A hillslope transect dataset with a resolution of 0.05 m (hyperspectral image) and a catchment dataset with a resolution of 0.5m (orthoimage). Vegetation pattern indices were calculated for both datasets.

Wu (2004) emphasized that using pattern indices must be based on the same spatial resolution and extent whereas no “optimal” or “general” scale for characterizing spatial heterogeneity is specified. We calculated the indices within 5m x 5m blocks (block statistics) for both images to obtain spatially distributed values of the vegetation measures. This block size was chosen since it provides a comparable basis to field findings and a sufficiently fine spatial resolution for mapping and interpretation of results. In summary, we calculated 263 blocks for each of the indices and both types of imagery, respectively.

The indices were calculated from the differently resolved image datasets to investigate their sensitivity to changes in image spatial resolution. We argue that if index values are insensitive against different spatial resolutions, the index is scale independent at least at the resolution range spanned by our imagery. Scale independent vegetation pattern indices calculated from the orthoimage are preferably used for further analysis. To examine scale dependence, the distributions of the vegetation indices calculated from both image were plotted as boxplots and visually compared. In addition, blockwise comparison of the indices was accomplished using linear regression (R^2) and by calculating the Root Mean Square Error (RMSE). A strong linear correlation and a low RMSE value indicate that the calculated vegetation pattern indices are independent from the resolution of the imagery used in this study.

Vegetation density was calculated as the aerial fraction covered by plant canopy from our imagery and was mapped by field observation.

Lacunarity describes the shape and the distribution of gap sizes in fractal geometric objects (Imeson & Prinsen 2004) obtained from a “moving window” algorithm (Mandelbrot 1983). Lacunarity for a box size r is defined as the mean-square deviation of the variation of mass distribution probability $Q(M,r)$ divided by its square mean, where $A(r)$ refers to the lacunarity at box size r and M indicates the mass respectively pixels of interest.

$$A(r) = \frac{\sum_M M^2 \, Q(M,r)}{[\sum_M M \, Q(M,r)]^2}$$

The number of boxes with radius r and mass M is defined as $n(M,r)$. $Q(M,r)$ is the probability distribution obtained by dividing $n(M,r)$ by the total number of boxes. The index and application is described in detail by Imeson & Prinsen (2004). Lacunarity was calculated with the Lacunarity Analysis Tool (Dong 2009). On the basis of the calculated lacunarity values vegetated patch clumpiness can be determined. High decay rates correspond to low lacunarity or a regular alternatively random distribution. Low decay rates correspond to high lacunarity and hence to more clumped patterns. An important advantage of the lacunarity index over other vegetation pattern indices is that the lacunarity curve depends on the pattern of aggregation. Hence the lacunarity index is independent from vegetation density.

The bare area fragmentation index was described by Jaeger (2000) to determine the degree of landscape division (D). The index is defined as the probability that two randomly chosen places in the map under investigation are not situated in the same undissected area (Jaeger 2000), where A_t is the total map area, A_i is the area of the n patches ($i=1, \ldots, n$) and n is the number of patches in the map. Imeson & Prinsen (2004) adopted this index for a semi-arid area in southeast Spain.

$$D = 1 - \sum_{i=1}^{n} \left(\frac{A_i}{A_t}\right)^2$$

An advantage to other measures is that the index is insensitive to omission or addition of very small patches. The bare area fragmentation index is used in this study to determine how strongly vegetated patches dissect the bare area. Hence areas, which are highly fragmented, have few small bare patches.

PUSLAR was calculated to determine the impact of the vegetation structure on runoff infiltration. Previous studies (Bergkamp et al. 1996, Imeson & Prinsen 2004) have shown that most of the runoff infiltrates at the upslope side of the vegetation patches. PUSLAR is calculated for the vegetation patches by dividing the number of cells of a patch that have minimum one upslope un-vegetated cell by the area of the patch using TopoToolbox (Schwanghart & Kuhn 2010), where n is the number of patches, A_i the area of n patches ($i=1, \ldots, n$), N_i the number of upslope side cells and L_c the cell length. The advantage of the calculated index is that it is insensitive especially for highly variable patch sizes.

$$U = \sum_{i=1}^{n} \frac{N_i * L_c}{A_i}$$

3.4 Decision Tree Modelling

A decision tree (IBM SPSS Version 20) approach was used to train and validate an EHE classification model based on the vegetation pattern indices. The classification tree approach evaluates a set of "if-then" logical conditions between the dependent and independent variables and splits the dataset according to the largest deviance produced (Rejwan et al. 1999). A decision tree model is a non-linear and non-parametric approach that automatically identifies interactions among variables and displays these interactions as a simple tree diagram. No implicit assumptions are made about the underlying relationships between the independent and the dependent variables (Rejwan et al. 1999). The Classification and Regression (CRT) growing method was chosen to generate the decision tree. The maximum tree depth which determines the maximum number of levels of growth beneath the root node was limited to five levels. The default value of 10 cases was defined for parent nodes as well as for child nodes. To avoid overfitting the model the decision tree was pruned by specifying the maximum difference in risk as zero. The branches of the tree are identified by leave-one-out cross validation (LOOCV) of the dataset. LOOCV uses a single observation from the original sample as validation data and the remaining observations as training data. This procedure is repeated such that each observation in the sample is used once for validation (Picard & Cook 1984). CRT splits the data into segments that are as homogeneous as possible with respect to the dependent variable. Terminal nodes in which all cases have the same value for the dependent variable are homogeneous "pure" nodes. A further output of the calculation is the predicting accuracy of the decision tree model. The results were visually revised and compared with the generated data based on field mapping.

4. Results and interpretation

4.1 Vegetation density

Table 1 shows the vegetation density values of the field observation dataset and of both remote sensing datasets. Vegetation density was calculated for each plot regarding the different EHEs (Figure 3). For further analysis the field observation dataset was used as reference. Linear regression analysis and the RMSE calculation shows a R^2=0.85 and a RMSE=0.5 comparing the orthoimage dataset with the field observation dataset and a R^2=0.89 respectively a RMSE=0.8 comparing the hyperspectral image dataset with the field observation dataset. Hence, it can be identified that vegetation density values do not differ significantly between the different analysis methods. The vegetation density values generated by field observation, hyperspectral image analysis and orthoimage analysis significantly ($p<0.05$, p: error probability) differ among each EHE. Due to the challenges in georeferencing the ground based imagery with the orthoimage an accordance of 100% is not within reach. The highest inaccuracy is found where image distortions are highest, such as at the upper edge of both transects and in the middle of the north-facing transect.

Table 1: Average vegetation density in percent for the different EHEs as calculated from the orthoimage and hyperspectral image analysis and obtained from field observation.

Ecohydrological unit	Orthoimage	Hyperspectral Image	Field Observation
FDP	10	9	11
SDP	17	15	15
BS	9	11	10
FBS	18	23	20
SVC	56	34	30

Based on these results we infer that some but not all EHEs can be discriminated using vegetation density alone since vegetation density lacks information on the spatial configuration of vegetation patches. In combination with the other indices, however, vegetation density is of use for the identification of different EHEs within the studied experimental watershed.

4.2 Scale dependence of vegetation pattern indices

The scale dependency of vegetation pattern indices is tested using the results of the vegetation classifications obtained from the hyperspectral, groundbased imagery and the airborne orthophoto. The hyperspectral image was used as reference. The results of the linear regression and the RMSE calculation are presented in Fig. 6. Albeit small vegetation patches (<0.5m) and single plants remain shrouded by the coarse resolution of the orthoimage, strong linear relations and a high coefficient of determination (R^2) is identified for vegetation density, lacunarity and bare area fragmentation index. Thus we infer that these indices are not sensitive or dependent to the difference in spatial resolution of our imagery. We suppose that small vegetation patches (<0.5m) are limited or alternatively are contiguously located to larger vegetation patches or that some indices are insensitive to omission or addition of very small patches.

In contrast to the previous indices, the correlation between PUSLAR calculated from both images is very low (R^2=0.02). This suggests that PUSLAR is sensitive to the lack of subgrid vegetation detection by the orthoimage analysis. The large discrepancy in PUSLAR values between both analysis methods points to a significant influence of small vegetation patches regarding the PUSLAR. Owing to the scale dependency of PUSLAR we refrained from including this index in the subsequent modeling approach.

Vegetation density (%)

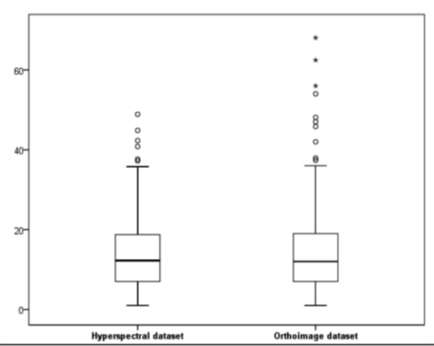

R^2=0.78

RMSE= 0.1

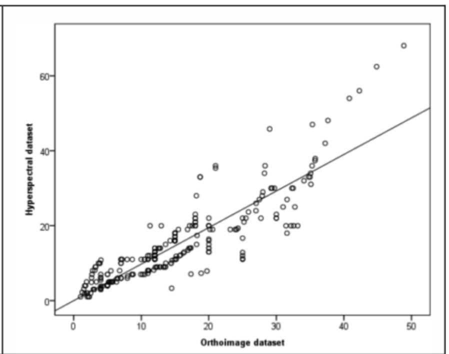

Lacunarity

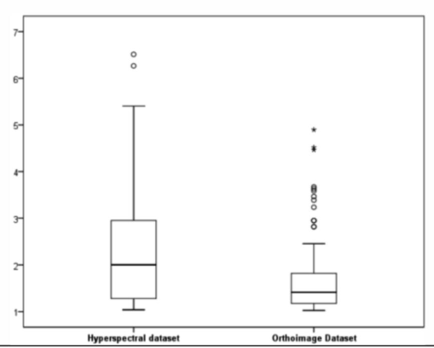

R^2=0.84

RMSE=0.1

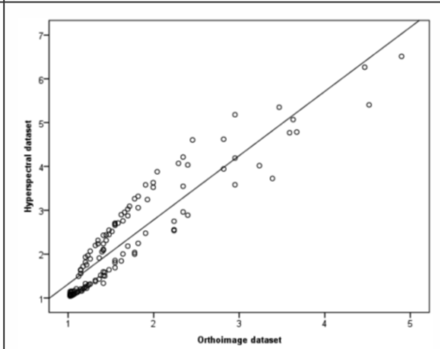

Bare Area Fragmentation Index

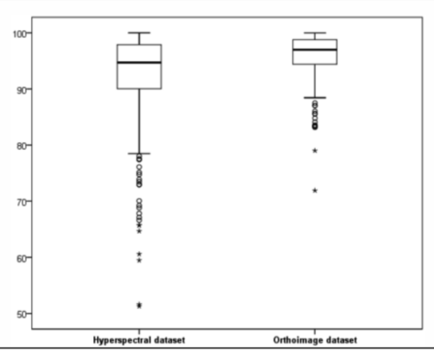

R^2=0.75

RMSE= 0.5

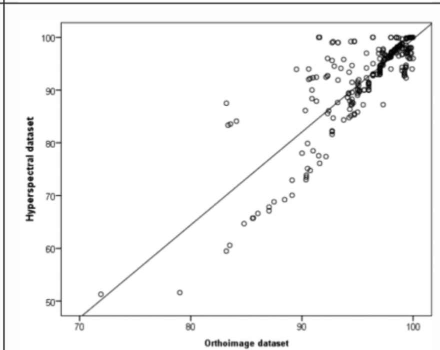

Patch Upslope Side Length / Area Ratio

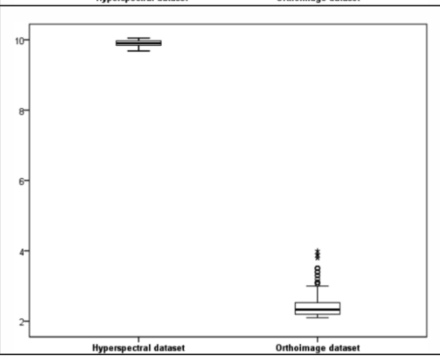

R^2=0.02

RMSE=1.2

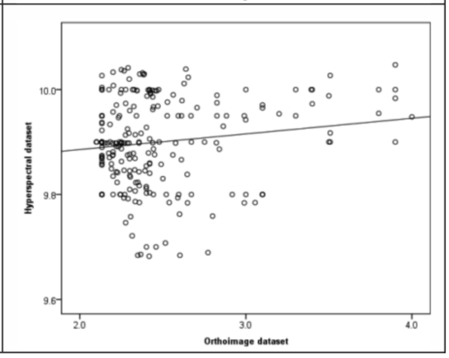

Figure 6: Boxplots, linear regression and RMSE comparing both remote sensing datasets regarding the different vegetation pattern indices to assess the dependence of vegetation pattern indices on the spatial resolution of imagery applied in this study.

4.3 Decision tree

The previous results indicate that three of the four extracted vegetation pattern indices are independent on the resolution of the two datasets. Thus, we anticipate that these indices can be used as discriminatory variables at the scale of the orthoimage, which is available for a larger spatial extent while still being representative for the details observed in the high-resolution, hyperspectral imagery.

Table 2 shows the results of the multiple mean comparisons between different vegetation indices grouped by EHE. For each index the groups with the highest degree of explanatory power ($p<0.05$) were identified. As an example, the averages of the vegetation indices vegetation density and bare area fragmentation index calculated for SVC are significantly different from all other EHEs (Table 2). Thus, we expect SVC to be distinguished well from the other EHEs. In contrast, FDP cannot clearly be distinguished from SDP and BS where no significantly different averages between these two vegetation indices are recorded. A discrimination of these EHEs based on vegetation density and bare area fragmentation index only is expected to be more difficult.

Table 2: Results of the multiple mean comparison between vegetation indices (vegetation density (veg), lacunarity (lac) and bare area fragmentation index (bar)) within EHEs. Significant differences (error probability $p<0.05$) are indicated bold.

	FDP			SDP			BS			FBS			SVC		
	veg	lac	bar	veg	lac	bar	veg	lac	bar	veg	lac	bar	veg	lac	bar
FDP	-	-	-	1.000	1.000	1.000	0.393	1.000	1.000	0.550	**0.026**	1.000	**0.000**	1.000	**0.000**
SDP	1.000	1.000	1.000	-	-	-	**0.019**	0.203	1.000	0.953	0.053	1.000	**0.000**	0.113	**0.000**
BS	0.393	1.000	1.000	**0.019**	0.203	1.000	-	-	-	**0.000**	**0.000**	0.837	**0.000**	1.000	**0.000**
FBS	0.550	**0.026**	1.000	0.953	0.053	1.000	**0.000**	**0.000**	0.837	-	-	-	**0.000**	**0.000**	**0.000**
SVC	**0.000**	1.000	**0.000**	**0.000**	0.113	**0.000**	**0.000**	1.000	**0.000**	**0.000**	**0.000**	**0.000**	-	-	-

Comparing the different vegetation pattern indices it can be identified that vegetation density determines a large part of the EHEs. BS and FDP can hardly be discriminated. Despite the different surface properties of BS and FDP, both units exhibit similar values of vegetation pattern indices. Extensive bedrock outcrops of massive limestone characterize BS. The surfaces are relatively smooth and strongly inclined. In small, local depressions shallow soil has been accumulated generating a small scale, patchy soil cover. Low soil volumes and the dominating rocky surfaces generate dry moisture conditions due to rapid runoff generation and reduced water storage capacity. Water availability and hence beneficial conditions for vegetation growth is related to the distinction in soil volume and distribution. Hence vegetation is concentrated in soil mounds and along small soil patches. The surface of FDP is covered by rocky substratum and shallow and patchy soils. Being exposed to strong winds most of the unconsolidated fine material has been blown out. The uniform surface of FDP is prone to crusting thus delimiting infiltration rates and promoting the generation of Hortonian overland flow. Similarly as in BS, aridity is promoted by the rapid, lateral export of surface waters. Hence, despite their structural difference, BS and FDP are expected to show a similar hydrological behaviour, promoting similar vegetation patterns.

The average lacunarity of FBS differs from that of FDP, BS and SVC, which indicates different patch clumpiness in this EHE. Bedrock in FBS consists of a stepped topography, structured in almost horizontal layers. Bare bedrock prevails but a dense network of joints enables the development of relatively deep soils. In addition, shallow soil patches occur along the base of the bedrock steps. Runoff deeply infiltrates at the interface between rock and soil covered surfaces. Hence this environment provides an improved moisture reservoir for vegetation at certain locations generating a clumped vegetation distribution. Vegetation is concentrated along the stepped environment and the soil filled joints thus following patterns governed by the structural properties of the bedrock not prevalent elsewhere.

FBS lacks a difference to SDP. SDP is situated in a transitional slope position between FDP and FBS. SDP consists largely of bare rock surface and soil surface covered by a rocky layer. In comparison to

FDP soil depth is higher and the covered area larger resulting in higher total infiltration capacities. Since more runoff is retained in the soil moister conditions are generated. Due to the less uniform surface conditions vegetation is distributed more clumped than FDP but less clumped than FBS.

The bare area fragmentation index discriminates SCV from the other EHEs. SVC is characterized by a thick uniform colluvial regolith and benefits from the circumstance that most of the water originated at the upper part of the slope infiltrates at this lower unit. Water deeply infiltrates at the interface between the above rock covered surfaces and the colluvial regolith. This implies that SVC is an environment of moderate water supply. Vegetation cover is relatively dense and less clumped with resulting in a highly area fragmentation characterized by few small bare patches.

FDP, SDP, BS and FBS are characterized by an array of extensive bare areas due to lower vegetation density values and a less uniform surface structure. In comparison to BS the EHEs SDP and FBS show more and smaller bare patches. SDP and FDP also differ regarding the bare area fragmentation index. FDP has less and larger bare patches than SDP but still more and smaller bare patches than BS. In general FDP and SDP are hard to establish due to nearly similar surface properties generating related values for the different vegetation pattern indices. Due to the higher vegetation density values and the higher fraction of rock fragments SDP shows more and smaller bare patches than FDP. The interpretation of the results strongly evidences that vegetation pattern indices are determined by hydrological and geomorphological processes related to variable surface properties, which take place at the small scale. In turn vegetation pattern indices provide an indication of the subsequent interactions and effects within each EHE.

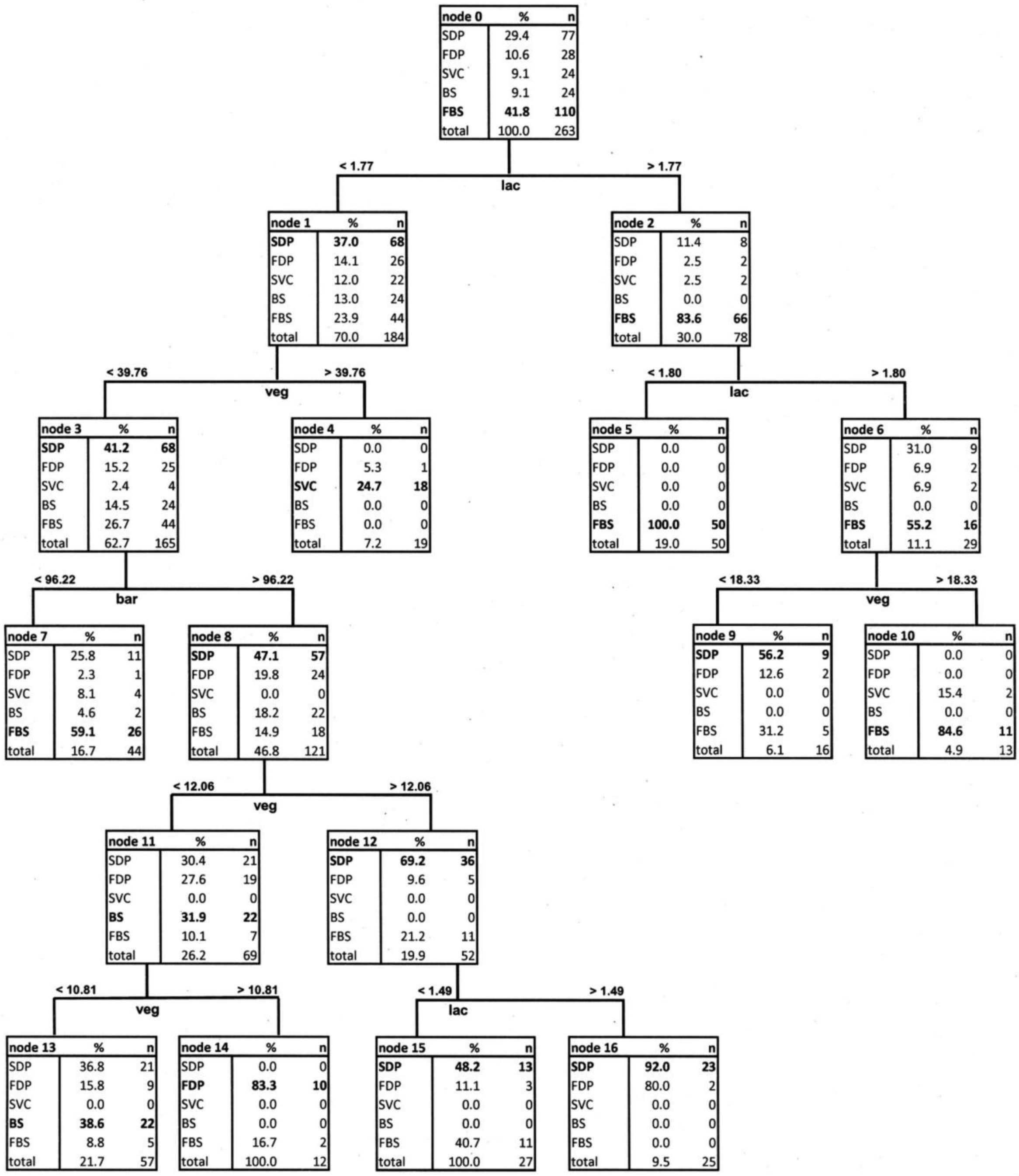

Figure 7: Tree classification results of the EHEs according to the interactive effect of the vegetation pattern indices such as vegetation density (veg), lacunarity (lac) and bare area fragmentation index (bar).

The classification tree that discriminates EHEs based on the vegetation pattern indices is shown in Fig. 7. The tree contains 17 nodes and thereof nine terminal nodes. The maximum tree depth is five. Among the included variables the vegetation pattern indices vegetation density and lacunarity are the most important variables in partitioning the dataset (Table 3). The dataset is first partitioned by lacunarity, which represents the maximum change in deviance where the root node is split in two branches. The left branch predicts the EHEs SVC, BS and FDP. Among the 184 samples 18 samples were correctly simulated as SVC (predicting accuracy of 75.0%), 22 as BS (predicting accuracy of 91.7%) and 10 as FDP (predicting accuracy of 35.7%). Compared to BS and FDP, SVC is determined by high vegetation density values and a low bare area fragmentation index. Vegetation density discriminates BS from SDP, where BS is characterized by lower vegetation density values. Both branches predicted the EHEs FBS and SDP at which both are hard to distinguish due to related surface properties. Compared to SDP and BS, FBS shows higher values for vegetation density and lacunarity resulting in a distinction of these EHEs. The predicting accuracy for FBS was 79.1%, for SDP 58.4%. In total 81 samples of the dataset were misclassified resulting in a prediction accuracy of the classification tree of 69.2% (Table 4). These results indicate that the proposed method is appropriate for simulating the different EHEs within the studied catchment.

Table 3: Discriminatory power (%) and normalized discriminatory power (%) of the three vegetation pattern indices in the decision tree model. Vegetation density has the highest discriminatory power.

Independent variable	Discriminatory Power (%)	Normalized Discriminatory Power (%)
Vegetation density	0.198	100.0 %
Lacunarity	0.155	78.3%
Bare area fragmentation index	0.129	64.9%

Table 4: Results of the decision tree analysis showing the observed and predicted classification of the EHEs and the prediction accuracy of the decision tree model.

	Predicted					
Observed	SDP	FDP	SVC	BS	FBS	Precise Percentage
SDP	45	0	0	21	11	58.4%
FDP	7	10	1	9	1	35.7%
SVC	0	0	18	0	6	75.0%
BS	0	0	0	22	2	91.7%
FBS	16	2	0	5	87	79.1%
Total Percentage	25.8%	4.6%	7.2%	21.7%	40.7%	69.2%

To obtain a mapping of estimates of EHEs the decision tree model was calculated with the vegetation pattern indices calculated from the entire spatial extent of the catchment covered by the orthophoto. Visual interpretation of the resulting prediction map of EHEs (Fig. 8) allows identifying and checking the plausibility of the general patterns of EHEs. The mapped estimates show a relatively consistent classification where the general patterns agree well with impressions obtained in the field. The EHEs are associated with slope positions, which are in line with the horizontal bedding of the main structural units. Despite this general agreement, numerous, randomly located misclassified areas (salt-and-pepper error, Langford et al. (2006)) prevail in the results and spatially homogeneous EHE segments are largely missing.

There are various possible origins of the salt-and-pepper misclassifications. First, EHE misclassifications can be related to errors originating in the initial vegetation classification and propagating to the final results. Second, misclassifications are attributed to the spatial heterogeneity within each EHE and the strong influence of vegetation density results. The spatial heterogeneity of surface properties in each EHE, especially the distribution of rock and soil covered surfaces determine vegetation density and spatial distribution. Atypically large bedrock outcrops in an EHE, which is characterized by a uniform surface structure and equally randomly distributed and dense vegetation coverage, lead to a misclassification of these areas. For instance we found areas within SVC that are void of vegetation. In contrast there are areas in BS that show a very high vegetation density because of runoff concentration and deep infiltration at the interface between rock and soil covered surfaces. Misclassifications occur more pronounced in EHEs that have previously been identified as being discriminated only poorly. The inset in Figure 8 shows the spatially defined classification for the EHEs FDP/SDP. It can be identified that number of samples are misclassified as BS and FBS. Due to very similar values for vegetation density for both ecohydrological units based on similar uniform surface properties an accurate differentiation is hard to establish.

Generalization filters are common tools to smooth classification maps. To obtain a more contiguous segmentation of EHEs and to smooth EHE outlines a majority filter with a von-Neumann neighbourhood was applied to the classification results. The majority definition was defined as HALF which means, that half of the cells must have the same value and be contiguous. This majority definition has an even stronger smoothing effect. The application of the majority results in a much smoother representation of EHEs with most of the misclassified cells being replaced by the expected EHE. The results (Fig. 8) show that the spatial variability within each EHE was reduced. The model and the generalization filter was run for the whole extent of the orthoimage (Fig. 8).

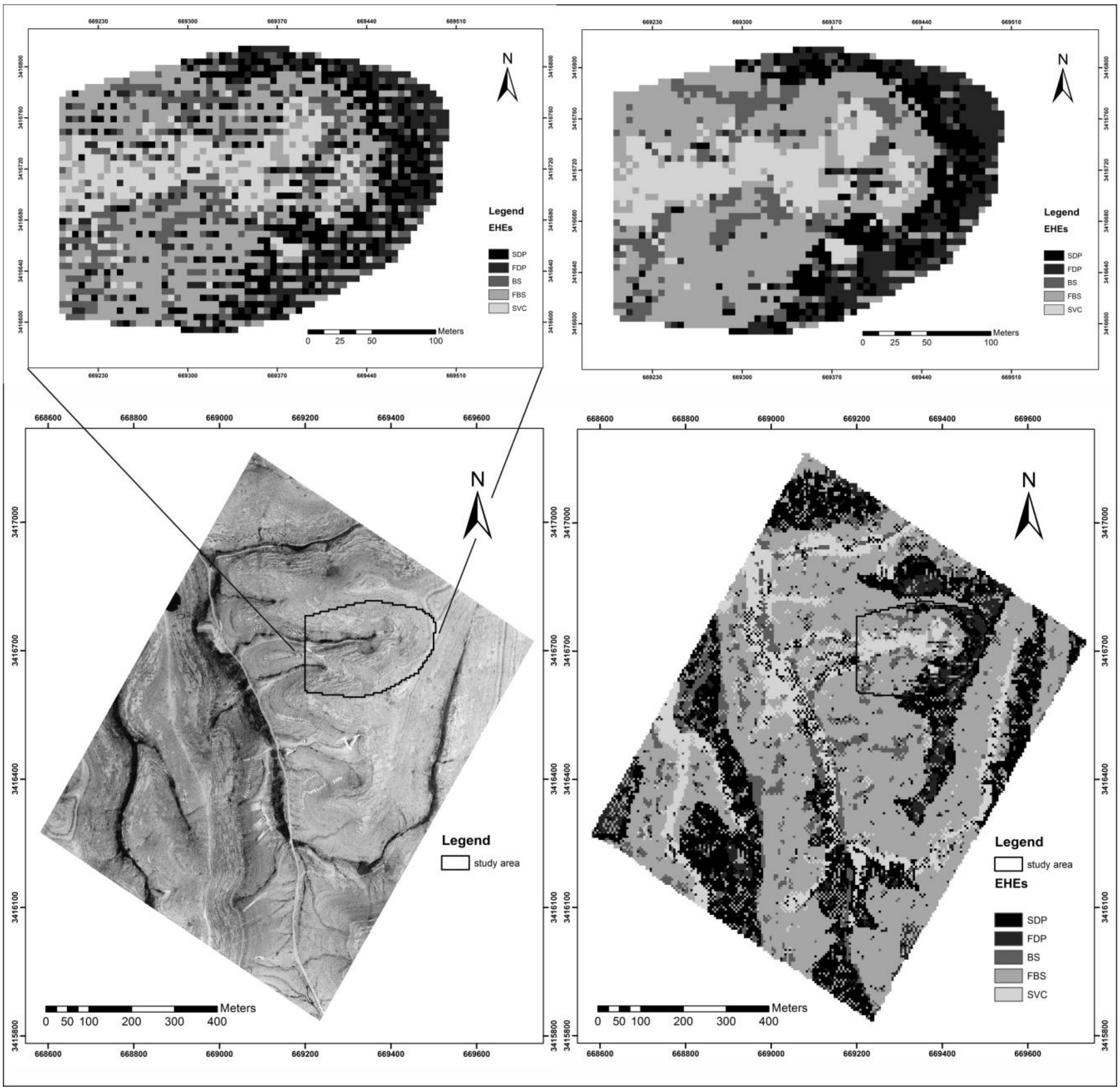

Figure 8: Results of the decision tree based classification model. Spurious misclassifications were removed using a majority filter. The classification model was run for the experimental catchment and for the whole extent of the image.

Whilst being relatively coarsely resolved the model captures the most fundamental spatial characteristics of the distribution of EHEs, which are the spatial sequence along the topographic gradient and the alignment parallel to the elevation contours as suggested by the horizontal bedding of the geological formations. The degree of generalization is dependent on the scale of the results. In general there is no common rule which degree of generalization is most suitable. But more often generalization is used the results will lose detailed spatial information. The tree-based classification model can predict with a relative high accuracy the affiliation to a defined EHE, but cannot compensate the natural homogeneity and spatial variability within each EHE.

5. Discussion

During the last decades, interactions between Earth surface processes such as runoff, soil erosion and vegetation have received increasing attention (Imeson & Prinsen 2004). Studies by Bergkamp (1998) and Cammeraat & Imeson (1999) showed that vegetation patterns indicate the location of runoff and sediment source and sink areas that determine vegetation growth and distribution (Tongway & Ludwig 1994, Puigdefábregas & Sánchez 1996). In turn, vegetation patterns provide information on dominant hydrology and geomorphological processes (Imeson & Prinsen 2004) and are thus potential proxies towards understanding these processes and their variability in space. With increasing availability of very high-resolution satellite imagery with submeter spatial resolution vegetation patterns become more precisely detectable. Detecting patterns from imagery will thus provide new insights into the variability of hydrological and geomorphological processes at unprecedented spatial extents. Amongst other, this information will be of value for the assessment of food production and carbon fluxes between plants and the atmosphere (Shoshany 2012).

Shoshany et al. (1995) suggested that the understanding of vegetation and vegetation patterns and how they reflect and respond to rainfall events is of value for the up- and down-scaling that is required to link remotely sensed and ground based studies. Spatial heterogeneity constitutes a great problem here. To incorporate spatial heterogeneity in modeling approaches requires large amounts of parameters, which are often not available for larger areas (Calver & Cammeraat 1993). An approach to translate fine-scale properties into a broader-scale framework is to define distinctive units which represent characteristic surface properties and specific process responses. Busch et al. (1999) and Becker & Braun (1999) used response units to characterize spatial heterogeneity within a study site. The identification of these response units is generally achieved using key indicators depending on the geo-ecosystem (Imeson & Cammeraat 2000). In this study different vegetation pattern indices were studied to identify different EHEs. We showed that some of these indices perform particularly well in quantitatively describing patterns that usually require very high resolution data. A machine learning based approach towards automated, supervised classification of spatially distributed indices was then shown to plausibly reconstruct the patterns previously mapped EHEs. It was shown that vegetation and vegetation distribution are related to previously mapped surface properties and that occurrence and extent of the latter can be spatially predicted using information on vegetation patterns.

Studies by Puigdefabregas & Sanchez (1996), Ludwig et al. (1999) and Cammeraat & Imeson (1999) underscore the importance of integrating vegetation patterns and their spatial distribution into hydrological and erosion research. Many models on erosion and sedimentation processes are based on highly simplified representations of spatial patterns of water redistribution which fail to account for the feedback mechanisms between runoff and surface properties (De Roo & Jetten 1999, Sun et al. 2002). Hence a good representation of water redistribution processes and patterns is therefore essential, especially in catchments with varying surface properties which yield very different water redistribution patterns (Buis & Veldkamp 2008). Modeling runoff and erosion at catchment scale makes simplifications unavoidable, but without taking processes and surface conditions at plot and hillslope scale into account runoff and sediment yield will often be overestimated (Lesschen et al. 2009). The introduced approach is based on the identification of EHEs which integrate distinctive surface properties that feedback with hydrological and geomorphological processes. At present we are still unable to quantify these feedback mechanisms, but we think that the presented approach is a significant step forward to regionalize such information when available. In addition, patterns of runoff source and sink areas will allow to investigate hydrological and sediment connectivity and will thus provide important input to the study of non-climatic factors governing water availability in drylands.

Remote sensed images with different spatial resolutions were frequently used to estimate vegetation coverage (Xiao & Moody 2005). Lesschen (2008) studied different vegetation indices on fractional vegetation cover in a semi-arid environment using QuickBird imagery. The results of this study show that vegetation indices derived from visible spectral bands are highly correlated with vegetation coverage. In contrast, vegetation indices based on red and NIR reflectance (e.g. NDVI) showed a low or weak correlation. The adaption of dryland vegetation to high temperature and low water availability cause a lack of a strong red edge, reduced leaf absorption in the visible spectra and strong wax absorptions (Calvao & Palmeirim 2004). The resulting limited detectability by remote sensing techniques leads to an underestimation of vegetation coverage. The identification of vegetation based on the differences in reflectance between ground and vegetation seem to be more appropriate for the determination of vegetation coverage than on the difference between the NIR and red reflectance (Sandholt et al. 2002).

The implemented remote sensing approach in this study bridges the gap between the need of high resolution and a differentiated detection of vegetation coverage based on bands in the visible spectra. It could be also shown that calibration based on field data (e.g. vegetation coverage estimation from georeferenced plots) is essential for correct estimation of vegetation coverage. Studies by Francis & Thornes (1990), Rogers & Schumm (1991) and Quinton et al. (1997) show that a vegetation coverage >30% is already enough to decrease soil erosion considerably. Maps combining information about vegetation coverage and ecohydrology (e.g. topography, geology, rock-soil ratio, soil distribution) provide a quick identification of erosion hotspots within a study site. The benefit of high resolution data is that areas of high erosion risks are identified at the scale it occurs. In a next step, conservation practices can be applied at locations with high erosion risk. In addition these maps can also be applied for vegetation monitoring as an indicator for desertification (Kefi et al. 2007) or as input for vegetation-climate models (Pitman 2003).

6. Conclusion

This study presents an automated approach towards mapping EHEs on the basis of vegetation patterns using very high-resolution ground imagery and an orthophoto with 0.5 m ground resolution. The study was conducted in the Negev Desert, Israel, where surface properties exert a strong influence on vegetation patterns and the distribution of runoff and thus plant available water in the landscape. The dependence of different vegetation pattern indices on the spatial resolution of the image data was investigated and indices identified that are insensitive against the resolution difference in our imagery. A decision tree model was successfully used to classify EHEs from different vegetation pattern indices the interactions of which were shown to have sufficient discriminative power even at a relatively coarse spatial scale. While being restricted to EHEs we assume that our approach can be transferred to other areas and research questions that address interactions between hydrological, geomorphological and vegetation patterns.

Acknowledgements

Wolfgang Schwanghart was supported by the Seed Money Fund of the University of Basel while Thomas Jarmer was supported by a Sam & Cecilia Neaman Fellowship at the Technion – Israel Institute of Technology, which is gratefully acknowledged.

References

Becker A., Braun P. 1999. Disaggregation, aggregation and spatial scaling in hydrological modelling. Journal of Hydrology 217. 239-252.

Bergkamp, G., Cammeraat, L.H., Martinez-Fernandez, J., 1996. Water movement and vegetation patterns on shrubland and an abandoned field in two desertification threatened areas in Spain. Earth Surface Processes and Landforms 21, 1073-1090.

Bergkamp, G.J.J., 1998. A hierarchical view of the interactions of runoff and infiltration with vegetation and microtopography in semiarid shrublands. Catena 33, 201-220.

Boeken, B., Shashak, M., 1994. Changes in desert plant communities in human-made patches and their implications for management of desertified landscapes. Journal of Applied Ecology 4, 702-716.

Buis, E., Veldcamp, A., Boeken, B., van Breemen, N., 2009. Controls on plant functional surface cover types along a precipitation gradient in the Negev Desert Israel. Journal of Arid Environments 73, 82-90.

Busch, G., Sutmöller, J., Krüger, J.P., Gerold, D., 1999. Regionalization of runoff formation by aggregation of hydrological response units: a regional approach. in: Diekkrüger, B., Kirkby, M.J., Schroeder, U. (Eds.), Regionalization in Hydrology. IAHS Press, Wallingford, 45-51.

Calvao ,T., Palmeirim, J.M., 2004. Mapping Mediterranean scrub with satellite imagery: biomass estimation and spectral behaviour. International Journal of Remote Sensing 25 (16), 3113–3126.

Calver, A., Cammeraat, L.H., 1993. Testing a physically-based runoff model against field observation on a Luxembourg hillslope.Catena 20, 273-288.

Cammeraat, L.H., Imeson, A.C., 1999. The evolution and significance of soil-vegetation patterns following land abandonment and fire in Spain. Catena 37 (1-2), 107-128.

De Roo, A.P.J., Jetten, V.G., 1999. Calibrating and validating the LISEM model for two data sets from the Netherlands and South Africa. Catena 37 (3/4), 477-493.

Dong, P., 2009. Lacunarity analysis of raster datasets and 1D, 2D, and 3D point patterns. Computer and Geoscience 35, 2100-2110.

Ferguson, C. W., 1964. Annual rings in big sagebrush. The University of Arizona Press, Tucson.

Hill, J., Schuett, B., 2000. Mapping complex patterns of erosion and stability in dry Mediterranean ecosystems. Remote Sensing of Environment 74, 557-569.

Imeson, A.C., Cammeraat, L.H., 2000. Scaling up from field measurements to large areas using the Desertification Response Unit and Indicator Approaches. in: Arnalds, O., Archer, S. (Eds), Rangeland Desertification. Advances in Vegetation Science 19. Kluwer Academic Publisher. Dordrecht. 99-114.

Imeson, A.C., Prinsen, H.A.M., 2004. Vergetation patterns as biological indicators for identifying runoff and sediment source and sink areas for semi-arid landscapes in Spain. Agriculture, Ecosystems and Environment 104, 333-342.

Jaeger, J.A.G, 2000. Landscape division, splitting index, and effective mesh size: new measures of landscape fragmentation. Landscape Ecology 15, 115-130.

Kefi, S., Rietkerk, M., Alados, C.L., Pueyo, Y., Papanastasis, V.P., ElAich, A., de Ruiterm P.C., 2007. Spatial vegetation patterns and imminent desertification in Mediterranean arid ecosystems. Nature 449, 213–217.

Kirkby, M.J., Imeson, A.C., Bergkamp, G., Cammeraat, L.H., 1996. Scaling up processes and models from the field plot to the watershed and regional areas. Journal of Soil and Water Conservation 51 (5), 391-396.

Langford, W.T., Gergel, S.E., Dietterich, T.G., Cohen, W., 2006. Map misclassification can cause large errors in landscape pattern indices: examples from habitat fragmentation. Ecosystems 9, 474-488.

Lesschen, J.P., 2008. Multi-scale interactions between soil, vegetation and erosion in the context of agricultural land abandonment in a semi-arid environment. Dissertation. University of Amsterdam. Faculty of Science.

Lesschen, J.P., Schoorl, J.M., Cammeraat, L.H., 2009. Modelling runoff and erosion for a semi-arid catchment using a multi-scale approach based on hydrological connectivity. Geomorphology 109, 174-183.

Ludwig, J.A., Tongway, D.J., Marsden, S.G., 1999. Stripes, strands or stripples: modeling the influence of three landscape banding patterns on resource capture and productivity in semi-arid woodlands, Australia. Catena 37, 257-273.

Mandelbrot, B.B., 1983. The Fractal Geometry of Nature. Freeman, New York.

Olsvig-Whittaker, L., Shachak, M., Yair, A., 1983. Vegetation patterns related to environmental factors in a Negev Desert watershed. Plant Ecology 54, 153.

Pariente, S., 2002. Spatial patterns of soil moisture as affected by shrubs in different climatic conditions. Environmental Monitoring and Assessment 73, 237-251.

Picard, R., Cook, D., 1984. Cross-Validation of Regression Models. Journal of the American Statistical Association 79, 575–583.

Pitman, A.J., 2003. The evolution of, and revolution in, land surface schemes designed for climate models. International Journal of Climatology 23, 479–510.

Puigdefabregas, J., 2005. The role of vegetation patterns in structuring runoff and sediment fluxes in drylands. Earth Surface Processes and Landforms 30, 133-147.

Puigdefabregas, J., Sanchez, G., 1996. Geomorphological implications of vegetation patchiness on semi-arid slopes. in: Anderson, G., Brooks, S.M. (Eds.), Advances in Hillslope Processes, Vol. 2.

Quinton, J.N., Edwards, G.M., Morgan, R.P.C., 1997. The influence of vegetation species and plant properties on runoff and soil erosion: results from a rainfall simulation study in south east Spain. Soil Use and Management 13, 143–148.

Qin, Z., Li, W., Burgmeier, J., Karnieli, A., 2006. Quantitative estimation of land cover structure in an arid region across the Israel-Egypt border using remote sensing data. Journal of Arid Environments 66, 336-352.

Rogers, R.D, Schumm, S.A., 1991. The effect of sparse vegetative cover on erosion and sediment yield. Journal of Hydrology 123 (1), 19–24.

Rejwan, C., Collins, N.C., Brunner, L.J., Shuter, B.J., Ridgway, M.S., 1999. Tree regression analysis on the nesting habitat of Smallmouth Bass. Ecology 80, 341-348.

Sandholt, I., Rasmussen, K., Andersen, J., 2002. A simple interpretation of the surface temperature/vegetation index space for assessment of soil moisture status. Remote Sensing of Environment 79, 213-224.

Schlesinger, W.H., Pilmanis, A.M., 1998. Plant-soil interactions in deserts. Biogeochemistry 42, 169-187.

Schreiber, K.F., Yair, A., Shachak, M., 1995. Ecological gradients along slopes of the Northern Negev Highlands, Israel. Advances in GeoEcology 28, 209-229.

Schwanghart, W., Kuhn, N.J., 2010. Topotoolbox – a set of Matlab functions for topographic analysis. Environmental Modelling and Software 25, 770-781.

Shashak, M., Sachs, M., Moshe, I., 1998. Ecosystem management of desertified shrublands in Israel. Ecosystems 1, 475 – 483.

Shoshany, M., 2012. The rational model of shrubland biomass, pattern and precipitation relationships along semi-arid climatic gradients. Journal of Arid Environments 78, 179-182.

Shoshany, M., Lavee, H., Kutiel, P., 1995. Seasonal vegetation cover changes as indicators of soil types along a climatological gradient: a mutual study of environmental patterns and controls using remote sensing. International Journal of Remote Sensing 16, 2137-2151.

Sun, H., Cornish, P.S., Daniell, T.M., 2002. Contour.based digital elevation modelling of watershed erosion and sedimentation: erosion and sedimentation estimation tool (EROSET). Water Resources Research 38, 1233.

Tongway D.J., Ludwig J.A. 1994. Small-scale resource heterogeneity in semi-arid landscapes. Pacific Conservation Biology 1, 201-208.

Wu, J., 2004. Effects of changing scale on landscape pattern analysis: scaling relations. Landscape Ecology 19, 125-138.

Xiao, J., Moody, A., 2005. Geographical distribution of global greening trends and their climatic correlates: 1982-1998. *International Journal of Remote Sensing* 26, 2371-2390.

Yair, A., Kossovsky, A., 2002. Climate and surface properties: hydrological response of small arid and semi-arid watersheds. Geomorphology 42, 43-57.

Yair, A., Shashak, M., 1982. A case study of energy, water and soil flow chains in an arid ecosystem. Oecologia 54, 389-397.

Yair, A., Danin, A., 1980. Spatial variations in vegetation as related to the soil moisture regime over an arid limestone hillside, Northern Negev Israel. Oecologia (Berl) 47, 83-88.

Zhang, X., Drake, N., Wainwright, J., 1998. Downscaling land surface parameters for global soil erosion estimation using no ancillary data. Proceeding of the 3rd International Conference on GeoComputation, University of Bristol (UK), Abrahart R.J. (producer). GeoComputation CD-ROM.

Zohary, M., 1962. Plant life of Palestine. The Roland Press Company. New York.

6. Spatial prediction of SOC-patterns in the Negev Desert (Israel) based on vegetation distribution and remote sensing

Hikel H., Kuhn N.J. (in prep.): Spatial prediction of SOC-patterns in the Negev Desert (Israel) based on vegetation distribution and remote sensing.

Spatial prediction of SOC-patterns in the Negev Desert (Israel) based on vegetation distribution and surface heterogeneity

Harald Hikel, Nikolaus J. Kuhn

Affiliation
Department of Environmental Science, Physical Geography and Environmental Change, University of Basel, Klingelbergstrasse 27, 4056 Basel, Switzerland

(✉) **Corresponding author:**
Harald Hikel
Tel: 0041-61-267 07 33
Fax: 0041-61-267 0740
e-mail: Harald.Hikel@unibas.ch

Abstract

In the context of global warming dryland ecosystems are considered to be highly sensitive to climate change. Despite the fact that a not insignificant portion of the world's total soil organic carbon (SOC) is stored in global drylands, there is insufficient research about the quantification of SOC sink and source capacity of soils in changing desert environments. Several studies in drylands document that dynamic geomorphic processes, small scale spatial variability of surface properties and vegetation distribution affects the formation and degradation of organic carbon in soils. This study aimed at the quantification of SOC-stocks at regional scale considering small scale spatial heterogeneity of SOC concentrations and driving processes at local scale. A GIS-based image analysis approach was therefore developed using vegetation coverage and ecohydrological environments (EHEs) as proxy indicators for SOC concentrations and patterns.

To determine vegetation coverage within the study site a GIS-based orthoimage analysis method was used. To imply the influence of the spatial variability of surface properties in the SOC-stock calculation an approach to determine EHEs within the study site was implemented. The distinctive EHEs are characterized by similar surface conditions (such as geology, rock/soil ratio, soil distribution) and vegetation density.

The results clearly show that the combination of field data and digital image processing approaches are practical and beneficial for the precise estimation of SOC-stocks at regional scale in arid environments. The calculated SOC-stock for the total area is 1.19t C ha^{-1}, indicating that dryland soil contain a significant amount of SOC.

Vegetation distribution and EHEs can be used as proxy variables for the estimation of SOC-stocks in arid environments. The results suggest that the implemented approach is generally applicable to estimate SOC inventory, spatial SOC patterns and to increase our knowledge in up-scaling data from local scale to regional scales.

Keywords Drylands • Ecohydrology • SOC-inventory • Soil Organic Carbon

1 Introduction

1.1 Soil organic carbon stocks in drylands

Deserts and semi-deserts occupy more than one-third of the Earth's land surface (LAITY, 2008). About 50% of these regions are dominated by rocky surfaces, where patches of bedrock and shallow soils or pavements prevail (BUIS & VELDKAMP, 2008). Despite the predominantly patchy and shallow soil cover, 15.5% of the world's total SOC to 1-meter depth (LAL, 2003; SCHIMEL ET AL., 2000) is stored in global dryland soils. Nevertheless literature is still dominated by studies in humid environments and the dynamics of the soil organic carbon (SOC) pool in drylands are still not well known (QUINTON ET AL., 2010; SEIP, 2001). In the context of global warming, dryland ecosystems seem to be regions sensitive to climate change (MISHRA ET AL., 2007; SMITH ET AL., 2008). Studies by FARAGE ET AL. (2003), LAL (2003) and YAIR (1999) show that changing climate conditions will result in large, rapid and variable responses of desert ecosystems. Dryland soils are determined as far from SOC saturation, which indicates a high potential of SOC uptake. Limited water availability in arid environments reduces SOC mineralization. As a result dryland soils are less likely to lose SOC and therefore the flux of SOC into the atmosphere is limited (FANG & MONCRIEFF, 2001; FARAGE ET AL., 2003; QI ET AL, 2000). According to the studies by FARAGE ET AL. (2003) and LAL (2009, 2001) the residence time of SOC in desert soils can be much longer than in humid regions. The ratio of the soil to living biomass SOC pool might be greater in drylands than in tropical forest. In the last 15 years SOC studies largely focused on the estimation of SOC stocks at plot scale or along transect (CERDAN ET AL., 2010; COLEMAN & JENKINSON, 1999; DOETTERL ET AL., 2012b). According to the Kyoto Protocol SOC inventories at coarser scales such as regional or global scale are required. Data are therefore generally extrapolated from small scale to coarser scale. But the results are only partially appropriate and characterized by large uncertainties due to high spatial heterogeneity of environmental factors and soil properties and limited sampling densities (ASBJORNSEN ET AL., 2011; DOETTERL ET AL., 2012a). Hence, there is a need for more case studies with precise measurements of SOC stocks at regional scale considering the spatial heterogeneity of SOC concentrations and patterns at local scale. This is particularly important for the quantification of SOC sink or source capacities of soils in changing desert environments.

1.2 Spatial variability of carbon sequestration

In arid areas vegetation patterns constitute hotspots of biological productivity and diversity of herbaceous plants (BOEKEN & SHACHAK, 1994; GOLODETS & BOEKEN, 2006). The mosaic of vegetated and non-vegetated patches is dynamically interdependent. Bare ground acts as a source of water and sediments; vegetated patches act as sinks where water and sediments are trapped (PARIENTE, 2002; PUIGDEFABREGAS, 2005). Vegetated patches absorb more water due to higher soil porosity, infiltration capacity, water holding capacity, hydraulic conductivity, structural stability, organic matter content, and lower bulk density (CAMMERAAT, 2002; PUIGDEFABREGAS, 2005). The variability of soil moisture availability generates a patchy vegetation distribution, which in turn exerts a strong control on carbon stocks (JOBBÁGY & JACKSON, 2000; LI ET AL., 2010; OLSVIG-WHITTAKER ET AL., 1983; SCHLESINGER ET AL., 1996).

HOFFMANN ET AL. (2012) determined SOC-stocks at plot scale (plot sizes vary between 9 to 100m^2) in a range of different ecohydrological environments (EHEs) in the Negev Desert, Israel and identified soil properties relevant for SOC concentrations and stocks. The results of the study show, that the soils in the study area contain a significant amount of SOC of 1.54 kg C m^{-2}, with an average SOC stock over the entire study site of 0.58 kg C m^{-2}. The SOC is determined by the different EHEs, which are characterised by (i) aspect-driven differences, (ii) microscale topography and soil formation, and (iii) vegetation coverage (HIKEL ET AL., 2012, 2013; HOFFMANN ET AL., 2012). The study also documented that in general high SOC concentrations and stocks are found at slope positions that favour high soil moisture and thus high vegetation densities (HOFFMANN ET AL., 2012). In addition, similar results are reported by JOBBÁGY & JACKSON (2000) and LI ET AL. (2010) who found a strong link between aboveground vegetation properties and SOC. Hence, EHEs and vegetation distribution need to be considered as a major controlling factor on SOC concentrations and stocks in arid environments.

1.3 Remote sensing and quantification of SOC-stocks

Vegetation coverage and EHEs have been demonstrated to provide a direct indicator of spatial pattern of SOC-concentrations in an arid catchment (HOFFMANN ET AL., 2012). This correlation can be of great value for up- and down-scaling that is required to link remotely sensed and ground based studies. In general spatial point data at local scale are interpolated to inventory at regional / global scale. Although plots and long transects have been intensely studied, it is difficult to extrapolate findings from field studies at small scale to larger areas (DOETTERL ET AL., 2012a,b; HILL & SCHUETT, 2000) because of many thresholds, non-linear processes, the large spatial variability of environmental factors, soil properties and limited sampling densities. These estimated SOC stocks are not well represented and a more detailed investigation is required (ASBJORNSEN ET AL., 2011; DOETTERL ET AL., 2012a).

For the precise quantification of SOC stocks an approach is necessary which considers small scale spatial SOC heterogeneity, its driving processes and the ability to incorporate these dependencies at coarser scales. For regional-wide assessment remote sensing with a commonly used spatial resolution of several decimetres seems to be a practical method of data collection (JARMER ET AL., 2010; PUIGDEFABREGAS, 2005; SCHWANGHART & JARMER, 2011). HIKEL ET AL. (2013) developed (i) a GIS-based image analysis approach to map vegetation patterns from orthoimages and (ii) an approach towards automated mapping of EHEs in drylands using vegetation pattern indices derived from high-resolution imagery. Both mentioned image analysis approaches were combined to one methodological procedure due to the major aim of this study to estimate SOC inventory and to map SOC patterns in an arid environment. The calculation of the SOC-stock is based on the strong correlation between SOC-concentrations with vegetation coverage and EHEs. In this study we focus on the quantification of a SOC inventory at regional scale considering SOC spatial heterogeneity at local scale.

2 Study site

The study was conducted near Sede Boqer (30°52’N, 34°48’E) in the Northern Highlands of the Negev Desert, Israel (Fig.1), which was ideally suited because of well-researched ecohydrology. EVENARI ET AL. (1980), OLSVIG-WHITTAKER ET AL. (1983) and YAIR (1999) intensively investigated there the influence of surface properties and rock and soil covered surfaces on ecohydrology and vegetation. The study area has an extent of about 1 km^2 and elevation ranges between 480 m and 540 m above zero.

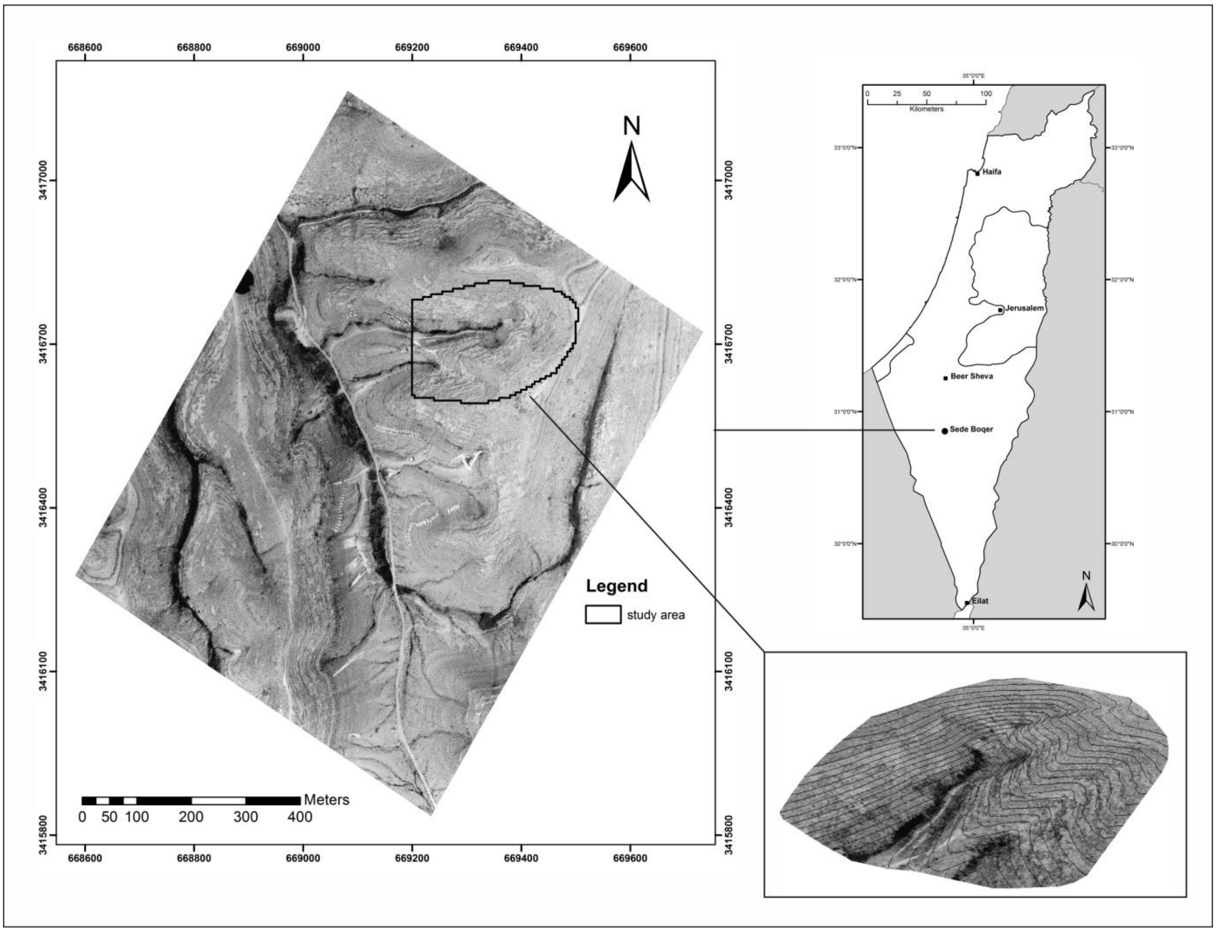

Figure 1: Study area (1 km^2) in the Negev Desert (Israel) and the experimental catchment site (0.05 km^2) studied by HIKEL ET AL. (2012) and HOFFMANN ET AL. 2012.

The mean annual air temperature is 20° C and mean monthly temperatures vary from 9 °C in January to 25 °C in August. Average annual rainfall, observed during a 30-y-period at the study site is 90 mm characterized by high interannual variability with extreme values between 34 mm and 167 mm (KUHN & YAIR, 2003; KUHN ET AL., 2004; YAIR & KOSSOVSKY, 2002). Rainfall is concentrated during the winter season between October and April. Potential evaporation rates vary between 2000 mm and 2600 mm, generating an arid climate (KIDRON & ZOHAR, 2010; NATIV ET AL., 1997). The Upper Cretaceous bedrock stratigraphy is composed of three limestone formations: the Netser, Shivta, and Drorim formation (Fig.2). The three formations are bedded almost horizontally and differ greatly in surface properties. The lithological formations within the study site provide distinctive structural properties creating different surface environments (OLSVIG-WHITTAKER ET AL., 1983; SCHREIBER ET AL., 1995; YAIR & SHACHAK, 1982). In accordance to HOFFMANN ET AL. (2012) and OLSVIG-WHITTAKER ET AL. (1983) following EHEs are distinguished within the study area at hillslope scale (Fig.2): flat desert pavement (FDP), gently sloped desert pavement (SDP), non-fissured bedrock slope (BS), stepped and fissured bedrock slope (FBS) and slope and valley colluvium (SVC). These EHEs differ regarding hydrology, lithology and water redistribution (OLSVIG-WHITTAKER ET AL., 1983; SCHREIBER ET AL., 1995; YAIR & DANIN, 1980).

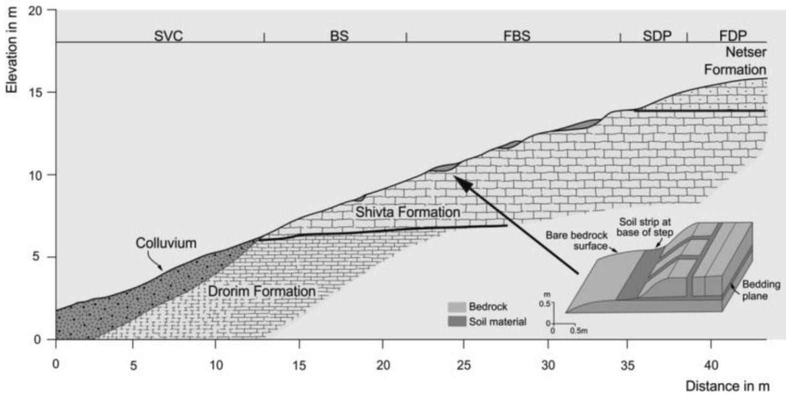

Figure 2: Lithological formations within the studied catchment (modified after YAIR & SHACHAK, 1982; OLSVIG-WHITTAKER ET AL., 1983; SCHREIBER ET AL., 1995) and the different EHEs at the hillslope scale: flat desert pavement (FDP), gently sloped desert pavement (SDP), non-fissured bedrock slope (BS), stepped and fissured bedrock slope (FBS) and slope and valley colluvium (SVC).

In-situ chemical weathering of bedrock is of minor importance for soil formation. The mineral substrate is not solely derived from the local limestone bedrock, but largely composed of loessial sediments deposited since the early Quaternary (BRUINS, 1986; YAALON & DAN, 1974). Based on the World Reference Base for Soil Ressources (FAO 2006), soils are dominantly classified as a desert brown Lithosol with patchy and thin soil coverage. Soils are rich in sand and silt (85-93%) while clay content varies between 14.5% in joints and 7-10% in soil patches covering bedrock (YAIR & DANIN, 1980).

Plant communities in the study area represent a transition between the Irano-Turanian plant geographical region and the Saharo-Arabian region (OLSVIG-WHITTAKER ET AL., 1983; YAIR & SHACHAK, 1982). The study area hosts a range of communities from semi-desert (10-30% perennials vegetation cover) on rocky upper slopes to some patches of true desert (less than 10% perennial cover) at the lower colluviums (OLSVIG-WHITTAKER ET AL., 1983; YAIR & DANIN, 1980).

3 Methods

The applied methodological approach is based on the results of the studies by HIKEL ET AL. (2012, 2013) and HOFFMANN ET AL. (2012). The main findings of both studies are that (i) vegetation distribution is a direct indicator for SOC concentrations and patterns, (ii) SOC concentrations are determined by the different EHEs which are characterized by similar surface conditions (such as geology, rock/soil ratio, soil distribution) and vegetation density and (iii) EHEs are detectable by remote sensing techniques using vegetation indices as a proxy indicators for the different EHEs. Combining this information is innovative in the field of SOC-stock quantification due to the fact that the spatial heterogeneity of SOC concentrations and patterns at local scale are considered for the estimation of SOC stocks and patterns at regional scale. This approach is especially applicable for (semi-) arid environments because vegetation is clearly distinguishable from soil and rock covered surfaces by strong contrasts in the Pixel Digital Numbers (QIN ET AL., 2006). Particularly in such dynamic geomorphic systems, which are considered as highly sensitive to climate change, precise measurements and estimates of the spatial distribution of SOC stocks and patterns are necessary to quantify the SOC sink and source capacity of changing environments.

Based on the aim of the study the following objectives for data analysis are derived: (i) determine vegetation coverage by orthoimage analysis (ii) map automatically EHEs by using vegetation pattern indices (iii) calculate the SOC inventory for the study area. The methodical procedure is described in detail below.

3.1 Measurement of aerial photograph

The aerial photograph used for the analysis has three channels in the visible range and a spatial resolution of 0.5m that is high enough to clearly distinguish the shrub canopies from their surrounding background. The approach applied in this study was described by HIKEL ET AL. (2013) to determine vegetation patterns and distribution within the study site. The basis for this approach is that pixels with low DN-values (Pixel Digital Number) are usually desert shrub canopies in the photograph (QIN ET AL., 2006) due to the fact that vegetation absorbs most incoming light at visible wavelengths. HIKEL ET AL. (2013) used grayscale image morphology to identify vegetation patches. To obtain a binary image representing vegetation and bare ground, regional minima were extracted from the band with the first principal component scores (PC1) using the flood fill operator in ArcGIS 10.0 (ESRI). In a next step the flooded image was subtracted from PC1 band and a threshold was defined to the difference image. The result is a map showing spatial vegetation distribution within the study site.

3.2 Mapping EHEs

The approach to determine EHEs within the study site was described by HIKEL ET AL. (2013). Vegetation and its spatial extent were mapped by analyzing the orthoimage. The subsequently generated dataset was used to calculate spatial vegetation pattern indices such as vegetation density, lacunarity and bare area fragmentation index. The indices were then used in a decision tree model for automated mapping of EHEs. This approach is an identification tool for EHEs in (semi-) arid environments supported by vegetation detection using remote sensing and digital image processing (HIKEL ET AL., 2013).

3.3 Calculation of SOC-stock

Based on an adapted sample strategy for this arid environment the SOC-stock was calculated for the different EHEs ($SOC_{stock,EHE}$). According to HOFFMANN ET AL. (2012) the estimation of $SOC_{stock,EHE}$ is based on three different equations.

With equation 1 the SOC-stock ($SOC_{stock,i}$ [kg C m^{-2}]) was estimated for each representative layer *i* of a soil sample with thickness $d_{soil,i}$ [cm]:

$$SOC_{stock,i} = 0.1 \times d_{soil,\,i} \times BD \times SOC_{ci} \times (1-CF_i / 100) \qquad \text{(equation 1)}$$

Equation 2 calculates SOC-stocks (SOC_{stock}) per sampling site by summarizing the SOC-stock of each layer *i* ($SOC_{stock,i}$) at the corresponding sampling site:

$$SOC_{stock} = \sum SOC_{stock,i}. \qquad \text{(equation 2)}$$

The stocks given in equation 2 were multiplied with the mean soil coverage of each unit (equation 3). Hence the SOC stock for each EHE ($SOC_{stock,EHE}$) was determined considering the limited soil coverage in each EHE.

$$SOC_{stock,EHE} = SOC_{stock} \times \text{soil coverage} \qquad \text{(equation 3).}$$

Based on these calculated SOC-stocks for each EHE ($SOC_{stock,EHE}$) the total SOC-stock ($SOC_{stock,total}$) was determined by summing up the $SOC_{stock,EHE}$.

4 Results

4.1 Determination of vegetation coverage

Vegetation density values were calculated for 40 plots based on the different EHEs within the study site by the introduced orthoimage analysis approach. HIKEL ET AL. (2012, 2013) and HOFFMANN ET AL. (2012) calculated in their studies vegetation density values for exact the same 40 plots by field observation. The field data were used to determine ground truth for the generated orthoimage dataset.

Table 1 shows the vegetation density values (%) of the field dataset and the orthoimage dataset. For further analysis the field dataset was used as reference. Linear regression analysis (Fig. 3) and the RMSE calculation show a R^2=0.86 and an $RMSE_{ges}$=0.2. The RMSE values for the different EHEs shows values between 0.3 - 1.3 (Table 1). Hence, it can be identified that vegetation density values do not differ significantly between the different analysis methods. Based on these results, the RGB image analysis approach could be validated by the field dataset. In a next step a vegetation distribution map was generated (Fig. 4) where the *ones* (black grid cells) in the binary image refer to vegetation and the *zeros* (grey grid cells) to bare ground.

Ecohydrological environments	Field dataset	Orthoimage dataset	RMSE
FDP	11	10	0.7
SDP	15	17	1.1
FBS	20	18	0.6
BS	10	9	0.3
SVC	30	36	1.3

Table 1: Average vegetation density in percent and the calculated coefficient of variation for the different EHEs as calculated from the orthoimage and obtained from field observation

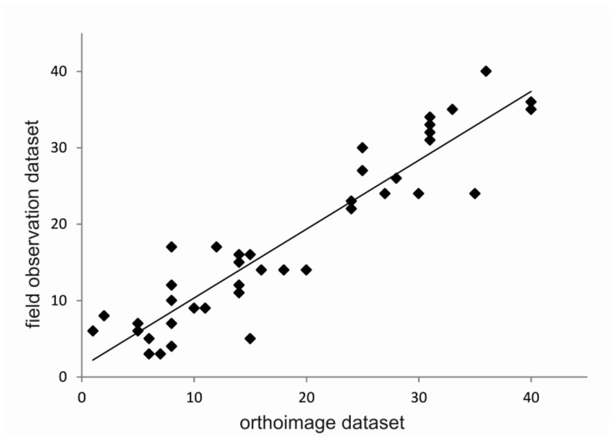

Figure 3: Relationship between the different vegetation density analysis methods plotted as linear regression (R^2=0.86).

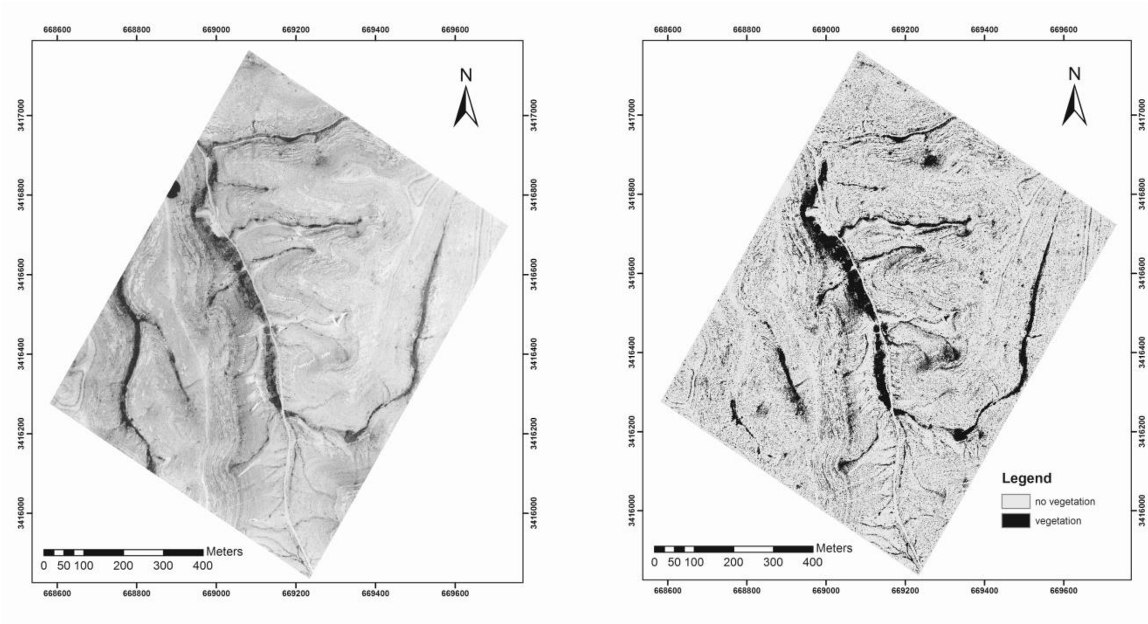

Figure 4: Binary image showing vegetation distribution within the study area.

4.2 Automated mapping of EHEs

The introduced decision tree model was run with the vegetation pattern indices calculated from the entire extent of the orthoimage. As a result a mapping of estimates of EHEs was obtained. The resulting prediction map of EHEs (Fig. 5) allows a visual interpretation for identifying and checking the plausibility of the general patterns of EHEs. As mentioned in the previous study by HIKEL ET AL. (2013) who implemented this methodological approach for automated mapping, the mapped estimates show a relatively consistent classification. In general, the patterns agree well with impressions obtained in the field. But it must be mentioned that misclassifications prevail in the results. This salt-and-pepper error (LANGFORD ET AL., 2006) inhibits the formation of spatially homogeneous EHE segments, which are largely missing in the resulting map. Nevertheless the decision tree model has a high predicting accuracy of ~70%. The spatial extent of the different EHEs is shown in Table 2.

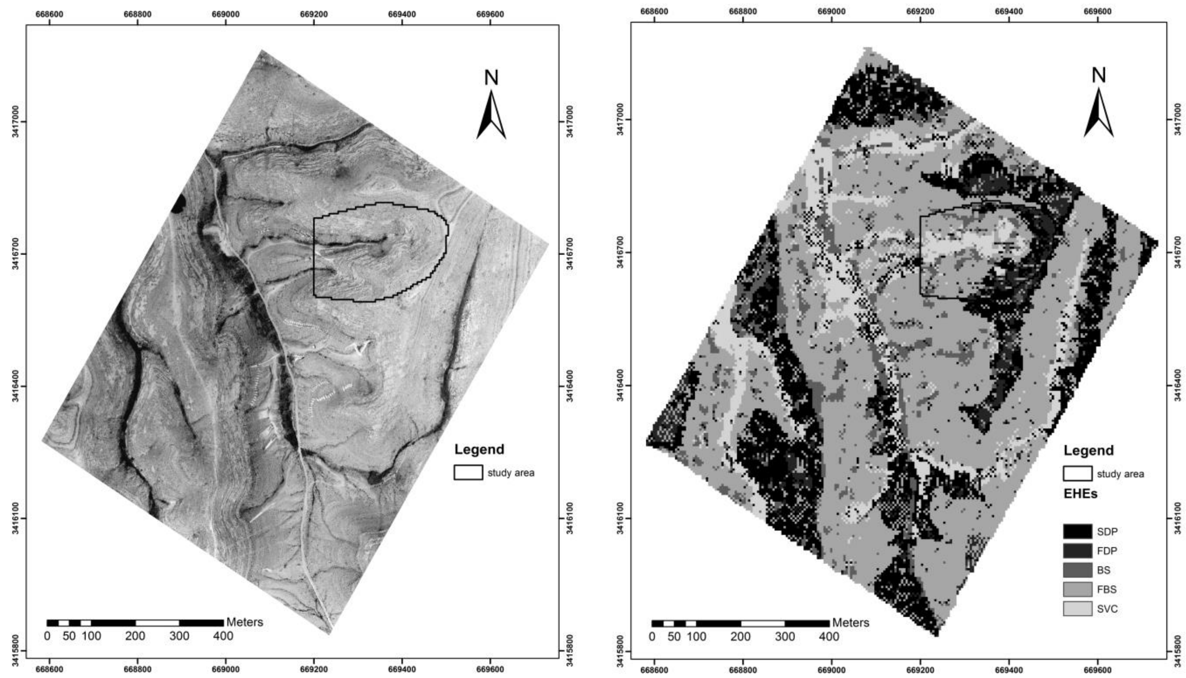

Figure 5: Results of the decision tree based classification model showing the estimated EHEs after removing spurious misclassification with a majority filter.

4.3 SOC-stock and SOC-patterns

Based on the field measurement data by HOFFMANN ET AL. (2012) and the calculated spatial extent of the different EHEs by the decision tree based classification model, the SOC-stocks for each EHE were determined. Table 2 shows the results of the calculation. The calculated SOC inventory for the total area is 1.19t C ha^{-2}. The SOC stocks of the different EHEs show a wide variability ranging from 0.095kg C m^{-2} to 1.065 kg C m^{-2}. The greatest SOC concentrations are shown in the EHE FBS, the lowest in the EHE BS. The trend of the $SOC_{stocks,EHE}$ is similar to the SOC concentrations.

Figure 6 shows the spatial patterns of SOC within the study site. The spatial patterns are related to the spatial variability of SOC concentrations within the study site, determined by vegetation distribution and the heterogeneity of surface properties. The results indicate in due consideration of soil moisture, vegetation coverage as well as surface properties as driving factors for SOC-concentrations and patterns, a proper and differentiated calculation of SOC inventory.

Ecohydrological environments (EHEs)	Area EHEs (km^2)	Vegetation covered area (km^2)	SOC-stock EHE (kg C m^{-2})	SOC-stock EHE (kg C)
FDP	0.064	0.006	0.245	1564
SDP	0.182	0.031	0.445	13774
FBS	0.378	0.068	1.065	72511
BS	0.098	0.009	0.095	838
SVC	0.089	0.032	0.930	29873

Table 2: Area, vegetation covered area, $SOC_{stocks,ehe}$ and $SOC_{stock,total}$ with respect to the different EHEs. The mean $SOC_{stock,ehe}$ (kg C m^{-2}) is based on the study by HOFFMANN ET AL. (2012)

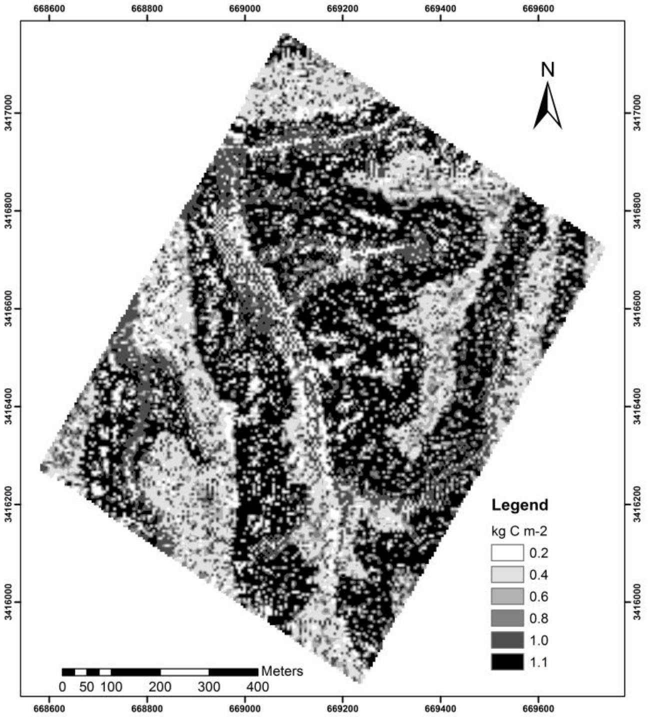

Figure 6: Spatial distribution of SOC-pattern within the study area controlled by vegetation distribution and surface properties.

5 Discussion

5.1 SOC stocks, surface properties and vegetation

The SOC concentrations and stocks show strong differences between the distinctive EHEs (Table 2). These results suggest that different ecohydrologic conditions affect the SOC stocks on the different EHEs. HIKEL ET AL. (2012) and HOFFMANN ET AL. (2012) investigated in their studies the influence of soil and surface properties and vegetation on SOC concentrations for the experimental site in the Negev Desert, Israel. The highest SOC concentrations and $SOC_{stock,EHE}$ are found at northern exposed slopes and lower slope positions which favour high soil moisture and thus high vegetation densities. Only a weak correlation (R^2 = 0.25) exists between the mean soil depths of the EHEs and SOC concentrations and no correlation (R^2 = 0.03) between soil depth and $SOC_{stock,EHE}$ (HOFFMANNN ET AL., 2012). In contrast to rocky desert slope environments, studies by BERHE ET AL. (2008) and YOO ET AL. (2006) show, that soil thickness is highly relevant for SOC stocks in more humid areas. The positive relationship (R^2 = 0.91) between vegetation coverage and SOC stocks at the experimental site (HOFFMANN ET AL., 2012) indicates that the findings by OLSVIG-WHITTAKER ET AL. (1983), who studied the effects of surface properties on vegetation, can also be applied to SOC stocks.

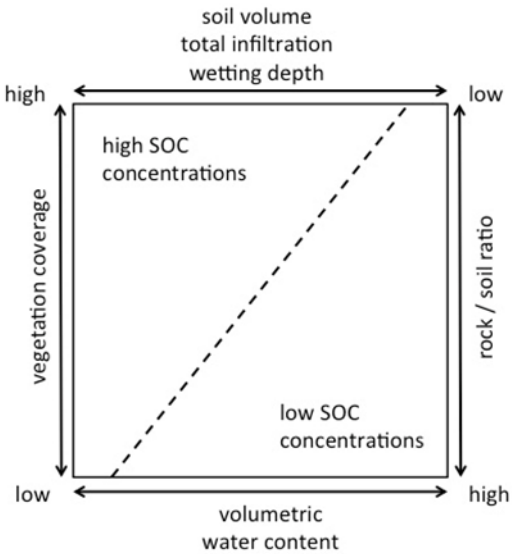

Figure 7: Conceptual model of the effect of surface properties, water availability and vegetation coverage on SOC concentrations.

The variability of soil properties and SOC stocks is associated with differences in net primary production (NPP) and the relative moisture supply (HOFFMANN ET AL., 201; OLSVIG-WHITTAKER ET AL., 1983). HIKEL ET AL. (2012) examined therefore the relevance of soil volume and rock-soil interactions for plant available water. The effects of surface properties and water availability on vegetation coverage and hence on SOC concentrations are shown in Fig. 7. The interactions between soil volume, total infiltration, wetting depth, rock-soil ratio, volumetric water content and vegetation coverage regarding SOC concentration were combined in a conceptual model (Fig. 7). Compared to soil covered surfaces, which are characterized by a high porosity and high water absorbing capacity, runoff generation is faster on relatively impermeable bare rocky surfaces. In turn lower flow frequency and lower magnitude of runoff are observed on soil-covered surfaces (HIKEL ET AL., 2012; YAIR & RAZ-YASSIF, 2004; YAIR, 1992). For the simulated rainfall total infiltration values range from 5.7 l on soil covered areas to 1.6 l on areas nearly devoid of any soil. In addition, runoff redistribution is determined by differences in infiltration rates due to rock and soil covered surfaces influencing the rate of transformation of rainfall into runoff. Rock-soil ratio declines with soil volume. Hence, small soil volumes receive their water from a proportionally greater rock surface than those with a high soil volume. Rock-soil ratio and soil volume are strongly correlated (R^2=0.8). For small soil volumes total infiltration is lower due to the fact that the limited soil volume reduces the amount of infiltration. Low infiltration rates indicate that only a limited amount of water entered the soil. The low depth of wetting which declines with rock-soil ratio confirms this. Hence, low soil volumes limit plant available water. Soil volume displays a moderate negative relationship (R^2=-0.56) with volumetric water content (water storage capacity) indicating that small soil volumes are filled up closer to their maximum water storage capacity than the large ones during the simulated rainfall. In contrast, low volumetric water content therefore indicates high total infiltration but also that the soil volume was not filled up to its maximum. Soil volume determines the frequency of watering that is required to maintain vegetation and the risk of drought stress. High vegetation coverage is therefore found where soil volume and total infiltration is high. In contrast low vegetation coverage is found where soil volume, total infiltration and wetting depth are low. According to the findings by CAMMERAAT (2002), PUIGDEFABREGAS (2005) and STAVI ET AL. (2009), vegetation patches absorb more water due to higher soil porosity, infiltration capacity water holding capacity, hydraulic conductivity, structural stability and organic matter content and lower bulk density. This suggests that high vegetation densities indicate high soil volumes and hence high SOC concentrations per unit area. Vegetation coverage and SOC concentrations and stock are strongly correlated (R^2=0.81, R^2=0.91). Vegetation is distributed patchily within the area due to soil and water availability resulting in a high spatial variability of SOC concentrations and stocks. SOC concentrations range between 3 g kg^{-1} and 15 g kg^{-1}. Soil depth varies on a centimetre to meter scale and the SOC concentration change is therefore limited by depth.

The presented approach bears some importance regarding the expected changing climate conditions related to the global warming process. YAIR & KOSSOVSKY (2002) state for the Negev Desert that the same regional climatic change may have different effects on the environmental responses. Different surface conditions and processes control the ecohydrological response and therefore lead to a non-uniform reaction to a regional climatic change. Determining spatial heterogeneity and interrelation between surfaces and processes as introduced by the experimental procedure contributes to a better understanding and estimation of the impact of climate change on the spatial variability of SOC concentrations and stocks in arid environments.

5.2 Estimation of SOC using remotely sensed data

For the last three decades remote sensing techniques are used for the assessment and monitoring of arid ecosystems (HEIN ET AL., 2011; MULDER ET AL., 2011; SCHMIDT & KARNIELI, 2000). Especially in arid ecosystems remote sensed images with different spatial resolutions were frequently utilized to estimate environmental properties and vegetation coverage (XIAO & MOODY, 2005). Several techniques exist to determine vegetation coverage by the analysis of remote sensing images (BARATI ET AL., 2011; FRANK & TWEDDALE, 2006; MCGLYNN & OKIN, 2006; XIAO & MOODY, 2005). ANDREW & USTIN (2008) for example used 128-band HyMap image data for the spectral analysis of *Lepidium* by aggregated classification and regression tree models (CART). QI ET AL. (2000) developed a modelling approach for the estimation of Leaf Area Index in semiarid regions, which are available from many sensors such as AVHRR, VEGETATION, MODIS and MISR. The adaption of dryland vegetation to high temperatures and lower water availability (e.g. strong wax absorptions, reduced leaf absorption) lead to a limited detectability by remote sensing techniques and hence an underestimation of vegetation coverage (LESSCHEN, 2008; CALVAO & PALMEIRIM, 2004). SANDHOLT ET AL. (2002) states that the identification of vegetation based on the differences in reflectance between surface (e.g. soil and rock cover) and vegetation seems to be more appropriate for the determination of vegetation coverage in drylands than on the difference between the NIR and red reflectance. The implemented GIS-based image analysis approach is based on the analysis of aerial imagery (orthophotos) using digital image processing and hence provides a simple solution for estimation of vegetation coverage and distribution in arid environments. This approach was developed on the actual vegetation and the vegetation density values of the image datasets used. The key to establish near natural and accurate vegetation coverage values is to use a sufficient large training dataset that covers a wide range of vegetation densities (from non-vegetated areas as well as low-, medium and high-density areas). Especially vegetation coverage and EHEs as a proxy variable for the estimation of SOC-concentrations and stocks provides to link remotely sensed and ground based studies. The GIS-based image analysis approach generated exact results for this specific area. The field data were used to determine the prediction accuracy of the implemented method. The results of 40 plot measurements were therefore compared with the generated results of the GIS-based image analysis approach. The approach shows a prediction accuracy of 86%. This analysis approach furthermore provides some key benefits such as (i) fast and comprehensive of vegetation coverage analysis, (ii) sparse long and expensive field trips, (iii) integrates small scale spatial

heterogeneity of SOC concentration and (iv) enables the precise determination of SOC sink and source areas at regional scale.
The GIS-based image analysis approach also bears some advantages regarding the estimation of SOC inventories using soil reflectance by remote sensing techniques. Using hyperspectral remote sensing for the estimation of SOC inventories is limited to soils devoid of any vegetation, which leads to large uncertainties (JARMER ET AL. 2010, SCHWANGHART & JARMER 2011). The GIS-based image analysis approach copes with the need to consider vegetation density and distribution and the relationship between SOC concentrations in the quantification of SOC inventories. The spatial resolution of the sensor is also a limiting factor (SCHWANGHART & JARMER, 2011) resulting in simplifying assumptions regarding the SOC spatial heterogeneity at local scale (COX ET AL., 2000; JONES ET AL., 2005). Based on the consideration of vegetation coverage and EHEs as proxy indicators for SOC concentrations and patterns in the implemented approach, SOC spatial heterogeneity at local scale is figured into the calculation of regional SOC inventory. SOC inventories generated by hyperspectral remote sensing techniques are generally limited to the uppermost 2 cm of topsoil (JARMER ET AL., 2010; SCHWANGHART & JARMER, 2011). By combining field data and digital image processing approaches soil volume is considered in the SOC-stock calculation.
But a certain limitation was brought for orthoimages with (i) a high variability in the greyscale values for vegetation and (ii) a very low albedo contrast between vegetation and bare ground. Detection errors are mostly based on these two aspects. Over-estimation was a result of an inability to distinguish a small range of high greyscale values representing vegetation as well as bare ground. Vegetation patterns, characterized by low greyscale values, were classified as bare ground when the surrounding raster cells also show low greyscale values. This results in an under-estimation of vegetation coverage. In general the detection of vegetation coverage is difficult if the albedo contrast between vegetation and bare ground is greatly diminished. Based on the generated image analysis approach, identification was very simple and for the most part very precise. This remote sensing approach shows the potential benefits of using image data with carefully located in situ field data in digital soil mapping.

5.3 SOC-stock comparison with other drylands

Table 3 summarizes results of SOC-studies in arid and semi-arid areas regarding the measured SOC-stocks. To compare the results of the different studies the SOC-stocks were calculated for the area of the spatial extent of the orthoimage (1 km^2). The estimated SOC-stock for the study site in Israel shows a medium to high value compared to those in other arid environments cited in Table 3. The even medium SOC-stock indicates an exact calculation of the generated analysis method due to the high variability of SOC-concentration values regarding previous studies (HOFFMANN ET AL., 2012). According to the findings of HOFFMANN ET AL. (2012) higher SOC-concentrations are attributed to the patchiness of the soil cover in the study area. The mosaic of soil and rock covered surfaces determines the distribution of vegetation. Vegetation is concentrated were soil cover prevails. These "islands of fertility" (SCHLESINGER & PILMANIS, 1998) are characterized by increased biochemical processes, net primary production (NPP) and SOC-concentrations (BONANOMI ET AL., 2008; SCHADE & HOBBIE, 2005). These higher SOC-concentrations can be also attributed to the reduced mineralization of SOC due to water scarcity in the Negev desert (YAO ET AL., 2010).

Reference	Region	Environment	SOC-stock (t C km^{-2})
Schlesinger (1977)	Global	World desert soils	18.6 - 44.6
Amundson (2001)	Global	Warm desert	1136.0
Watson et al. (2000)	Global	Deserts and semi-deserts	3546.0
Feng et al. (2002)	Land region of china	Different desert types	16.2 - 1882.3
Feng et al. (2002)	Land regions of china	Different desert types	16.2 - 908.7
Ardö (2003)	Sudan	Semi-arid Sudan	48.7
This study	Negev, Israel	Rocky desert	118.6

Table 3: Calculated SOC-stock (t C) for an extent of 1km^2 based on studies in several arid environments.

The comparison of the different SOC studies (Table 3) remains limited due to the fact that the studies rely on different measurement techniques, up-scaling approaches and variable reference soil depths. Hence differences in SOC stocks may not represent environmental conditions but simply the different methodologies applied for inventorying (HOFFMANN ET AL., 2012). But the comparison indicates that the number of high-resolution SOC inventories in drylands is very limited. This implies that more case studies should focus on comparable methodology to evaluate the importance and potential changes of SOC in arid environments. In contrast to the notion that rocky deserts do not contain significant soil or SOC, the results of the SOC-stock calculation in the Negev Desert Israel show that the SOC-stock is higher than generally expected. Due to the fact that SOC-stocks in arid environments are highly sensitive to climate change and thus represent a major unstable C-pool within the global carbon cycle monitoring approaches are needed to detect and quantify changes at the scale they occurs. The implemented GIS-based image analysis approach ensures the required consideration of spatial heterogeneity regarding SOC distribution at local scale for the calculation of SOC inventories at regional scale as mentioned in the introduction.

6 Summary and conclusions

This article describes the combination of field data and digital image processing approaches for the calculation of SOC-stocks in arid environments. Vegetation density and EHEs within the study site were used as proxy variables for SOC-concentrations. The combination of the different approaches facilitates the assessment of spatial SOC patterns. High-resolution satellite imagery (1 m and higher) are recently more and more available which enables to detect small single plants and hence to calculate more exactly SOC patterns and distribution. This approach can be then implemented on broader regional scales to facilitate mapping of the estimated SOC stocks. The use of remotely sensed data in the manner proposed in this paper can also be used to monitor and better understand the impact of climate change on SOC-pools. But further empirical assessment of the approach in wide arid and semi-arid areas and at different spatial scales is needed. Future developments of the approach may include vegetation type and utilize other vegetation pattern indices combined with seasonal variability and a drought index.

References

ANDREW, M.E. & USTIN, S.L., 2008: The role of environmental context in mapping invasive plants with hyperspectral image data. Remote Sensing of Environment **112**, 4301-4317.

ASBJORNSEN, H., GOLDSMITH, G.R., ALVARADO-BARRIENTOS, M.S., REBEL, K., VAN OSCH, F.P., RIETKERK, M., CHEN, J., GOTSCH, S., TOBÓN, C., GEISSERT, D.R., GÓMEZ-TAGLE, A., VACHE, K., DAWSON, T.E., 2011: Ecohydological advances and applications in plant-water relations research: a review. Journal of Plant Ecology **4 (1-2)**, 3-22.

BARATI, S., RAYEGANI, B., SAATI, M., SHARIFI, A., NASRI, M., 2011: Comparison the accuracies of different spectral indices for estimation of vegetation cover fraction in sparse vegetated areas. The Egyptian Journal of Remote Sensing and Space Science **14 (1)**, 49-56.

BERHE, A.A., HARDEN, J.W., TORN, M.S., HARTE, J., 2008: Linking soil organic matter dynamics and erosion-induced terrestrial carbon sequestration at different landform positions. Journal of Gepphysical Research **113**, 1-12.

BOEKEN, B. & SHACHAK, M., 1994: Desert plant communities in human-made patches-implications for management. Ecololgical Applications **4**, 702-716.

BONANOMI, G., RIETKERK, M., DEKKER, S.C., MAZZELONI, S., 2008: Islands of fertility induce co-occuring negative and positive plant-soil feedbacks promoting coexistence. Plant Ecology **197**, 207-218.

BRUINS, H., 1986: Desert Environment and Agriculture in the Central Negev and Kadesh Barnea During Historical Times, PhD-Thesis. Wageningen Agricultural University, Nijkerk, The Netherlands.

BUIS, E. & VELDKAMP, A., 2008: Modelling dynamic water redistribution patterns in arid catchments in the Negev Desert of Israel. Earth Surface Processes and Landforms **33**, 107–122.

CALVAO, T. & PALMEIRIM, J.M., 2004: Mapping Mediterranean scrub with satellite imagery: biomass estimation and spectral behavior. International Journal of Remote Sensing **25 (16)**, 3113-3126.

CAMMERAAT, L.H., 2002: A review of two strongly contrasting geomorphological systems within the context of scale. Earth Surface Processes and Landforms **27**, 1201-1222.

CERDAN, O., GOVERS, G., LE BISSONNAIS, Y., VAN OOST, K., POESEN, J., SABY, N., GOBIN, A., VACCA, A., QUINTON, J., AUERSWALD, K., KLIK, A., KWAAD, F.J.P.M., RACLOT, D., IONITA, I., REIJMAN, J., ROUSSEVA, S., MUXART, T., ROXO, M.J., DOSTAL, T., 2010: Rates and spatial variations of soil erosion in Europe: a case study based on erosion plot data. Geomorphology **122 (1-2)**, 167-177.

COLEMAN, K. & JENKINSON, D.S., 1999 : ROTHC-26.3. A Model for the Turnover of Carbon in Soil. Model Description and Users Guide. IACR, Rothamsted, Harpenden, UK.

COX, P.M., BETTS, R.A., JONES C.D., SPALL, S.A., TOTTERDELL, I.J., 2000: Acceleration of global warming due to carbon-cycle feedbacks in a coupled climate model. Nature **408**, 184-187.

DOETTERL, S., SIX, J., VAN WESEMAEL, B., VAN OOST, K., 2012a: Carbon cycling in eroding landscapes: geomorphic controls on soil organic C pool composition and C stabilization. Global Change Biology **18**, 2218-2232.

DOETTERL, S., VAN OOST, K., SIX, J., 2012b: Towards constraining the magnitude of global agricultural sediment and soil organic carbon fluxes. Earth Surface Processes and Landforms **37**, 642-655.

EVENARI, M., MASIG, D., ROGEL, A., 1980 : Runoff-farming in the Negev Desert of Israel (VI). Jacob Blaustein Institute for Desert Research, Sede Boqer.

FAO, 2006: World reference base for soil resources, Rome.

FANG, C. & MONCRIEFF, J.B., 2001: The dependence of soil CO_2 efflux on temperature. Soil Biology and Biochemistry **33**, 155-165.

FARAGE, P., PRETTY, J., BALL, A., 2003: Biophysical Aspects of Carbon Sequestration in Drylands, University of Essex.

FRANK, T.D. & TWEDDALE, S.A., 2006: The effect of spatial resolution on measurement of vegetation coverage in three Mojave Desert shrub communities. Journal of Arid Environments **67**, 88-99.

GOLODETS, C. & BOEKEN, B., 2006: Moderate sheep grazing in semiarid shrubland alters small scale soil surface structure and patch properties. Catena **65**, 285-291.

HEIN, L., DE RIDDER, N., HIERNAUX, P., LEEMANS, R., DE WIT, A., SCHAEPMANN, M., 2011: Desertification in the Sahel : Towards better accounting for ecosystem dynamics in the interpretation of remote sensing. Journal of Arid Environments **75 (11)**, 1164-1172.

HIKEL, H., YAIR, A., SCHWANGHART, W., HOFFMANN, U., STRAEHL, S., KUHN, N.J., 2012: Experimental investigation of soil ecohydrology on rocky desert slopes in the Negev Highlands, Israel. Zeitschrift für Geomorphologie **57**, Suppl. 1, 039-058.

HIKEL, H., JARMER, T., KUHN, N.J., SHOSHANY, M., SCHWANGHART, W., 2013: Combining remote sensing and spatial statistics for the analysis of shrub patterns in arid regions. Journal of Arid Environments, (in Review).

HILL, J. & SCHUETT, B., 2000: Mapping complex patterns of erosion and stability in dry Mediterranean ecosystems. Remote Sensing of Environment **74**, 557-569.

HOFFMANN, U., YAIR, A., HIKEL, H., KUHN, N.J., 2012. Soil organic carbon in the rocky desert of northern Negev (Israel). Journal of Soils and Sediments **12**, 811-825.

JARMER, T., HILL, J., LAVEE, H., SARAH, P., 2010: Mapping soil organic carbon in non-agricultural semi-arid and arid ecosystems of Israel. Photogrammetric Engineering and Remote Sensing **75**, 85-94.

JOBBÁGY, E.G. & JACKSON, R.B., 2000: The vertical distribution of soil organic carbon and its relation to climate and vegetation. Ecological Applications **10**, 423-436.

JONES, C., McCONNELL, C., COLEMAN, K., COX, P.M., FALLON, P., JENKINSON, D., POWLSON, D., 2005: Global climate change and soil carbon stocks; predictions from two contrasting models for the turnover of organic carbon in soil. Global Change Biology **11 (1)**, 154-166.

KIDRON, G.J. & ZOHAR, M., 2010: Spatial evaporation patterns within a small drainage basin in the Negev Desert. Journal of Hydrology **380**, 376-385.

KUHN, N.J., YAIR, A., 2003: Spatial distribution of surface conditions and runoff generation in small arid watersheds, Zin Valley Badlands, Israel. Geomorphology **57**, 183-200.

KUHN, N.J., YAIR, A., KASANIN-GRUBIN, M., 2004: Spatial distribution of surface properties, runoff generation and landscape development in the Zin Valley Badlands, northern Negev, Israel. Earth Surface Processes and Landforms **29**, 1417-1430.

LAITY L., 2008: Deserts and desert environments, 342. Wiley-Blackwell, Singapore.

LAL, R., 2001: Potential of desertification control to sequester carbon and mitigate the greenhouse effect. Climatic Change **51**, 35-72.

LAL, R., 2003: Carbon Sequestration in Dryland Ecosystems. Environmental Management **33 (4)**, 528-544.

LAL, R., 2009: Sequestering Carbon in Soils of Arid Ecosystems. Land Degradation and Development **20**, 441-454.

LANGFORD, W.T., GERGEL, S.E., DIETTERICH, T.G., COHEN, W., 2006: Map misclassification can cause large errors in landscape pattern indices: examples from habitat fragmentation. Ecosystems **9**, 474-488.

LESSCHEN, J.P., 2008: Multi-scale interactions between soil, vegetation and erosion in the context of agricultural land abandonment in a semi-arid environment. Dissertation. University of Amsterdam. Faculty of Science.

LI, Y., 2010: Can the spatial prediction of soil organic matter contents at various sampling scales be improved by using regression kriging with auxiliary information? Geoderma **159**, 63-75.

MCGLYNN, I.O. & OKIN, G.S., 2006: Characterization of shrub distribution using high spatial resolution remote sensing: Ecosystem implications for a former Chihuahuan Desert grassland. Remote Sensing of Environment **101 (4)**, 554-566.

MISHRA, U., LAL, R., SLATER, B., CALHOUN, F., LIU, D., VAN MEIRVENNE, M., 2007: Predicting soil organic carbon stock using profile depth distribution functions and ordinary kriging. Soil Science Society of America Journal **73 (2)**, 614-621.

MULDER,V.L., DE BRUIN, S., SCHAEPMANN, M.E., MAYR, T.R., 2011: The use of remote sensing in soil and terrain mapping – A review. Geoderma **162 (1-2)**, 1-19.

NATIV, R., ADAR, E., DAHAN, O., NISSIM, I., 1997: Water salinization in arid regions – observations from the Negev desert, Israel. Journal of Hydrology **196**, 271-96.

OLSVIG-WHITTAKER, L., SHACHAK, M., YAIR, A., 1983: Vegetation patterns related to environmental factors in a Negev Desert watershed. Plant Ecology **54**, 153-165.

PARIENTE, S., 2002: Spatial patterns of soil moisture as affected by shrubs in different climatic conditions. Environmental Monitoring and Assessment **73**, 237-251.

PUIGDEFABREGAS, J., 2005: The role of vegetation patterns in structuring runoff and sediment fluxes in drylands. Earth Surface Processes and Landforms **30**, 133-147.

QI, J., KERR, Y.H., MORAN, M.S., WELTZ, M., HUETE, A.R., SOROOSHIAN, S., BRYANT, R., 2000: Leaf Area Index Estimates Using Remotely Sensed Data and BRDF Models in a Semiarid Region. Remote Sensing of Environment **73**, 18-30.

QIN, Z., LI, W., BURGMEIER, J., KARNIELI, A., 2006: Quantitative estimation of land cover structure in an arid region across the Israel-Egypt border using remote sensing data. Journal of Arid Environments **66**, 336-352.

QUINTON, J.N., GOVERS, G., VAN OOST, K., BARDGETT, R.D., 2010: The impact of agricultural soil erosion on biogeochemical cycling. Nature Geosciences **3**, 311-314.

SANDHOLT, I., RASMUSSEN, K., ANDERSEN, J., 2002: A simple interpretation of the surface temperature/vegetation index space for assessment of soil moisture status. Remote Sensing of Environment **19**, 213-224.

SCHADE, J.D. & HOBBIE, S.E., 2005: Spatial and temporal variation in islands of fertility in the Sonoran Desert. Biogeochemistry **73**, 541-553.

SCHIMEL, D., MELILLO, J., TIAN, H., 2000: Contribution of increasing CO^2 and climate to carbon storage by ecosystems in the United states. Science **287**, 2004-2006.

SCHLESINGER, W.H, PILMANIS, A.M., 1998: Plant-Soil Interactions in Deserts. Biogeochemistry **42**, 169-187.

SCHLESINGER, W.H., RAIKES, J., HARTLEY, A., CROSS, A., 1996: On the spatial pattern of soil nutrients in desert ecosystems. Ecology **77**, 364-374.

SCHMIDT, H. & KARNIELI, A., 2000: Remote Sensing of the seasonal variability of vegetation in a semi-arid environment. Journal of Arid Environments **45 (1)**, 43-59.

SCHREIBER, K.F., YAIR, A., SHACHAK, M., 1995: Ecological Gradients Along Slopes of the Northern Negev Highlands, Israel. Advances in GeoEcology **28**, 209-229.

SCHWANGHART, W., JARMER, T., 2011: Linking spatial patterns of soil organic carbon to topography - A case study from south-eastern Spain. Geomorphology **126**, 252-263.

SEIP, H.M., 2001: We know too little about the carbon cycle, Oslo.

SMITH, P., FANG, C., DAWSON, J.J.C., MONCREIFF, J.B., 2008: Impact of global warming on soil organic carbon. Advances in Agronomy **97**, 1-43.

STAVI, I., LAVEE, H., UNGAR, E.D., SARAH, P., 2009: Ecogeomorphic feedbacks in semiarid rangelands: a review. Pedosphere **19 (2)**, 217-229.

XIAO, J. & MOODY, A., 2005: Geographical distribution of global greening trends and their climatic correlates: 1982-1998. International Journal of Remote Sensing **26**, 2371-2390.

YAALON, D.H. & DAN, J., 1974 : Accumulation and distribution of loess-derived deposits in the semi-desert and desert fringe areas of Israel. Zeitschrift für Geomorphologie **20**, 91-105.

YAIR, A., 1992: The control of headwater area on channel runoff in a small arid watershed. In: PARSONS, T., ABRAHAMS, A., (Eds.). Environmental Change in Drylands: Biogeophysical and Geomorphological Perspectives, 199-227.

YAIR, A., 1999: Spatial variability in the runoff generated in small arid watersheds: implications for water harvesting, in: HOEKSTRA, T.M. & SHACHAK, M., (Eds.), Arid Land Management, toward Ecological Sustainability, 212-222.

YAIR, A., DANIN, A., 1980: Spatial variations in vegetation as related to the soil moisture regime over an arid limestone hillside, Northern Negev Israel. Oecologia **47**, 83-88.

YAIR, A., KOSSOVSKY, A., 2002: Climate and surface properties: hydrological response of small arid and semi-arid watersheds. Geomorphology **42 (1/2)**, 43-57.

YAIR, A., SHACHAK, M., 1982: A case study of energy, water and soil flow chains in an arid ecosystem. Oecologia **54 (3)**, 389-397.

YAIR, A., RAZ-YASSIF, N., 2004: Hydrological processes in a small arid catchment: scale effects of rainfall and slope length. Geomorphology **61**, 155-169.

YAO, S.H, ZHANG, B., HU, F., 2010: Biophysical controls over mineralization and sequestration of amended organic carbon in soil: Effects of intensity and frequency of drying and wetting cycles. World Congress of Soil Science: Soil solutions for a changing world, Brisbane, Australia.

YOO, K., AMUNDSON, R., HEIMSATH, A.M., DIETRICH, W.E., 2006: Spatial patterns of soil organic carbon on hillslopes: integrating geomorphic processes and the biological C cycle. Geoderma **130**, 47-65.

7. Synthesis

This thesis proposes the development of a GIS-based image analysis approach for the quantification of SOC stocks at regional scale considering SOC spatial heterogeneity at local scale in arid environments by combining field data and digital image processing approaches. Based on field measurements, ecohydrological conditions and processes; controlling SOC concentrations and patterns at local scale were determined. A major focus was the determination of parameters characterizing environmental heterogeneity in dynamic geomorphic systems. Special attention was put on small-scale surface properties, the spatial heterogeneity of SOC stocks, data extrapolation of spatially limited sampling densities and the identification of proxy indicators for SOC concentrations and patterns such as vegetation density and EHEs. The results (Chapter 6, Research Paper, 4.3) show that the developed image analysis approach (Chapter 4, Research Paper, 3) in combination with field sampling strategies (Chapter 3, Research Paper, 3; Chapter 2, Research Paper, 4) provides an effective tool to quantify SOC stocks in highly heterogeneous arid environments and to improve the methodological setup of future regional SOC inventories.

The results of the individual studies have already been discussed above in more detail. However, the following synthesis briefly summarizes the results of the four studies and then discusses the major findings with reference to the questions raised in the introduction.

7.1 Relationship between surface characteristics, vegetation coverage and SOC

The relationship between surface characteristics, vegetation coverage, SOC concentrations and stocks was identified for the study site in the Negev Desert, Israel (Chapter 3, Research Article, 4). The results show a large spatial variability of SOC depending on differences in micro-topography, surface processes, soil formation and properties and vegetation. These differences were mapped within the study site based on EHEs, which provide an effective tool to detect ecological processes governing the spatial patterns of SOC. The calculated SOC stocks show that soil in the study site contains a significant amount of SOC (Chapter 3, Research Paper, 4). Despite the fact that this amount is smaller than in more humid environments, it is still substantial and important for the functioning and thus conservation of arid ecosystems. Data analyses derived from field sampling indicates that soil moisture and vegetation coverage affect and control SOC concentrations. High SOC concentrations and SOC stocks are found at slope positions which favour high soil moisture and thus high vegetation densities (Chapter 3, Research Paper, Fig. 3, Fig. 4). In turn, high vegetation densities indicate high SOC concentrations. The positive relationship between vegetation coverage and SOC stocks at the study site shows that the findings of Olsvig-Whittaker et al. (1983), who studied the surface properties on vegetation, can also be applied to SOC stocks. This strong link between SOC and aboveground vegetation properties, such as vegetation density and spatial vegetation distribution is also reported in studies by Jobbágy & Jackson (2000) and Li et al. (2010). Furthermore the results indicate that vegetation coverage provides a direct index for the spatial patterns of SOC stocks in drylands. In general the variability of SOC stocks, driven by precipitation, soil volume, water redistribution and vegetation density also implies that SOC stocks in arid environments are highly sensitive to climate change. The impact of climate change will result in a major unstable SOC-pool within the global carbon cycle of the twenty-first century.

7.2 Relationship between environmental properties and vegetation coverage

To determine the relationship between precipitation, soil volume, water redistribution and vegetation density the study aimed at the examination of rock-soil interactions and the relevance of soil volume for storing plant available water in the Northern Negev, Israel (Chapter 4, Research Paper, 2). Therefore, a suitable rainfall simulation procedure was developed. Short and low magnitude rainfall events, which occur in a high frequency in the study area, only lead to a limited amount of rainfall and runoff infiltrating into the soil, resulting in a partial wetting of the soil profile. Soil volume potentially affects plant water supply when the infiltration capacity of the soil body is smaller than the amount of water required by the vegetation until the next rainfall. High vegetation densities are found, where soil volume is high. The results clearly show (Chapter 4, Research Paper, 5) that micro-scale water supply and soil volume determine vegetation density. In turn this suggests that high vegetation densities indicate high soil volumes and hence high SOC concentrations per unit area. Furthermore the analysis of rainfall magnitude and frequency in this region in conjunction with the critical role of soil volume and infiltration rate indicate that the duration of periods without rainfall seem to be more important for vegetation growth than the absolute event or annual rainfall amount. Soil volume and infiltration regulate whether drought stress occurs once the water in the soil has evaporated. Overall, rainfall frequency rather than magnitude or annual precipitation amount appear to determine plant available water in an area with a given pattern of rock-soil cover and soil volumes. This is highly relevant for the assessment of the impact of climate change on SOC stocks and patterns in arid environments.

7.3 Automated mapping of ecohydrological environments (EHEs)

The distinctive EHEs reflect the spatial variability of environmental and ecohydrological conditions within the study site. Each EHE is characterized by distinctive relationships between precipitation, soil volume, water redistribution, vegetation density and SOC concentrations and patterns. Micro-scale water supply and soil volume determine vegetation density and spatial distribution. In turn, high vegetation densities indicate high soil volumes and hence high SOC concentrations per unit area. The different surface conditions of the distinctive EHEs lead to variable SOC concentrations and vegetation patterns regarding vegetation density and spatial distribution. The aim of the study was therefore to develop an approach towards automated mapping of EHEs on the basis of vegetation patterns using imagery with different resolutions (Chapter 5, Research Paper 1). The dependence of different vegetation pattern indices on the spatial resolution of the image data was investigated and indices identified that are insensitive to the resolution difference in the imagery. Indices with a high degree of explanatory power were then used as variables in a decision tree model. The results of the decision tree based classification model show that spatial pattern indices can be used as an identification tool for EHEs (Chapter 5, Research Paper, 4). The implemented remote sensing approach bridges the gap between the need for high resolution and the detection of vegetation coverage based on bands in the visible spectra. The benefit of high-resolution data is that areas of interest are identified as the scale processes occur. This approach represents an easy way to map EHEs using vegetation pattern indices and the adaptability of a range of differently generated satellite imageries (e.g. orthophoto (RGB), Quickbird, Iconos or GeoEye-1 images). Further potentially valuable studies could take the form of a more detailed determination of the SOC-pool regarding sink and source areas and a better assessment of the impact of climate change in desert environments.

7.4 Spatial prediction of SOC stock and patterns

The study aimed at the estimation of SOC stocks and patterns at regional scale considering small-scale spatial heterogeneity of SOC concentration (Chapter 6, Research Paper, 1). As identified in the previous studies, spatial vegetation patterns are related to the different EHEs and SOC concentrations and patterns. Therefore vegetation coverage and EHEs were implemented as proxy indicators for SOC concentration and spatial distribution. Finally SOC stocks and patterns were calculated for the study site using the interrelations and methodological procedures derived from the previous investigations by remote sensing and digital image processing. The results (Chapter 6, Research Paper, 4) show that the adopted image analysis approach for arid environments provides a simple solution for the estimation of vegetation coverage and EHEs and hence the precise estimation of SOC stocks and patterns. In combination with the identified relationships between precipitation, soil, vegetation, water redistribution and SOC, this method delivers some key benefits such as being (i) fast and comprehensive (ii) cheap, due to shortened field trips and easy and often free access to orthoimages and (iii) scale-invariant. Nevertheless, a certain limitation of this approach exists for images with (i) a high variability in the greyscale values for vegetation and (ii) a very low albedo contrast between vegetation and bare ground. By taking these limitations into consideration, the resulting adequate selection of remotely sensed images diminishes detection and analysis errors. This is intended to be the first study that has employed SOC-stock calculation by using spatial distribution of vegetation coverage and EHEs as proxy variables for SOC-concentrations. In contrast to the notion that rocky desert environments do not contain significant soil or SOC, the results of this study show that the SOC-stock is higher than generally expected. This fact confirms the necessity to quantify the SOC sink and source capacity of soils in changing desert environments.

7.5 Discussion of the guided research questions

Based on the results of the four studies, the major research questions that were raised in the introduction (chapter 1) are addressed below:

Question 1: How much are surface properties, water availability and vegetation coverage related to SOC concentrations and stocks?

The study site in the Negev Desert is characterized by highly complex and variable environmental settings (Chapter 3, Research Paper, Table 1). Surface properties range between a mosaic of small soil patches and soil filled bedrock fissures to soil free bedrock surfaces prohibiting the formation and storage of SOC (Hoffmann et al. 2012, Olsvig-Whittaker et al. 1983, Schreiber et al. 1995). The variability of surface properties and SOC stocks is related to the different EHEs within the study site (Chapter 4, Research Paper, Table 1) and water availability as a key limiting factor (Hoffmann et al. 2012). The effects of surface properties and water availability on vegetation coverage and hence on SOC concentrations are shown in Fig.2.

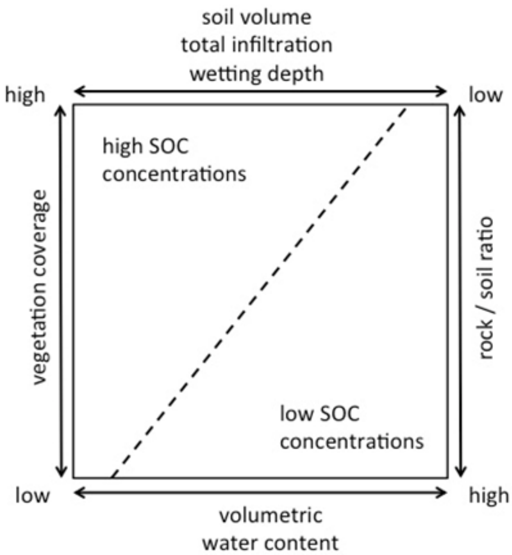

Fig. 2: Conceptual model of the effect of surface properties, water availability and vegetation coverage on SOC concentrations.

The relationships between soil volume, total infiltration, wetting depth, rock-soil ratio, volumetric water content and vegetation coverage regarding SOC concentrations are reflected in this conceptual model. Compared to soil covered surfaces, which are characterized by a high porosity and high water absorbing capacity, runoff generation is faster on relatively impermeable bare rocky surfaces. In turn lower flow frequency and lower magnitude of runoff are observed on soil-covered surfaces (Hikel et al. 2012, Yair & Raz-Yassif 2004, Yair 1992). For the simulated rainfall, total infiltration values range from 5.7 l on soil covered areas to 1.6 l on areas nearly devoid of any soil. In addition, runoff redistribution is determined by differences in infiltration rates due to rock and soil covered surfaces influencing the rate of transformation of rainfall into runoff (Chapter 4, Research Paper, Table 3 and Figure 9). Rock-soil ratio declines with soil volume (Chapter 4, Research Paper, Figure 11). Hence, small soil volumes receive their water from a proportionally greater rock surface than those with a high soil volume. Rock-soil ratio and soil volume are strongly correlated (R^2=0.8). For small soil volumes total infiltration is lower due to the fact that the limited soil volume reduces the amount of infiltration. Low infiltration rates indicate that only a limited amount of water entered the soil. The low depth of wetting which declines with rock-soil ratio confirms this. Hence, low soil volumes limit plant available water. Soil volume displays a moderate negative relationship (R^2=-0.56) with volumetric water content (water storage capacity) indicating that small soil volumes are filled up closer to their maximum water storage capacity than the large ones during the simulated rainfall. In contrast, low volumetric water content therefore indicates high total infiltration but also that the soil volume was not filled up to its maximum (Chapter 4, Research Paper, Figure 11). Soil volume determines the frequency of watering that is required to maintain vegetation and the risk of drought stress. High vegetation coverage is therefore found where soil volume and total infiltration is high. In contrast low vegetation coverage is found where soil volume, total infiltration and wetting depth are low. According to the findings by Cammeraat (2002), Puigdefabregas (2005) and Stavi et al. (2009), vegetation patches absorb more water due to higher soil porosity, infiltration capacity water holding capacity, hydraulic conductivity, structural stability, organic matter content and lower bulk density. This suggests that high vegetation densities indicate high soil volumes and hence high SOC concentrations per unit area. Vegetation coverage and SOC concentrations and stock are strongly correlated (R^2=0.81, R^2=0.91) (Chapter 3, Research Paper, 4). Vegetation is distributed patchily within the area due to soil and water availability resulting in a high spatial variability of SOC concentrations and stocks. SOC concentrations range between 3 g kg^{-1} and 15 g kg^{-1}. Soil depth varies on a centimetre to meter scale and the SOC concentration change is therefore limited by depth.

The presented approach bears some importance regarding the expected changing climate conditions related to the global warming process. Yair & Kossovsky (2002) state for the Negev Desert that the same regional climatic change may have different effects on the environmental responses. Different surface conditions and processes control the ecohydrological response and therefore lead to a non-uniform reaction to a regional climatic change. Determining spatial heterogeneity and interrelation between surfaces and processes as introduced by the experimental procedure contributes to a better understanding and estimation of the impact of climate change on the spatial variability of SOC concentrations and stocks in arid environments.

Question 2: At which level of detail and accuracy can SOC inventories be made using field measurements, remote sensing and digital image processing?

The results generated to address research question 1 show that micro-scale differences in topography and soil and surface properties determine the spatial distribution of vegetation and hence the spatial variability of SOC concentrations and stocks (Chapter 3, Research Paper, 4; Chapter 4, Research Paper, 5). It was shown that vegetation density and spatial distribution are related to previously mapped EHEs which consider the small-scale spatial variability of environmental properties and that the occurrence and extent of the latter can be spatially predicted using information on vegetation patterns (Chapter 5, Research Paper, 4). Several studies (Cammeraat & Imeson 1999, Imeson & Prinsen 2004, Lesschen 2008, Puigdefabregas 2005) show that vegetation patterns provide information on dominant hydrology and geomorphological processes and are thus potential proxies towards understanding these processes and their variability in space. This implies the need for a precise detection of vegetation coverage using imagery with submeter spatial resolution.

The implemented GIS-based image analysis approach bridges the gap between the need for high resolution and a differentiated detection of vegetation coverage and generated exact results for the specific area. Due to the detection of vegetation coverage based on bands in the visible spectra using digital image processing, this approach provides a simple solution for the accurate estimation of vegetation coverage (accuracy of 89%, RMSE=0.8) and spatial patterns in arid environments. The precise estimation of vegetation coverage and the subsequent identification of EHEs using vegetation indices, as proxy variables for SOC concentrations and patterns (prediction accuracy of ~70%) provide a link between remotely sensed and ground based studies (Chapter 5, Research Paper, 4).

A certain limitation was brought for orthoimages with (i) a high variability in the greyscale values for vegetation and (ii) a very low albedo contrast between vegetation and bare ground. Detection errors are mostly based on these two aspects. Vegetation patterns, characterized by low greyscale values were classified as bare ground when the surrounding raster cells also show low greyscale values resulting in an under-estimation of vegetation coverage. If a small range of high greyscale values was representing vegetation as well as bare ground, vegetation coverage was over-estimated. In general the estimation of vegetation coverage is difficult if the albedo contrast between vegetation and bare ground is greatly diminished.

But the approach provides some key benefits. First, it allows the estimation of vegetation coverage and its spatial patterns from orthoimages with a high spatial resolution. Second, the identification of distinctive EHEs using vegetation indices are possible. Third, the precise quantification of SOC stocks and patterns are possible at regional scale (prediction accuracy of 86%) using vegetation distribution and EHEs as proxy variables for SOC concentrations and patterns (Chapter 6, Research Paper, 4). Compared to SOC studies in other arid environments (e.g. Amundson 2001, Ardö & Olsson 2003, Feng et al. 2003, Schlesinger 1977), the estimated SOC concentrations and stocks for the study site in Israel show medium to high values (see Chapter3, Table 4). The SOC stock averaged over the entire study site is 0.58 kg C m^{-2}. SOC stocks vary between zero in uncovered areas and 1.54 kg C m^{-2} in soil covered areas. Jarmer et al. (2010) identified in his study similar SOC concentrations in this area (3 g kg^{-1} - 15 g kg^{-1}). The even medium SOC-stock indicates an exact quantification due to the high variability of SOC-concentration values regarding previous studies (Hoffmann et al. 2012). Higher SOC-concentrations in the Negev Desert are attributed to the patchy nature of the rock and soil cover. This is in accordance with the "islands of fertility" (Schlesinger & Pilmanis 1998) with increased biogeochemical processes, NPP, SOC-concentrations, reduced

mineralization of SOC due to water scarcity (Yao et al. 2010) and/or soil degradation (Bolton et al. 1993).
The potential benefit of the implemented GIS-based image analysis approach for the quantification of SOC inventories is that the spatial heterogeneity of SOC concentrations at local scale is considered in the SOC stock calculation at regional scale (Chapter 6, Research Paper, 6). Studies at regional scale are generally based on simplified relations where uncertainty associated with small scale variability at local scale is not considered (Cox et al. 2000, Jones et al. 2005). The results are therefore characterized by large uncertainties of regional SOC estimates. The uncertainties based on commonly used interpolation or extrapolation techniques are diminished by using the GIS-based image analysis approach which shows a prediction accuracy of 86% (Chapter 6, Research Paper, 5). The relationship between surface properties, water availability, vegetation coverage and SOC concentrations related to the different EHEs is identified at local scale (Chapter 3, Research Paper, 5; Chapter 4, Research Paper, 5). In turn these relationships are determined at regional scale by using vegetation indices as an identification tool for the distinctive EHEs (Chapter 5, Research Paper, 3). By combining field measurements, remote sensing and digital image processing the implemented approach therefore ensures the required consideration of spatial heterogeneity regarding SOC-distribution at local scale for the quantification of SOC stocks at regional scale as mentioned in the introduction (Chapter 1).

Question 3: How does the GIS-based image analysis approach contribute to reducing the uncertainty of SOC inventories in arid environments?

The GIS-based image analysis approach shows the potential benefits of using image data with carefully located in situ field data in digital SOC mapping (Chapter 6, Research Paper, 4.3). The results also indicate the benefit of combining ecohydrologic studies with spatial data analysis. A detailed mapping of small scale surface properties and processes (Chapter 3, Research Paper, 3; Chapter 4, Research Paper, 4) and the stratification of the study site into EHEs of similar surface process regimes (Chapter 5, Research Paper, 3) provides the potential to decrease the uncertainty of SOC inventories in arid environments. The calculated SOC concentrations are in accordance with the findings by Jarmer et al. (2010) who studied SOC variability in this area. The implemented GIS-based image analysis approach shows a prediction accuracy of 86% and bears some advantages regarding generally used methods for SOC stock assessment at regional scale such as remote sensing and / or interpolation / extrapolation approaches. First, using remote sensing for the estimation of SOC inventories is limited to soils devoid of any vegetation which leads to large uncertainties (Schwanghart & Jarmer 2011). SOC concentrations and stocks are strongly correlated with aboveground vegetation (Jobbágy & Jackson 2000, Li et al. 2010). As a result, these “islands of fertility” (Schlesinger & Pilmanis 1998, Austin et al. 2004, Cánton et al. 2004) therefore remain hidden from airborne monitoring. Vegetation density and distribution and the relationship with SOC concentrations are considered in the quantification of SOC inventories using the GIS-based image analysis approach. Second, the spatial resolution of the sensor is a limiting factor

(Schwanghart & Jarmer 2011) resulting in simplifying assumptions regarding the SOC spatial heterogeneity at local scale (Cox et al. 2000, Jones et al. 2005). In contrast interpolation and extrapolation techniques are used to estimate SOC inventories at coarser scales (Li & Heap 2011, Liu et al. 2006, Mondini 2012). Both approaches lead to large uncertainties in the assessment of SOC stocks (Aufdenkampe et al. 2011). Using vegetation coverage and EHEs as proxy indicators for SOC concentrations and patterns SOC spatial heterogeneity at local scale is considered in the calculation of regional SOC inventory by the implemented GIS-based image analysis approach. Third, by combining field data and digital image processing approaches, SOC inventories are not limited to the uppermost 2cm of topsoil as provided by common remote sensing techniques (Jarmer et al. 2010, Schwanghart & Jarmer 2011) due to the fact that soil volume is considered in the SOC stock calculation.

Based on the GIS-based image analysis approach the uncertainties in the estimation of SOC inventories are reduced. Compared to previous studies in arid environments it is difficult to quantify the reduction of uncertainty due to different applied methods and environmental conditions.

For this reason examples are presented below to illustrate how the implemented GIS-based image analysis approach can be applied to existing studies to reduce the uncertainty in the quantification of SOC inventories.

For the quantification of regional SOC inventories soil groups are defined and for each group SOC densities are calculated by soil sampling. SOC densities of each group are then multiplied with their respective area for the quantification of SOC stock (Feng et al. 2002, Singh et al. 2007, Sinoga et al. 2012). Data from the FAO/UNESCO Soil Map of the World (FAO-UNESCO, 1995) are generally used (Alam et al. 2013, Henry et al. 2009, Jobbágy & Jackson 2000). The results show that uncertainties exist, due to the fact that FAO soil data are based on extrapolation and substitution from similar soil types and soil formation factors rather than actual survey and sampling (Alam et al. 2013, Selvaradjou et al. 2005). The implemented GIS-based image analysis approach copes with the need for point measurements and regional assessment of SOC stock quantification. The determination of the relationship between SOC concentrations and stocks and environmental conditions provides the required information at local scale. At regional scale the mapped small scale surface properties and processes defined by EHEs of similar surface process regimes are detectable using remote sensing techniques and spatial statistics. Combining both information uncertainties in the estimation of SOC stocks are reduced. While a strong link between SOC and ecohydrological processes has been recognized (Lal 2009, Yoo et al. 2006) there is no simple and straightforward way to quantitatively determine these relationships on a local scale basis for a study site with an extent of regional scale.

Yoo et al. (2006) measured the relationship between SOC storage, soil thickness and topographic curvature to create SOC storage maps at regional scale for two watersheds. But questions remain about the broad applicability of one or two local scale attributes to a regional scale. The SOC stock calculation using the implemented GIS-based image analysis approach is based on the spatial distribution of vegetation coverage and EHEs as proxy variables for SOC-concentrations. Each EHE is characterized by distinctive relationships between precipitation, soil volume, water redistribution, vegetation density and SOC concentrations and patterns at local scale. Due to the fact that the distinctive EHEs are detectable by remote sensing techniques at regional scale, the driving factors for SOC concentrations and patterns at local scale are considered in the calculation of SOC stocks at regional scale. The quantification of SOC inventories at regional scale is therefore not reduced to one or two attributes at local scale which improves the accuracy of SOC inventories.

For the estimation of SOC inventories, ecosystem models are frequently used (Falloon et al. 1998, Falloon et al. 2002, Poussart et al. 2004a, b). Ecosystem models require input data of high quality for reliable SOC estimates and are therefore generally combined with field measurements (Ardö & Olsson 2003). However, modelling at regional scale makes simplifications unavoidable resulting in uncertain model outputs (Ardö et al. 2000, Poussart 2002, Poussart et al. 2004a,b). The input data are mostly based on the FAO Soil Map of the World (FAO-UNESCO, 1995) or the IGBP soil dataset (Global Soil Data Task, 2000) (Ardö & Olsson 2004, 2003, Farage et al. 2007) which do not represent the environmental conditions at local scale. The implemented GIS-based image analysis approach provides the required high quality input data for such ecosystem models due to the fact that environmental conditions and relationships between environmental factors at local scale are detectable at regional scale. Using the generated data in ecosystem models suggests reducing the uncertainty of the model output.

The implemented GIS-based image analysis approach copes with the need to observe the spatial structure and extent of the studied system, whilst simultaneously observing the functional components. The increasing availability of diversified remote sensing data concerning spatial resolution and eco/geomorphic system structure (Mulder et al. 2011) complies with the required observation of multiple biotic and abiotic parameters over various spatial and temporal times.

8. Outlook

This PhD thesis applied a GIS-based image analysis approach for the estimation of SOC stocks and patterns at regional scale in the arid Negev Highlands, Israel. The approach provides reliable estimates of SOC inventories and copes with the need to consider the spatial heterogeneity of SOC concentrations at local scale and the necessity to determine the importance and potential changes of SOC stocks in arid environments. The approach thus fulfils the increasing demand on spatially distributed, quantitative information on SOC inventories in arid ecosystems and contributes to recent endeavours of digital SOC mapping and monitoring. The study site was analysed with regard to the relationship between surface characteristics, vegetation coverage, water availability and SOC concentrations and stocks. Based on the generated dataset distinctive EHEs were identified which reflect dominant processes and surface properties and specific hydro-geomorphological responses in reaction to rainfall. The results show a large spatial variability of SOC regarding the different EHEs at which ecohydrologic conditions and hence vegetation density and distribution exerts a strong control on SOC concentrations. The variability of SOC stocks, driven by aspect, soil moisture availability and vegetation coverage also implies that SOC stocks in arid environments are highly sensitive to climate change and thus represent a major unstable C pool within the global carbon cycle. The generated dataset on vegetation densities and distribution derived from hyperspectral remote sensing and orthoimage analysis was applied to automatically map the distinctive EHEs at regional scale using a decision tree model. The results show that the proposed method is appropriate for simulating the different EHEs within the study site with a prediction accuracy of the classification tree of 70%. Vegetation coverage and EHEs were used as proxy indicators for SOC concentrations and patterns in a GIS-based image analysis approach for the calculation of SOC inventory at regional scale. The results show that the study site contains a significant amount of SOC (1.19t C ha^{-2}). The results also show that the combination of field data and digital image processing approaches lead to a precise estimation of SOC stocks (accuracy of 86%) at regional scale considering local scale SOC heterogeneity in arid environments. So far our findings refer only to rocky desert environments in the Negev Highlands, Israel and further studies are required to test if the approach is applicable in other (rocky) desert environments. The literature review on SOC inventories in these dynamic geomorphic systems has indicated that studies are characterized by different measurement techniques, variable reference soil depth and different interpolation or extrapolation techniques respectively. The comparison of the calculated SOC inventories therefore proved to be difficult. More comparable and detailed SOC inventories are therefore needed to verify the results of this study in arid environments. Our data provides only a snapshot of present SOC stocks and patterns. But SOC stocks and patterns are related to vegetation density and spatial distribution, which are sensitive to changing climate conditions. This temporal aspect could not be covered in our analysis but should be included in future research in this area. Additionally, the results of the implemented approach regarding the detailed mapping of small scale surface properties and processes and the stratification of the study site into EHEs of similar surface process regimes could be applied in hydrological and erosion models and research. By combining information about vegetation coverage and ecohydrology, the efficient identification of erosion hotspots within a study site could be provided. Nevertheless future studies should first focus on testing the implemented approach in different desert environments and comparing the results using standardised methods.

Acknowledgements

I would like to thank my doctoral supervisor Prof. Dr. Nikolaus J. Kuhn who has always supported me in every possible way. I am grateful for his supervision and guidance over the past five years. I also thank Dr. Holly Croft for her willingness to supervise my work and for her time and support.

Special thanks go to my colleagues and friends at the University of Basel who supported me during my work. I am very thankful to Heidi Strohm, Marianne Caroni, Hans-Rudolf Rüegg and Ruth Strunk for technical support, Dr. Wolfgang Schwanghart, Dr. Thomas Jarmer (University of Osnabrueck) and the Israel field-crew for the great time we had in the Negev. Your support and friendship created a motivating and fun working environment.

I thank my family and friends for their support and encouragement in every way before and during my PhD.

My PhD was financially supported by Freie Akademische Gesellschaft, Stiftung Dr. Joachim de Giacomi and by Nikolaus und Bertha Burckhardt-Bürgin Stiftung.

References

Adams J.B., Smith M.O., Gillespie A.R., 1989. Simple methods for complex natural surfaces: A strategy for the hyperspectral era of remote sensing. Proceedings of the IGARSS Symposium, 16-21, 10-14 July, IEEE, Vancouver, Canada.

Alam S.A., Starr M., Clark B.J.F., 2013. Tree biomass and soil organic carbon densities across the Sudanese woodland savannah: A regional carbon sequestration study. Journal of Arid Environments 89, 67-76.

Andrew M.E., Ustin S.L., 2008. The role of environmental context in mapping invasive plants with hyperspectral image data. Remote Sensing and Environment 112, 4301-4317.

Amundson R., 2001. The Carbon Budget in Soils. Annual Review of Earth and Planetary Science 29, 535-562.

Ardö J., Barkman A., Arvidsson P., 2000. Critical Levels of SO_2 in northern Czech Republic - uncertainties and relationship to regional forest decline. Geographical and Environmental Modelling 4, 131-161.

Ardö J., Olsson L., 2003. Assessment of soil organic carbon in semi-arid Sudan using GIS and the CENTURY model. Journal of Arid Environments 54, 633-651.

Ardö J., Olsson L., 2004. Soil carbon sequestration in traditional farming in Sudanese drylands. Environmental Management 33, 318-319.

Arkin Y., Braun M., 1965. Type sections of Upper Cretaceous formations in the northern Negev. Israel - Geological Survey. Stratigraphic Section No. 2a. Jerusalem.

Asbjornsen H., Goldsmith G.R., Alvarado-Barrientos M.S., Rebel K., Van Osch F.P., Rietkerk M., Chen J., Gotsch S., Tobón C., Geissert D.R., Gómez-Tagle A., Vache K., Dawson T.E., 2011. Ecohydrological advances and applications in plant-water relations research: a review. Journal of Plant Ecology 4 (1-2), 3-22.

Asner G.P, Borghi C.E, Ojeda R.A, 2003. Desertification in Central Argentina: changes in ecosystem carbon and nitrogen from imaging spectroscopy. Ecological Applications 13, 629-648.

Aufdenkampe A.K., Mayorga E., Raymond P.A., Melack J.M., Doney S.C., Alin S.R., 2011. Riverine coupling of biogeochemical cycles between land, oceans, and atmosphere frontiers. Ecology and Environment 9 (1), 53-60.

Austin A.T., Yahdjian L., Stark J.M., Belnap J., Porporato A., Norton U., Ravetta D.A., Schaeffler S.M., 2004. Water pulses and biogeochemical cycles in arid and semiarid ecosystems. Oecologia 141, 221-235.

Barati S., Rayegani B., Saati M., Sharifi A., Nasri M., 2011. Comparison the accuracies of different spectral indices for estimation of vegetation cover fraction in sparse vegetated areas. The Egyptian Journal of Remote Sensing and Space Science 14 (1), 49-56.

Batjes N.H., 1996. Total carbon and nitrogen in the soils of the world. European Journal of Soil Science 47, 151-163.

Baumgardner M., Silva L., Biehl L., Stoner E., 1985. Reflectance properties of soils. Advances in Agronomy 38, 1-44.

Bell M.J., Worral F., 2009. Estimating a region's soil organic carbon baseline: The undervalued role of land-management. Geoderma 152, 74-84.

Ben-Dor E., Banin A., 1994. Visible and near-infrared (0.4-1-1µm) analysis of arid and semiarid soils. Remote Sensing of Environment 48, 261-274.

Ben-Dor E., Banin A., 1995. Near-infrared analysis as a rapid method to simultaneously evaluate several soil properties. Soil Science Society of America Journal 59, 364-372.

Bergkamp G., Cerda A., Imeson A.C., 1999. Magnitude-frequency analysis of water redistribution along a climate gradient in Spain. Catena 37, 129-146.

Berhe A.A., Harden J.W., Torn M.S., Harte J., 2008. Linking soil organic matter dynamics and erosion-induced terrestrial carbon sequestration at different landform positions. Journal of Geophysical Research 113, 1-12.

Boeken B., Shashak M., 1994. Changes in desert plant communities in human-made patches and their implications for management of desertified landscapes. Journal of Applied Ecology 4, 702-716.

Bohn H.L., 1982. Estimate of organic-carbon in world soils II. Soil Science Society of America Journal 46, 1118-1119.

Bolin B., 1970. The carbon cycle. Scientific American 223, 124-132.

Bolstad P.V., Vose J.M., 2001. The Effects of Terrain Position and Elevation on Soil C in the Southern Appalachians. In: Lal R., Kimble J.M., Follet R.F., Stewart B.A., (eds.). Assessment methods for soil carbon, 45-52. Boca Raton (FL), Lewis Publishers.

Bolton J.H., Smith J.J., Link S.O., 1993. Soil microbial biomass and activity of a disturbed and undisturbed shrubsteppe ecosystem. Soil Biology and Biochemistry 25, 545-552.

Brown D., Shepherd K., Walsh M., Mays M., Reinsch T., 2006. Global soil characterization with VNIR diffuse reflectance spectroscopy. Geoderma 132, 273-290.

Bruins H., 1986. Desert Environment and Agriculture in the Central Negev and Kadesh Barnea During Historical Times, PhD-Thesis. Wageningen Agricultural University, Nijkerk, The Netherlands.

Budge K., Leifeld J., Hiltbrunner E., Fuhrer J., 2011. Alpine grassland soils contain large proportion of labile carbon but indicate long turnover times. Biogeosciences 8, 1911-1923.

Buis E., Veldkamp A., 2008. Modelling dynamic water redistribution patterns in arid catchments in the Negev Desert of Israel. Earth Surface Processes and Landforms 33, 107-122.

Burke I.C., Lauenroth W.K., Riggle R., Brannen P., Madigan B., Beard S., 1999. Spatial Variability of Soil Properties in the Shortgrass Steppe: The Relative Importance of Topography, Grazing, Microsite, and Plant Species in Controlling Spatial Patterns. Ecosystems 2, 422-438.

Burnham J., Sletten H., Sletten R.S., 2010. Spatial distribution of soil organic carbon in northwest Greenland and underestimates of high arctic carbon stores. Global Biogeochemical Cycles 24, 1-14.

Calvao T., Palmeirim J.M., 2004. Mapping Mediterranean scrub with satellite imagery: biomass estimation and spectral behaviour. International Journal of Remote Sensing 25 (16), 3113-3126.

Cammeraat L.H., 2002. A review of two strongly contrasting geomorphological systems within the context of scale. Earth Surface Processes and Landforms 27, 1201-1222.

Cammeraat L.H., Imeson A.C., 1999. The evolution and significance of soil-vegetation patterns following land abandonment and fire in Spain. Catena 37 (1-2), 107-128.

Cánton Y., Solé-Benet A., Domingo F., 2004. Temporal and spatial patterns of soil moisture in semiarid badlands of SE Spain. Journal of Hydrology 285, 199-214.

Cerdan O., Govers G., Le Bissonnais Y., Van Oost K., Poesen J., Saby N., Gobin A., Vacca A., Quinton J., Auerswald K., Klik A., Kwaad F.J.P.M., Raclot D., Ionita I., Reijman J., Rousseva S., Muxart T., Roxo M.J., Dostal T., 2010. Rates and spatial variations of soil erosion in Europe: a case study based on erosion plot data. Geomorphology 122 (1-2), 167-177.

Coleman K., Jenkinson D.S., 1999. ROTHC-26.3. A Model for the Turnover of Carbon in Soil. Model Description and Users Guide. IACR, Rothamsted, Harpenden, UK.

Cox P.M., Betts R.A., Jones C.D., Spall S.A., Totterdell I.J., 2000. Acceleration of global warming due to carbon-cycle feedbacks in a coupled climate model. Nature 408, 184-187.

Dan J., Yaalon D.H., Koyumdjiski H., Raz Z., 1972. The soil association map of Israel. Israel Journal of Earth Science 21, 29-49.

Djukic I., Zeheter F., Tatzber M., Gerzabek M.H., 2010. Soil organic-matter and characteristics along an Alpine elevation gradient. Journal of Plant Nutrition and Soil Science 173, 30-38.

D'Odorico P., Porporato A. (eds.), 2006. Dryland Ecohydrology. Springer.

Doetterl S., Six J., Van Wesemael B., Van Oost K., 2012a. Carbon cycling in eroding landscapes: geomorphic controls on soil organic C pool composition and C stabilization. Global Change Biology 18, 2218-2232.

Doetterl S., Van Oost K., Six J., 2012b. Towards constraining the magnitude of global agricultural sediment and soil organic carbon fluxes. Earth Surface Processes and Landforms 37, 642-655.

Don A., Schumacher J., Freibauer A., 2011. Impact of tropical land-use change on soil organic carbon stocks - a meta-analysis. Global Change Biology 17, 1658-1670.

Dregne H.E., 2002. Land degradation in drylands. Arid Land Research and Management 16, 99-132.

Egli M., Sartori G., Mirabella A., Favilli F., Giaccai D., Delbos E., 2009. Effect of north and south exposure on organic matter in high Alpine soils. Geoderma 149, 124-136.

Evenari M., Shanan L., Tadmor N.H., 1971. The Negev. The challenge of a desert. Harvard University Press, Cambridge, Massachusetts, 344 pp.

Evenari M., Masig D., Rogel A., 1980. Runoff-Farming in the Negev Desert of Israel VI. Jacob Blaustein Institute for Desert research, Sede Boker, Israel.

Falloon P.D., Smith P., Smith J.U., Szabo J., Coleman K., Marshall S., 1998. Regional estimates of carbon sequestration potential: linking the Rothamsted carbon model to GIS databases. Biology and Fertility of soils 27, 236-241.

Falloon P.D., Smith P., Szabo J., Pásztor L., 2002. Comparison of approaches for estimating carbon sequestration at the regional scale. Soil Use and Management 18, 164-241.

Fang C., Moncrieff J.B., 2001. The dependence of soil CO_2 efflux on temperature. Soil Biology and Biochemistry 33, 155-165.

FAO (ed.), 2004. Carbon Sequestration in dryland soil. World soil resources reports, 102. Rome. (available online at http://fao.org/docrep/007/y5738e/y5738e0d.htm.).

FAO-UNESCO, 1995. The digital soil map of the world (DSMW). Paris, FAO-UNESCO.

Farage P., Pretty J., Ball A., 2003. Biophysical aspects of carbon sequestration in drylands. Seminar paper presented at University of Essex, 1-25.

Farage P., Ardö J., Olsson L., Rienzi E.A., Ball A.S., Pretty J.N., 2007. The potential for soil carbon sequestration in three tropical dryland farming systems of Africa and Latin America: A modeling approach. Soil and Tillage Research 94, 457-472.

Feng Q., Endo K.N., Guodong C., 2002. Soil carbon in desertified land in relation to site characteristics. Geoderma 106, 24-43.

Feng Y., Motta A.C., Reeves D.W., Burmester C.H., Van Santen E., Osborne J.A., 2003. Soil microbial communities under conventional till and no-till continuous cotton systems. Soil Biology and Biochemistry 35, 1693-1703.

Foley J.A., De Fies R., Asner G.P., Barford C., Bonan G., Carpenter S.R., Shapin F.S., Coe M.T., Daily G.C., Gibbs H.K., Helkowski J.H., Holloway T., Howard E.A., Kucharik C.J., Monfreda C., Patz J.A., Prentice C., Ramankutty N., Snyder P.K., 2005. Global Consequences of Land Use. Science 309, 570-574.

Frank T.D., Tweddale S.A., 2006. The Effect of Spatial Resolution on Measurement of Vegetation Cover in Three Mojave Desert Shrub Communities. Journal of Arid Environments 67, Special Issue on the Changing Mojave Desert, Supplement 1, 88-99.

Friedlingstein P., Cox P., Betts R., Bopp L., Von Bloh W., Brovkin V., Cadule P., Doney S., Eby M., Fung I., Bala G., John J., Jones C., Joos F., Kato T., Kawamiya M., Knorr W., Lindsay K., Matthews H.D., Raddatz T., Rayner P., Reick C., Roeckner E., Schnitzler K.G., Schnur R., Strassmann K., Weaver A.J., Yoshikawa C., Zeng N., 2006. Climate-Carbon Cycle Feedback Analysis: Results from the C4MIP Model Intercomparison. Journal of Climate 19, 3337-3353.

Frogbrook Z.L., Oliver M.A., 2001. Comparing the spatial predictions of soil organic matter determined by two laboratory methods. Soil Use and Management 17, 235-244.

Garcia-Pausas J., Casals P., Camarero L.S., Huguet C., Sebastià M.T., Thompson J.A., Romanyà J., 2007. Soil organic carbon storage in mountain grasslands of the Pyrenees: effects of climate and topography. Biogeochemistry 82, 279-289.

Glatzel S., Sommer M., 2005. Colluvial soils and landscape position: field studies on greenhouse gas exchange and related ecological characteristics. Zeitschrift für Geomorphologie, N.F. Supplement 139, 87-99.

Glenn E., Squired V., Olson M., Frye R., 1993. Potential for carbon sequestration in the drylands. Water Air and Soil Pollution 70, 341-355.

Global Soil Data Task (2000). Global Soil Data Products CD-ROM (IGBP-DIS). Available online at http://www.daac.ornl.gov/ from the ORNL Distributed Active Archive Center, Oak Ridge National Laboratory, Oak Ridge, TN, USA: International Geosphere-Biosphere Programme - Data and Information Services.

Gomez C., Viscarra Rossel R., McBratney A., 2008. Soil organic carbon prediction by hyperspectral remote sensing and field VIS-NIR spectroscopy: an Australian case study. Geoderma 146, 403-411.

Grayson R.B., Western A.W., Chiew F.H., 1997. Preferred states in spatial soil moisture patterns: local and nonlocal controls. Water Resources Research 33, 2897-2908.

Griffiths R.P., Madritch M.D., Swanson A.K., 2009. The effects of topography on forest soil characteristics in the Oregon Cascade Mountains (USA): implications for the effects of climate change on soil properties. Forest Ecology and Management 257, 1-7.

Grüneberg E., Schöning I., Kalko E.K.V., Weisser W.W., 2010. Regional organic carbon stock variability: A comparison between depth increments and soil horizons. Geoderma 155, 426-433.

Hancock G.R., Murphy D., Evans K.G., 2010. Hillslope catchment scale soil organic carbon concentration: An Assessment of the role of geomorphology and soil erosion in an undisturbed environment. Geoderma 155, 36-45.

Haynes R.J., Dominy C.S., Graham M.H., 2003. Effect of agricultural land use on soil organic matter status and the composition of earthworm communities in KwaZulu-Natal, South Africa. Agriculture, Ecosystems and Environment 95, 453-464.

Heckmann K., Welty-Bernard A., Rasmussem C., Schwartz E., 2009. Geologic controls of soil organic cycling and microbial dynamics in temperate conifer forests. Chemical Geology 267, 12-23.

Hein L., De Ridder N., Hiernaux P., Leemans R., De Wit A., Schaepman M., 2011. Desertification in the Sahel: Towards better accounting for ecosystem dynamics in the interpretation of remote sensing images. Journal of Arid Environments 75 (11), 1164-1172.

Henry M., Valentini R., Bernoux M., 2009. Soil carbon stocks in ecoregions of Africa. Biogeosciences Discussions 6, 797-823.

Hikel H., Yair A., Schwanghart W., Hoffmann U., Straehl S., Kuhn N.J., 2012. Experimental investigation of soil ecohydrology on rocky desert slopes in the Negev Highlands, Israel. Zeitschrift für Geomorphologie 57, Suppl. 1, 039-058.

Hill J., Schuett B., 2000. Mapping complex patterns of erosion and stability in dry Mediterranean ecosystems. Remote Sensing of Environment 74, 557-569.

Hoffmann T., Glatzel S., Dikau R., 2009. A carbon storage perspective on alluvial sediment storage in the Rhine catchment. Geomorphology 108, 127-137.

Hoffmann U., Yair A., Hikel H., Kuhn N.J., 2012. Soil organic carbon in the rocky desert of northern Negev (Israel). Journal of Soils and Sediments 12, 811-825.

Homann P.S., Sollins P., Chappell H.N., Stangenberger A.G., 1995. Soil Organic Carbon in a Mountainous, Forested Region: Relation to Site Characteristics. Soil Science Society of America Journal 59, 1468-1475.

Houghton R.A., 2007. Balancing the Global Carbon Budget. Annual Review of Earth and Planetary Science 35, 313-347.

Hummel J.W., Sudduth K.A., Hollinger S.E., 2001. Soil moisture and organic matter prediction of surface and subsurface soils using an NIR soil sensor. Computers and Electronics in Agriculture 32, 149-165.

Imeson A.C., Prinsen H.A.M., 2004. Vegetation patterns as biological indicators for identifying runoff and sediment source and sink areas for semi-arid landscapes in Spain. Agriculture, Ecosystems and Environment 104, 333-342.

IPCC, 2007. Climate Change 2007: The Physical Science Basis. Contribution of Working Group I to the Fourth Assessment Report of the Intergovernmental Panel on Climate Change. Solomon S., Qin D., Manning M., Chen Z., Marquis M., Averyt K.B., Tignor M., Miller H.L., (eds.). Cambridge University Press, Cambridge, UK and New York, NY, USA.

IUSS Working Group WRB, 2006. World reference base for soil resources 2006. World soil resources reports no. 103, FAO, Rome.

Jarmer T., Hill J., Lavee H., Sarah P., 2010. Mapping soil organic carbon in non-agricultural semi-arid and arid ecosystems of Israel. Photogrammetric Engineering and Remote Sensing 75, 85-94.

Jobbágy E.G., Jackson R.B., 2000. The vertical distribution of soil organic carbon and its relation to climate and vegetation. Ecoogical Applications 10, 423-436.

Jones H.G., 1992. Plants and Microclimate: A Quantitative Approach to Environmental Plant Physiology, 2nd edn. Cambridge University Press.

Jones C., McConnell C., Coleman K., Cox P.M., Falloon P., Jenkinson D., Powlson D., 2005. Global climate change and soil carbon stocks; predictions from two contrasting models for the turnover of organic carbon in soil. Global Change Biology 11 (1), 154-166.

Kaplan J.O., Krumhardt K.M., Ellis E.C., Ruddiman W.F., Lemmen C., Goldewijk K.K., 2010. Holocene carbon emissions as a result of anthropogenic land cover change. The Holocene 21, 775-791.

Kaplan J.O., Krumhardt K.M., Zimmermann N.E., 2012. The effects of land use and climate change on the carbon cycle of Europe over the past 500 years. Global Change Biology 18, 902-914.

Kern J.S., 1994. Spatial patterns of soil organic carbon in the contiguous United States. Soil Science Society of America Journal 58, 439-455.

Kidron G.J., Zohar M., 2010. Spatial evaporation patterns within a small drainage basin in the Negev Desert. Journal of Hydrology 380, 376-385.

Kirschbaum M.U.F., 2000. Will changes in soil organic carbon act as a positive or negative feedback on global warming? Biogeochemistry 48, 21-51.

Konen M.E., Burras C.L., Sandor J.A., 2003. Organic carbon, texture, and quantitative color measurement relationships for cultivated soils in North Central Iowa. Soil Science Society of America Journal 67, 1823-1830.

Kramer P.J., Boyer J.S., 1995. Water Relations of Plants and Soils. Academic Press. San Diego, California.

Kuhn N.J., Yair A., 2003. Spatial distribution of surface conditions and runoff generation in small arid watersheds, Zin Valley Badlands, Israel. Geomorphology 57, 183-200.

Kuhn N.J., Yair A., Kasanin-Grubin M., 2004. Spatial distribution of surface properties, runoff generation and landscape development in the Zin Valley Badlands, northern Negev, Israel. Earth Surface Processes and Landforms 29, 1417-1430.

Kutsch W.L., Bahn M., Heinemeyer A., 2009. Soil carbon relations: an overview. In: Kutsch W.L., Bahn M., Heinemeyer A., (eds.). Soil Carbon Dynamics. An Integrated Methodology. Cambridge University Press.

Kutzbach J., Bonan G., Foley J., Harrison S.P., 1996. Vegetation and soil feedbacks on the response of the African monsoon to orbital forcing in the early to middle Holocene. Nature 384, 623-626.

Laity J., 2008. Deserts and desert environments, 342. Wiley-Blackwell, Singapore.

Lal R., 2001. Potential of desertification control to sequester carbon and mitigate the greenhouse effect. Climatic Change 51, 35-72.

Lal R., 2002a. Soil carbon dynamics in crop land and rangeland. Environmental Pollution 116, 353-362.

Lal R., 2002b. Carbon sequestration in dryland ecosystems of west Asia and north Africa. Land Degradation and Development 13, 45-59.

Lal R., 2003. Carbon sequestration in dryland ecosystems. Environmental Management 33, 528-544.

Lal R., 2005. Soil erosion and Carbon dynamics. Soil and Tillage Research 81 (2), 137-142.

Lal R., 2009. Sequestering carbon in soils of arid ecosystems. Land Degradation and Development 20, 441-454.

Lal R., Kimble J.M., Stewart B.A., 2011. Importance of soil bulk density and methods of its measurement. In: Kimble J.M., Follett R.F., Stewart B.A., (eds.). Assessment methods for soil carbon, 31-44. CRC Press, Boca Raton.

Larcher W., 1995. Physiological Plant Ecology, New York, Springer Verlag.

Lavee H., Imeson A.C., Pariente S., Benjamini Y., 1991. The response of soils to simulated rainfall along a climatological gradient in an arid and semi-arid region. Catena Supplement 19, 19-37.

Lavee H., Imeson A.C., Pariente S., 1998. The impact of climate change on geomorphology and desertification along Mediterranean - arid transect. Land Degradation and Development 9, 407-422.

Leifeld J., Bassin S., Fuhrer J., 2005. Carbon stocks in Swiss agricultural soils predicted by land-use, soil characteristics, and altitude. Agriculture, Ecosystems and Environment 105, 255-266.

Lesschen J.P., 2008. Multi-scale interactions between soil, vegetation and erosion in the context of agricultural land abandonment in a semi-arid environment. Dissertation. University of Amsterdam. Faculty of Science.

Lesschen J.P., Cammeraat L.H., Kooijman A.M., Van Wesemael B., 2008. Development of spatial heterogeneity in vegetation and soil properties after land abandonment in a semi-arid ecosystem. Journal of Arid Environments 72, 2082-2092.

Lesschen J.P., Schoorl J.M., Cammeraat L.H., 2009. Modelling runoff and erosion for a semi-arid catchment based on hydrological connectivity to integrate plot and hillslope scale influences. Geomorphology 109, 174-183.

Lettens S., Van Orshoven J., Van Wesemael B., Muys B., 2004. Soil organic carbon and inorganic carbon contents of landscape units in Belgium derived using data from 1950 to 1970. Soil Use and Management 20, 40-47.

Lettens S., Van Orshoven J., Van Wesemael B., De Vos B., Muys B., 2005. Stocks and fluxes of soil organic carbon for landscape units in Belgium derived from heterogeneous data sets for 1990 and 2000. Geoderma 127, 11-23.

Li X.G., Li Y.K., Li F.M., Ma Q., Zhang P.L., Lin P., 2009. Changes in soil organic carbon, nutrients and aggregation after conservation of native desert soil into irrigated arable land. Soil and Tillage Research 104, 263-269.

Li P., Wang Q., Endo T., Zhao X., Kakubari Y., 2010. Soil organic carbon stock is closely related to aboveground vegetation properties in cold-temperate mountainous forests. Geoderma 154, 407-441.

Li J., Heap A.D., 2011. A review of comparative studies of spatial interpolation methods in environmental sciences: Performance and impact factors. Ecological Informatics 6, 228-241.

Lieb G., Kellerer-Pirklbauer-Eulenstein A., Strasser U., (eds.), 2011. Effekte des Klimawandels im Naturraum des Hochgebirges. Geographie für eine Welt im Wandel: Umwelt - Gesellschaft - Geokommunikation. Vienna University Press.

Liebens J., Van Molle M., 2003. Influence of estimation procedure on soil organic carbon stock assessment in Flanderns, Beldium. Soil Use and Management 19 (4), 364-371.

Liu D., Wang Z., Zhang B., Song K., Li X., Li J., Li F., Duan H., 2006. Spatial distribution of soil organic carbon and analysis of related factors in croplands of the black soil region, Northeast China. Agriculture, Ecosystems and Environment 113, 73-81.

Ludwig J.A., Wilcox B., Bresheards D., Tongway D.J., Imeson A., 2005. Vegetation patches and runoff-erosion as interacting ecohydrological processes in semiarid landscapes. Ecology 86, 288-297.

Luyssaert S., Schulze E.D., Börner A., Knohl A., Hessenmöller D., Law B.E., Ciais P., Grace J., 2008. Old-growth forests as global carbon sinks. Nature 455, 213-215.

Meersmans J., De Ridder F., Canters F., De Baets S., Van Molle M., 2008. A multiple regression approach to assess the spatial distribution of Soil Organic Carbon (SOC) at the regional scale (Flanders, Belgium). Geoderma 143, 1-13.

Mishra U., 2009. Predicting storage and dynamics of soil organic carbon at regional scale. Dissertation.

Mishra U., Lal R., Slater B., Calhoun F., Liu D., Van Meirvenne M., 2009. Predicting soil organic carbon stock using profile depth distribution functions and ordinary kriging. Soil Science Society of America Journal 73, 614-621.

Mondini C., Coleman K., Whitmore A.P., 2012. Spatially explicit modelling of changes in soil organic C in agricultural soils in Italy, 2001-2100: Potential for compost amendment. Agriculture, Ecosystems and Environment 153, 24-32.

Morgan J.A., Follet R.F., Allen L.H.J., Del Grosso S., Derner J.D., Dijkstra F., Franzluebbers A., Fry R., Paustian K., Schoeneberger M.M., 2010. Carbon sequestration in agricultural lands of the United States. Journal of soil and water conservation 65 (1), 6A-13A.

Mulder V.L., de Bruin S., Schaepmann M.E., Mayr T.R., 2011. The use of remote sensing in soil and terrain mapping – A review. Geoderma 162 (1-2), 1-19.

Ni J., 2001. Carbon storage in terrestrial ecosystems of China: estimates at different spatial resolutions and their responses to climate change. Climatic Change 49, 339-358.

Olsvig-Whittaker L., Shachak M., Yair A., 1983. Vegetation patterns related to environmental factors in a Negev Desert watershed. Vegetation 54, 153-165.

Parsons A.J., Abrahams A.D., (eds.), 2009. Geomorphology of desert environments, 2nd edn. Springer, New York.

Parton W.J., Schimel D.S., Cole C.V., Ojima D.S., 1987. Analysis of factors controlling soil organic matter levels in Great Plains grasslands. Soil Science Society of America Journal 51, 1173-1179.

Perruchoud D., Walthert L., Zimmermann S., Lüscher P., 2000. Contemporary carbon stocks of mineral forest soils in the Swiss Alps. Biogeochemistry 50, 111-136.

Ping C.L., Michaelson G.J., Jorgenson M.T., Kimble J.M., Epstein H., Romanovsky V.E., Walker D.A., 2008. High stocks of soil organic carbon in the North American Arctic region. Nature Geoscience 1, 615-619.

Post W.M., Kwon K.C., 2000. Soil Carbon Sequestration and Land-Use Change: Processes and Potential. Change Biology 6, 317-328.

Poussart J.N., 2002. Verification of soil carbon sequestration - uncertainties of assessment methods. M.Sc. thesis, Lund, Lund University. 64pp.

Poussart J.N., Ardö J., Olsson L., 2004a. Effects of data uncertainties on soil organic carbon in the Sudan. Environmental Management 33, 405-415.

Poussart J.N., Ardö J., Olsson L., 2004b. Verification of soil carbon sequestration: sample requirements. Environmental Management 33, 425-426.

Puigdefabregas J., 2005. The role of vegetation patterns in structuring runoff and sediment fluxes in drylands. Earth Surface Processes and Landforms 30, 133-147.

Qi Y., Xu M., Wu J., 2002. Temperature sensitivity of soil respiration and its effects on ecosystem carbon budget: nonlinearity begets surprises. Ecological Modelling 153:131-142.

Qin Z., Li W., Burgmeier J., Karnieli A., 2006. Quantitative estimation of land cover structure in an arid region across the Israel-Egypt border using remote sensing data. Journal of Arid Environments 66, 336-352.

Quinton J.N., Govers G., Van Oost K., Bardgett R.D., 2010. The impact of agricultural soil erosion on biogeochemical cycling. Nature Geoscience 3, 311-314.

Ravi S., Breshears D.D., Huxman T.E., D'Odorico P., 2010. Land degradation in drylands: Interactions among hydrologic-aeolian erosion and vegetation dynamics. Geomorphology 116, 236-245.

Reeves III J., McCarty G., Mimmo T., 2002. The potential of diffuse reflectance spectroscopy for the determination of carbon inventories in soils. Environmental Pollution 116, 277-284.

Reifenberg A., 1947. The Soils of Palestine. Murby, London.

Roberts D.A., Smith M.O., Adams J.B., 1993. Green vegetation, nonphotosynthetic vegetation, and soils in AVIRIS data. Remote Sensing of Environment 44, 255-269.

Rotenberg E., Yakir D., 2010. Contributing of Semi-Arid Forests to the Climate System. Science 327, 451-454.

Rosenbloom N.A., Harden J.W., Neff J.C., Schimel D.S., 2006. Geomorphic control of landscape carbon accumulation. Journal of Geophysical Research - Biogeosciences 111, 1-10.

Rodriguez-Iturbe I., Porporato A., (eds.), 2004. Ecohydrology of water-controlled ecosystems. Cambridge University Press.

Sandholt I., Rasmussen K., Andersen J., 2002. A simple interpretation of the surface temperature/vegetation index space for assessment of soil moisture status. Remote Sensing of Environment 79, 213-224.

Schimel D., 2010. Drylands in the earth system. Science 327, 418-419.

Schimel D., Melillo J., Tian H., 2000. Contribution of increasing CO_2 and climate to carbon storage by ecosystems in the United States. Science 287, 2004-2006.

Schlesinger W.H., 1977. Carbon balance in terrestrial detritus. Annual Review of Ecology and Systematics 8, 51-81.

Schlesinger W.H., 1990. Evidence from chronosequence studies for a low carbon-storage potential of soils. Nature 348, 232-234.

Schlesinger W.H., 1991. Biogeochemistry: An Analysis of Global Change, 588. Academic Press, San Diego.

Schlesinger W.H., 1995. An Overview of the carbon cycle. In: Lal R., Kimble J., Levine E., Stewart B.A., (eds.). Soils and Global Change. Advances in Soil Science, 9-25. Lewis Publisher.

Schlesinger W.H., Raikes J.A., Hartley A.E., Cross A.F., 1996. On the spatial patterns of soil nutrients in desert ecosystems. Ecology 77, 364-374.

Schlesinger W.H., Pilmanis A.M., 1998. Plant-soil interactions in deserts. Biogeochemistry 42, 169-187.

Schlesinger W.H., Winkler J.P., Megonigal J.P., 2000. Soils and the Global Carbon Cycle. In: Wigley T.M.L., (ed.). Carbon Cycle, 93-101. Cambridge University Press.

Schreiber K.F., Yair A, Shachak M., 1995. Ecological gradients along slopes of the Northern Negev Highlands, Israel. Advances in Geoecology 28, 209-229.

Schwanghart W., Jarmer T., 2011. Linking spatial patterns of soil organic carbon to topography - A case study from south-eastern Spain. Geomorphology 126, 252-263.

Seip H.M., 2001. We know too little about the carbon cycle. Oslo.

Selvaradjou S.K., Montanarella L., Spaargaren O., Dent D., 2005. European Digital Archive of Soil Maps (EuDASM) - Soil Maps of Africa, 386 pp. EUR 21657.

Sheikh M.A., Kumar M., Bussmann R.W., 2009. Altitudinal variation in soil organic carbon stock in coniferous subtropical and broadleaf temperate forests in Garhwal Himalaya. Carbon Balance and Management 4 (6), (published online).

Singh S.K., Singh A.K., Sharma B.K., Tarafdar J.C., 2007. Carbon stock and organic carbon dynamics in soils of Rajasthan, India. Journal of Arid Environments 68, 408-421.

Sinoga J.D.R., Pariente S., Diaz A.R., Murillo J.F.M., 2012. Variability of relationships between soil organic carbon and some soil properties in Mediterranean rangelands under different climatic conditions (South of Spain). Catena 94, 17-25.

Sitch S., Smith B., Prentice I.C., Arneth A., Bondeau A., Cramer W., Kaplan J.O., Levis S., Lucht W., Sykes M.T., Thonicke K., Venevsky S., 2003. Evaluation of ecosystem dynamics, plant geography and terrestrial carbon cycling in the LPJ dynamic global vegetation model. Global Change Biology 9, 161-185.

Smith K.A., Ball T., Conen F., Dobbie K.E., Massheder J., Rey A., 2003. Exchange of greenhouse gases between soil and atmosphere: interactions of soil physical factors and biological processes. European Journal of Soil Science 54, 779-791.

Smith P., 2004. Soils as carbon sinks: the global context. Soil Use and Management 20, 212-218.

Spielvogel S., Jörg P., Auerswald K., Kögel-Knabner I., 2009. Site-specific spatial patterns of soil organic carbon stocks in different landscape units of a high-elevation forest including a site with forest dieback. Geoderma 152, 218-230.

Stallard R.F., 1998. Terrestrial sedimentation and the carbon cycle: coupling weathering and erosion to carbon burial. Global Biogeochemical Cycles 12, 231-257.

Stavi I., Lavee H., Ungar E.D., Sarah P., 2009. Ecogeomorphic feedbacks in semiarid rangelands: a review. Pedosphere 19 (2), 217-229.

Stutter M.I., Lumsdon D.G., Billett M.F., Low D., Deeks L.K., 2009. Spatial Variability in Properties Affecting Organic Horizon Carbon Storage in Upland Soils. Soil Science Society of America Journal 73, 1724-1732.

Su Z.Y., Xiong Y.M., Zhu J.Y., Ye Y.C., Ye M., 2006. Soil organic carbon content and distribution in a small landscape of Dongguan, South China. Pedosphere 16, 10-17.

Tan Z.X., Lal R., Smeck N.E., Calhoun F.G., 2004. Relationships between surface organic carbon pool and site variables. Geoderma 121, 187-195.

Tan Z.X., Lal R., 2005. Carbon sequestration potential estimates with changes in land use and tillage practice in Ohio, USA. Agriculture, Ecosystem and Environment 111, 140-152.

Trumbore S., 2009. Radiocarbon and soil carbon dynamics. Annual Review of Earth and Planetary Sciences 37, 47-66.

Tsui C.C., Chen Z.S., Hsieh C.F., 2004. Relationships between soil properties and slope position in a lowland rain forest of southern Taiwan. Geoderma 123, 131-142.

Turner W.R., Brandon K., Brooks T.M., Costanza R., De Fonseca G.A.B., Portela R., 2007. Global conservation of biodiversity and ecosystem services. BioScience 57, 868-873.

Udelhoven T., Emmerling C., Jarmer T., 2003. Quantitative analysis of soil chemical properties with diffuse reflectance spectrometry and partial-least-square regression: a feasibility study. Plant and Soil 251, 319-329.

Van Wesemael B., Paustian K., Meersmans J., Goidts E., Barancikova G., Easter M., 2010. Agricultural management explains historic changes in regional soil carbon stocks. Proceedings of the National Academy of Sciences 107, 14926–14930.

Viscarra Rossel R., Walvoort D., McBratney A., Janik L., Skjemstad L., 2006. Visible, near infrared or combined diffuse reflectance spectroscopy for simultaneous assessment of various soil properties. Geoderma 131, 59-75.

Wang D.D., Shi X.Z., Wang H.J., Weindorf D.C., Yu D.S., Sun W.X., Ren H.Y., Zhao Y.C., 2010. Scale Effect of Climate and Soil Texture on Soil Organic Carbon in the Uplands of Northeast China. Pedosphere 20 (4), 525-535.

Wang H.Q., Hall C.A.S., Cornell J.D., Hall M.H.P., 2002. Spatial dependence and the relationship of soil organic carbon and soil moisture in the Luquillo Experimental Forest, Puerto Rico. Landscape Ecology 17, 671-684.

Wang Y., Zhang X.C., Zhang J.L., Li S.J., 2009. Spatial Variability of Soil Organic Carbon in a Watershed on the Loess Plateau. Pedosphere 19 (4), 486-495.

Wang Y., Fu B., Lü Y., Chen L., 2011. Effects of vegetation restoration on soil organic carbon sequestration at multiple scales in semi-arid Loess Plateau, China. Catena 85 (1), 58-66.

Webster R., Oliver M.A., 2001. Geostatistics for environmental science, 271 pp. John Wiley and Sons LTD. Toronto, Canada.

Wigley T.M.L., Schimel D.F., (eds.), 2005. The Carbon Cycle. Cambridge University Press.

Wills S.A., Burras C.L., Sandor J.A., 2007. Prediction of SOC content using field and laboratory measurements of soil color. Soil Science Society of America Journal 71, 380-388.

Xiao J., Moody A., 2005. Geographical distribution of global greening trends and their climatic correlates: 1982-1998. International Journal of Remote Sensing 26, 2371-2390.

Xu X., Liu W., Kiely G., 2010. Modeling the change in soil organic carbon of grassland in response to climate change: Effects of measured versus modelled carbon pools for initializing the Rothamsted Carbon model. Agriculture, Ecosystems and Environment 140 (3-4), 372-381.

Yaalon D.H., Dan J., 1974. Accumulation and distribution of loess-derived deposits in the semi-desert and desert fringe areas of Israel. Zeitschrift für Geomorphologie 20, 91-105.

Yair A., 1990. The role of topography and surface cover upon soil formation along hillslopes in arid climates. Geomorphology 3, 287-299.

Yair A., 1992. The control of headwater area on channel runoff in a small arid watershed. In: Parsons T., Abrahams A., (eds.). Overland flow: hydraulics and erosion mechanics, 53-68. UCL Press, London.

Yair A., 1994. The ambiguous impact of climate change at a desert fringe: Northern Negev, Israel. In: Millington A.C., Pye K., (eds.). Environmental Change in Drylands: Biogeophysical and Geomorphological Perspectives, 199-227.

Yair A., 1999. Spatial variability in the runoff generated in small arid watersheds: implications for water harvesting. In: Hoekstrat T.M., Shachak M., (eds.). Arid Land Management, toward Ecological Sustainability, 212-222.

Yair A., Danin A., 1980. Spatial variations in vegetation as related to the soil moisture regime over an arid limestone hillside, Northern Negev Israel. Oecologia 47, 83-88.

Yair A., Shachak M. 1982. A case study of energy water and soil flow chains in an arid ecosystem. Oecologia 54 (3), 389-397.

Yair A., Lavee H., 1985. Runoff generation in arid and semi-arid zones. In: Anderson M.G., Burt T.P., (eds.). Hydrological Forecasting, 183-220.

Yair A., Kossovsky A., 2002. Climate and surface properties: hydrological response of small arid and semi-arid watersheds. Geomorphology 42 (1/2), 43-57.

Yair A., Raz-Yassif N., 2004. Hydrological processes in a small arid catchment: scale effects of rainfall and slope length. Geomorpholohgy 61, 155-169

Yao S., Lan H., Zhang F., 2010. Variation of seed heteromorphism in Chenopodium album and the effect of salinity stress on the descendants. Annals of Botany 105, 1015-1025.

Yoo K., Amundson R., Heimsath A.M., Dietrich W.E., 2006. Spatial patterns of soil organic carbon on hillslopes: integrating geomorphic processes and the biological C cycle. Geoderma 130, 47-65.

Zeng N., Neelin J.D., Lau K.M. Tuker C.J., 1999. Enhancement of interdecadal climate variability in the sahel by vegetation interaction. Science 286, 1537-1540.

Zeng N., Qian H., Munoz E., Iacono R., 2004. How strong is carbon cycle - climate feedback under global warming? Geophysical Research Letters 31 (20).

Zhang X., Drake N., Wainwright J., 1998. Downscaling land surface parameters for global soil erosion estimation using no ancillary data. Proceeding of the 3rd International Conference on GeoComputation, University of Bristol (UK), Abrahart R.J. (producer). GeoComputation CD-ROM.

Zhang C.S., McGrath D., 2004. Geostatistical and GIS analysis on soil organic carbon concentrations in grassland of southeastern Ireland from two different periods. Geoderma 119, 261-275.

Zhao Y.C., Shi X.Z., Yu D.S., Zhao Y.F., Sun W.X., Wang H.J., 2005. Different methods for prediction of spatial patterns of soil organic carbon density in Hebei Province, China. Acta Pedologica Sinica 42, 379-385.

Zhou G., Liu S., Li Z., Zhang D., Tang X., Zhou C., Yan J., Mo J., 2006. Old-Growth Forests can accumulate Carbon in Soils. Science 314, 1417.

Zhou Z.Y., Li F.R., Chen S.K., Zhang H.R., Li G., 2011. Dynamics of vegetation and soil carbon and nitrogen accumulation over 26 years under controlled grazing in a desert shrubland. Plant and Soil 341, 257-268.

Zohary M., 1962. Plant life of Palestine. The Roland Press Company. New York.

Curriculum vitae **HIKEL HARALD**

Personaldaten	Geburtsdatum	22. März 1979
	Nationalität	Deutsch
Ausbildung	2014	Promotion
	2007 – 2013	Universität Basel, Physiogeographie und Umweltwandel
	2007	Diplom Geographie
	2001 – 2007	Universität Würzburg (D), Physische Geographie

Derzeitige Funktion

- Projektleiter / Sachbearbeiter Verkehr und Umwelt

Facherfahrung

- Lärmschutz
- Umweltschutz

Spezielle Erfahrung

- Lärm- und Umweltschutz
- Geographische Informationssysteme
- Boden- und Wasseranalysen

Berufliche Aktivität

seit 2014 Ingenieurbureau A. Aegerter & Dr. O. Bosshardt AG, Basel

- Strassenlärmsanierungsprojekte LSP
- Close Proximity (CPX) - Messungen

2008 – 2013 Universität Basel, Basel

- Wissenschaftlicher Mitarbeiter
- Durchführung unterschiedlicher Lehrveranstaltungen
- Forschung im Bereich Umwelt- und Klimawandel

2008 – 2012 Gruner AG, Basel

- Akustische Projekte Schallschutzfenster
- Durchführung diverser Lärmmessungen
- Bodenanalysen, Baubegleitung

2007 – 2008 Universität Würzburg, Würzburg

- Wissenschaftlicher Mitarbeiter
- Durchführung unterschiedlicher Lehrveranstaltungen
- GIS-Schulungen in Djibouti, Djibouti